PROPER ORTHOGONAL DECOMPOSITION FOR PERFORMANCE BASED DESIGN AND MODELLING CONCRETE

Thesis

Submitted in partial fulfilment of the requirements of the degree of

DOCTOR OF PHILOSOPHY

by

A. MANOJ

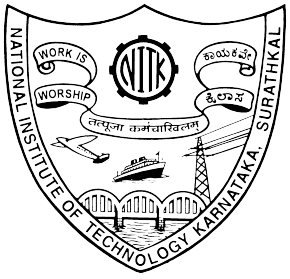

DEPARTMENT OF CIVIL ENGINEERING

NATIONAL INSTITUTE OF TECHNOLOGY KARNATAKA,

SURATHKAL, MANGALORE - 575 025

JUNE, 2022

PROPER ORTHOGONAL DECOMPOSITION FOR PERFORMANCE BASED DESIGN AND MODELLING CONCRETE

Thesis

Submitted in partial fulfillment of the requirements of the degree of

DOCTOR OF PHILOSOPHY

by

A. MANOJ

165037 CV16F01

Under the guidance of

Dr. K. S. BABU NARAYAN

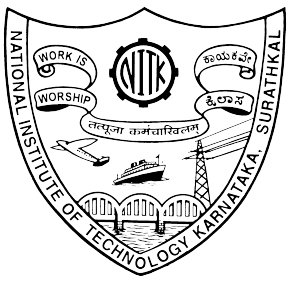

DEPARTMENT OF CIVIL ENGINEERING

NATIONAL INSTITUTE OF TECHNOLOGY KARNATAKA,

SURATHKAL, MANGALORE - 575 025

JUNE, 2022

DECLARATION

by the Ph.D Research Scholar

I hereby *declare* that the Research Thesis entitled **"Proper Orthogonal Decomposition for Performance Based Design and Modelling Concrete"** which is being submitted to the **National Institute of Technology Karnataka, Surathkal** in partial fulfillment of the requirements for the award of the Degree of **Doctor of Philosophy** in **Civil Engineering** is a *bonafide report of the research work carried out by me*. The material contained in this Research Thesis has not been submitted to any University or Institution for the award of any degree.

A. MANOJ
165037 CV16F01
Department of Civil Engineering
NITK, Surathkal - 575 025

Place: NITK, SURATHKAL
Date: JUNE 03,2022

CERTIFICATE

This is to *certify* that the Research Thesis entitled **"Proper Orthogonal Decomposition for Performance Based Design and Modelling Concrete"** submitted by **A. Manoj** (Register Number: 165037 CV16F01) as the record of research work carried out by him, *is accepted as Research Thesis submission* in partial fulfillment of the requirements for the award of degree of **Doctor of Philosophy**.

K.S.B.

Dr. K. S. BABU NARAYAN
Research Guide

Jayalekshmi
06/06/22

Dr. B. R. JAYALEKSHMI
Chairman - DRPC

Chairman (DRPC)
Department of Civil Engineering
National Institute of Technology Karnataka, Surathkal
Mangalore - 575 025, Karnataka INDIA

NATIONAL INSTITUTE OF TECHNOLOGY KARNATAKA, SURATHKAL
DEPT. OF CIVIL ENGG.

DEDICATED AT

LOTUS FEET OF,

GODDESS

SHRI SHARADAMBA

DISPELLER OF IGNORANCE

SHRI ADI SHANKARACHARYA

& TO

LIGHT OF MY LIFE

MY PARENTS

MY GURU, OCEAN OF KNOWLEDGE & WISDOM

Prof. K. S. BABU NARAYAN

ACKNOWLEDGEMENT

Foremost, I thank GOD for bestowing and channelizing me to pursue research, which has been an elevating life experience. I feel very happy and proud to accomplish the research taken up, satisfactorily fulfilling the institute norms and requirements.

All credits belong to my Guru, life coach, research supervisor Dr. K. S. Babu Narayan, Professor, Department of Civil Engineering and Dean P&D, National Institute of Technology Karnataka, Surathkal, who has enriched my thinking and approach towards research, multi-folded structural design and consultancy skills, and taught a better living. His ideologies, creative thinking, shrewdness, voracious reading habit, in-depth knowledge in a wide range of subjects, interest in literature & music and charming personality have always been inspiring. I am very fortunate and glad to be his understudy, and lifelong indebted for his care, concern and love. I am grateful to him for introducing me to the topic “Proper Orthogonal Decomposition” and budding interest in “Mathematical Modelling”. His keen interest and ceaseless efforts in preparation of the thesis have definitely enhanced its quality. I bow and submit my heartfelt gratitude and profound thanks to him.

Deep sense of gratitude to RPAC members Dr. Subhash C. Yaragal, Professor, Department of Civil Engineering, and Dr. P. Sam Johnson, Associate Professor, Department of Mathematical and Computational Sciences, National Institute of Technology Karnataka, Surathkal, for critical evaluation of my research progress and providing constructive inputs which have been value addition in bringing out this thesis. Dr. Subhash C. Yaragal’s support in acquisition of the data and collection of reference materials has been substantial and needs a special mention.

I am grateful to Dr. B. R. Jayalekshmi, Professor & Head, Department of Civil Engineering, former Heads Dr. D. Venkat Reddy, Dr. Varghese George and Dr. K. Swaminathan, National Institute of Technology Karnataka, Surathkal, for their immense support and encouragement by providing departmental resources, which have helped in timely completion of my research work.

Lectures by Dr. Shyam S. Kamath and Dr. Muralidhar N., Professors, Department of Mathematical and Computational Sciences, National Institute of Technology

Karnataka, Surathkal, greatly eased analysis of data in the study, for which I am very thankful to them. Meetings and interactions with Dr. Moray D. Newlands, Dundee University, Dr. Kevin Paine, University of Bath at UCC2019, Jalandhar and Dr. Akanshu Sharma, Stuttgart University at EACEF 2019 has been a memorable experience and I thank them for their insightful research inputs.

Opportunity given to visit Kumamoto University, Japan by Dr. Katta Venkataramana, Professor, Department of Civil Engineering, National Institute of Technology Karnataka, Surathkal, and Dr. Shuichi Tori, Professor, Department of Mechanical System Engineering, Kumamoto University is greatly acknowledged.

I record my sincere and special gratitude to Dr. B. M. Sunil, Dr. A. S. Balu, Dr. M. C. Narasimhan, Dr. M. H. Prashanth, Dr. B. B. Das, Dr. Palanisamy T., faculty members in Department of Civil Engineering, National Institute of Technology Karnataka, Surathkal, Dr. S. Raviraj, Sri Jayachamrajendra College of Engineering, Mysore, my school teacher Dr. Shivadasan, Jawahar Navodaya Vidyalaya, Mudipu, my music teachers Dr. Sudarshan M. L., Vivekananda College of Engineering and Technology, Puttur and Mr. Krishna Kumar, Assistant Manager, Federal Bank, Kadaba, for their technical and non-technical support. Technical discussions, research interactions with my good friends Dr. Umesh B., National Institute of Technology, Warangal and Dr. Bhaskar S. Malwa, National Institute of Technology Karnataka, Surathkal, have always been very valuable, and I profusely thank them.

I extend my thankfulness to all the teaching and non-teaching staff of Civil Engineering department of the Institute for their support. Institute fellowship, TEQIP–III fund, and contingency grants provided have facilitated in fulfilling my essentials for attending conferences during my research tenure. Timely support from the institute healthcare crew, academic section staff, library authorities and A1 printers is sincerely appreciated.

With a special mention, my indebtedness goes to my good friends Mr. Noothan Kaliveer, Mr. Anup Kanoj, Ms. Kushitha U., Mr. Shrushanth K. S., Mr. Manohar Shanbhogue K., Mr. Sandesh K., and fellow-researchers Dr. Supriya R. Kulkarni, Ms. Ujwala Shenoy, Dr. Chethan B. A., Mr. Raghuram K. C., Dr. Avinash H. T., Dr. Chethan Kumar B., Mr. Venkanagouda B. B. Patil, Dr. Krishnamurthy M. P., Dr.

Rajesh Kalli, Dr. Kishor Kumar M. J., Mr. Sachin H., Dr. Sheeka Chinnappa, Dr. Kesava Rao B. and Dr. Desalegn Girma Mengistu.

Life wouldn’t have been easy without the care and support of my wife, parents and brothers, for which I express my deepest sense of gratitude, love and reverence toward them all.

June 03, 2022 A. MANOJ

NITK, Surathkal – 575 025

ABSTRACT

Reduction in the usage of Portland cement as the primary cementitious component in concrete has become a key driver for accomplishment of the UN sustainable development goals (SDGs). Utilization of secondary cementitious materials, recycled materials and performance-based design of concrete by innovative cement combinations are being attempted to make concrete the most versatile and widely used construction material and sustainable too. Nevertheless, achieving desired workability, strength and durability characteristics, is still challenging owing to the complex interaction of many variables. Performance-based design demands thorough qualitative and quantitative appraisal of concrete characteristics. Knowledge of significant variables will provide directions to performance-based design methods for accomplishing targeted levels. Data analytics help enhance state-of-the-art. Mathematically, in such complex systems, random experiments further add to sources of redundancy and lead to unnecessary complications, if all the variables are to be included in performance appraisal. Identification of significant variables, elimination of redundant helps in dimensionality reduction of data and meaningful representation of system's behaviour. Statistical methods, group method of data handling, machine learning techniques are very popularly employed in modelling complex systems of this kind.

Proper Orthogonal Decomposition (POD) has been considered in this work for dimensionality reduction in performance-based design of concrete. An account of employment of data handling techniques in performance-based design has been provided and utility of POD in such assignments has been demonstrated and highlighted. Sequential steps adopted in current research have been described. Available-published data sets have been adopted for study. Correlation matrix obtained from screened data has been decomposed to obtain eigenvalues and eigenvectors. Orthogonal components extracted from dimensionality reduction have been further used to draw inferences. A method to identify significant variables and their hierarchy has been ordered, which is of prime importance in performance-based design to for accomplishment of targets. A performance quality index has been proposed for evaluating relative quality of different mixes. Potential utility of POD in refinement of

available concrete models to predict and project behaviour of concrete with inclusion of emerging data in decision-making for redefining such models have been investigated.

General outcomes on utility of POD in concrete performance evaluation and specific conclusions on concrete workability, strength, durability and performance at elevated temperature exposure have been brought out as inferences. It is found that POD can be an effective tool in exploration of complex concrete data. Identification of crucial variables and ordering of hierarchy based on their significance can aid in quick calibration of concrete characteristics depending upon specific target requirements of performance-based design. Utilization of POD can open up new vistas to extend existing concrete capabilities and possibilities.

Key words: Concrete, Data, Correlation, Eigenvalue, Eigenvector, Dimensional and variable reduction, Component plot, POD, Performance index, Models.

TABLE OF CONTENTS

LIST OF FIGURES

LIST OF TABLES

SYMBOLS AND ACRONYMS

The principal symbols and acronyms used in the text are presented here for quick reference. However, it may be noted that uncommon and case-specific notations are explained in the text as and when they occur.

$\mathbf{x}_i$	:	i^{th} variable
n, N	:	Total number of observations
p, P	:	Total number of variables
σ_j	:	Standard deviation
$\boldsymbol{R}$, (r)	:	Correlation matrix, (correlation value)
λ	:	Eigenvalue
α, v	:	Eigenvector
D	:	Dimension (or component)
Q	:	Quality of representation
χ^2	:	Chi-square value

OPC	:	Ordinary Portland cement
GPC	:	Geo-polymer concrete
SCC	:	Self-compacting concrete
PCA	:	Principal component analysis
POD	:	Proper orthogonal decomposition
RMA	:	Reduced major axis
DF	:	Degree of freedom
SD	:	Standard deviation

CHAPTER 1
INTRODUCTION

1.1 GENERAL

Though behaviour of Nature is very complex and chaotic, it is very much fascinating. This makes humans think, understand phenomena, and use them to the best of their ability. Quest of scientists, researchers, academicians and almost every being is to find, explore, observe, understand, predict and advance the knowing and relishing these wonders.

A researcher's expedition is to bring all these complexities onto paper or lab, organise and model them in simplified form and apply it in future tasks.

1.2 CONCRETE

Mould-ability of concrete to any shape, water-resistant characteristics and cost-effectiveness have made it the most popular and widely used construction material. Advent of modern cement (OPC) in 1824 by Joseph Aspdin, relegated Roman cement to the back feat (Neville and Brooks 2010). Continuous efforts from investigators have provided a spectrum of concrete having site-specific applications.

Workability, strength and durability are the cardinal properties of concrete affected by a large number of variables, and many of these have been identified. It is recognised that concrete is a composite and is heterogeneous material at different scales (Mehta and Monteiro 2014) and also its behaviour is non-linear (Boukhatem et al. 2011b) at different loading conditions. Notwithstanding the advancements made in concrete technology, accomplishment of targeted performance levels is still challenging.

Variation in material characteristics, methods of mixing and placing, degree of compaction, curing techniques, structural boundary conditions and environmental factors (Pan et al. 2017) have an effect on the properties and performance of concrete.

As the extent to which the characteristics of concrete are affected by such variables itself has a wide range, dimensionality reduction of data in assessment and projection of concrete characteristics is of great importance in resource optimization. Evolution of

computer and information technology (Boukhatem et al. 2011b) has aided in handling concrete data consisting of multiple variables and in identification of those that influence the desired and targeted behaviour.

1.3 STATISTICAL TECHNIQUES

Organised data is essential in developing predictive models. In systems with many variables, data handling and analysis itself is a very challenging exercise. In such cases, statistical methods can be used to infer the nature and degree of correlation of parameters involved. Proper Orthogonal Decomposition (POD) is one multivariate technique that helps in understanding correlation among variables and assists in addressing big data handling difficulties employing dimensionality reduction without much information loss.

1.4 PROPER ORTHOGONAL DECOMPOSITION

POD is a popular dimensionality reduction technique (Jolliffe 2002). The central idea of POD is to look through directions or plane of largest variance in dataset consisting of a large number of interrelated variables. Directions (or dimensions) of largest variation are considered to be most important (or principal) in POD analysis. Hence, POD is also popularly called as Principal Component Analysis (PCA). Smith (2002) says – "It is a way of identifying patterns in data, and expressing the data in such a way as to highlight their similarities and differences".

When data is projected onto newly formed reduced orthogonal space (preferably ≤ 3 dimensions), it leads to easy visualisation and interpretation of variable dependence, interdependence and independence, and retention of most of the original information. Thus POD serves as a valid decision-making tool in judicious selection of important variables from among the vast database to make relevant data less exhaustive and more meaningful. In other words, POD helps to remove unimportant variables with very little information loss. Systematic utility of POD finds a vital place in reorganisation of data and mathematical model development that are operational to reduced computational efforts and time. Thus state of the art can enhance the Science – the knowing, and the Art – the doing of Concrete!

1.4.1 POD – Graphical interpretation

Physical meaning of POD can be understood by conducting a simple photography experiment on a teapot (Li 2009). Aim of this experiment is to take picture(s) of the teapot in such a way that the image alone would be sufficient to explain most of its features. This can be done in two ways.

1. Many pictures can be taken in different directions, such that each picture would explain in detail different characteristics of the teapot.
2. Taking a single picture that can explain most important details of the teapot that would be sufficient to describe its characteristics.

The first method is not an efficient technique to achieve the aim of this experiment and hence is not of interest. Considering the second method, in order to get most details of the teapot in a single image, it has to be rotated, and axes capturing maximum information of visibility has to be found, which is the utmost important task. Finding such axes help in extracting most of the data variance, which is the main theme of POD.

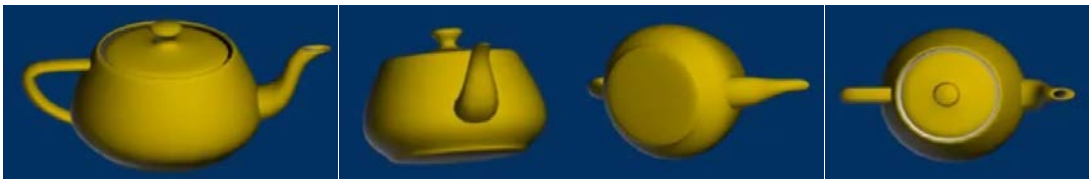

Figure 1.01 Rotation of teapot (Li 2009)

As seen in Fig. 1.01, the first image gives comprehensive information than others, which makes it most preferred image. It can be learned that by suitable axis orientation, maximum details can be construed. It is apparent from Fig. 1.02 that; red and green lines are the major and minor axes of most preferred configuration, respectively.

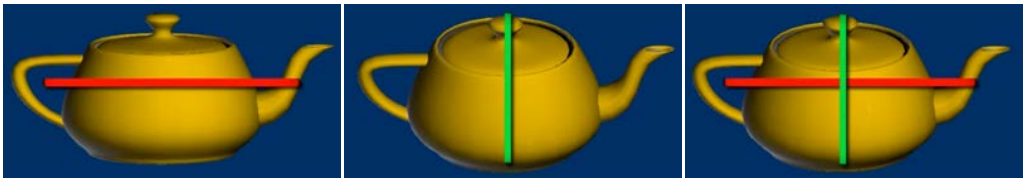

Figure 1.02 Axes of preferred configuration of teapot (Li 2009)

Hence, to summarise, the whole exercise of POD revolves around finding the best configuration in which description of data would be the most. In order to find the best configuration, POD follows a definite stepwise procedure of finding axis of the largest variation, whose mathematical gist has been explained in the chapter that follows.

1.4.2 Similar methods as POD for dimensionality reduction

Under dimensionality reduction tools, there are a plethora of options available. Other than POD, some popular tools are,

1. Reduced major axis (RMA)
2. Factor analysis
3. Independent component analysis

1.4.2.1 *POD and RMA*

Linear regression is a method of finding best fit line by trying to minimise the vertical distance between the point(s) and the assumed best fit. By doing so, it defines the direction of the best fit and thereby incorporating some error in analysis.

But, instead of calculating the vertical distance, in RMA, the orthogonal distances between the assumed line and the data point is calculated. Without knowing the best fit, it is impossible to calculate the orthogonal distance. Hence, it becomes an iterative process to find the best fit, where the orthogonal distances are to be minimised.

This process of minimising the orthogonal distance in 2–dimensions and determining the transformed orthogonal axes representing the variation of a dataset is called reduced major axis method. In comparison, POD (or PCA) can be thought of as RMA applied to higher dimensions.

1.4.2.2 *POD and factor analysis*

POD and factor analysis are very similar in operation. Factor analysis is a statistical method used to describe variability among observed, correlated variables in terms of a potentially lower number of unobserved, uncorrelated variables called factors. In other words, it is possible, for example, that variations in three or four observed variables mainly reflect the variations in fewer such unobserved variables. Factor analysis is related to POD, but the two are not identical. Factor analysis uses regression modelling techniques to test hypothesis producing error terms, while POD is a descriptive statistical technique. POD is used to find optimal ways of combing variables into a small number of subsets, while factor analysis is used in identification of the structure underlying such variables. When an investigator has a set of hypotheses that form the conceptual basis for the factor analysis, the investigator performs confirmatory factor analysis. On the contrary, when there are no guiding hypotheses and when the question

is simply what are the underlying factors, the investigator conducts an exploratory factor analysis. The factors in factor analysis are conceptualized as "real world" entities such as depression, anxiety and disturbed thought. This contrasts with POD, where the components are simply geometrical abstractions that may not map easily onto real-world phenomena. So, based on the data, one has to decide the analysis method. The structure of factor analysis is as presented in Eq. 1.01.

$$\mathrm{x} = \mathbf{\Lambda}\mathrm{f} + e \tag{1.01}$$

1.4.2.3 *POD and independent component analysis*

(Jolliffe 2002) The main objective of POD is to obtain a set of linear functions with the successive maximisation of variance, and the orthogonality and un-correlatedness are extras, which are included to ensure that the different components are measuring separate things. In contrast, independent component analysis (ICA) aims at the separation of components and begins with the vision of statistical independency (Jolliffe 2002; Shlens 2003).

$$P(\mathrm{x}_1, \mathrm{x}_2) = P(\mathrm{x}_1)\, P(\mathrm{x}_2) \tag{1.02}$$

where *P*() denotes the probability density. ICA model is,

$$\mathrm{x} = \mathbf{\Lambda}(f) \tag{1.03}$$

where $\mathbf{\Lambda}$ is some, not necessarily linear, function and the elements of f are independent. The components (factors) f are estimated by $\hat{f}$, which is a function of x and the family of functions from which $\mathbf{\Lambda}$ can be chosen must be defined.

1.4.3 POD – Advantages and applications

1.4.3.1 *Advantages*

The popularity of POD is due to the following essential properties.

a) It is the optimal (in terms of mean squared error) linear scheme for compressing a set of high dimensional vectors into a set of lower-dimensional vectors and then reconstructing the data.
b) The model parameters can be computed directly from the data.
c) Compression and decompression are easy operations to perform given the model parameters; they require only matrix multiplication.
d) POD is usually a robust solution (Shlens 2003) even to slightly deviated non-Gaussian data.

1.4.3.2 *Applications*

The apparent simplicity of the technique has made POD a widely used data handling technique in agriculture, biology, chemistry, climatology, demography, ecology, economics, food research, genetics, geology, meteorology, oceanography, psychology and quality control. It is now attracting the attention of concrete technologists and investigations are on in understanding behaviour of concrete and enhancement of concrete performance.

1.5 THESIS ORGANIZATION

The need, mode, method and potential of POD in concrete performance appraisal have been introduced with brevity in Chapter 1.

Chapter 2 presents a comprehensive review of relevant literature, research objectives and scope of the work. Chapter 3 outlines the methodology adopted to accomplish objectives set. Data analysis, results, critical observations, case-specific conclusions and application in computational mechanics have been put forward in Chapter 4. General conclusions drawn from the present research have been penned in Chapter 5. List of publications and References have been appended subsequently.

1.6 SUMMARY

The first chapter introduces POD and describes its potential in addressing the complexity of Concrete. At the chapter end, organisation of the research thesis has also been detailed.

CHAPTER 2
LITERATURE REVIEW

2.1 INTRODUCTION TO REVIEW

POD history, its mathematical background and literature related to application of POD (or PCA), factor analysis and cluster analysis in the field of concrete technology have been reviewed in this chapter. Essence of collected scientific works, motivation for this research, objectives and scope have been penned. Summary of the chapter has also been briefed.

2.2 POD – A BRIEF HISTORY

POD is one of the best multivariate techniques to reduce the dimensionality of data. Beltrami (1873) and Jordan (1874) developed singular value decomposition, which forms the basis of POD. Later, POD was independently developed by Pearson (1901) and Hotelling (1933).

Interestingly Pearson writes 'his method can easily be applied to numerical problems', even before 50 years of the widespread availability of computers. Although he mentions – the calculations become 'cumbersome' for four or more variables and suggest that they are quite feasible.

Hotelling derives it using Lagrange multipliers in 1933 (Hotelling 1933) and Power method in 1936 (Hotelling 1936). As per Jolliffe (2002), there has been only small amount of work from an application point of view for 25 years after Hotelling's paper. Widespread utilisation of electronic computers in 1960s, works of Anderson (1963), Rao (1964), Gower (1966) and Jeffers (1967) gave an impetus to tap the power of POD and bring out its value of practical application in the field of Science, Engineering and Technology (Jolliffe 2002; Liang et al. 2002).

2.2.1 POD – Mathematical background

A brief explanation of mathematical operations of matrix manipulations in POD is provided in this section.

Vector **x** (eq. 2.01) is a vector of p random variables $\subset \mathbb{R}$. Correlations between these variables are of fundamental interest, which are to be understood by their variances and co-variances.

$$\mathbf{x} = \begin{Bmatrix} x_1 \\ x_2 \\ \vdots \\ x_p \end{Bmatrix} \tag{2.01}$$

When the number of variables is limited, it is possible to observe all the variances, co-variances and correlations. When structure is complex, a technique to hold vital information by looking at a very few of the derived variables is of great help.

A first consideration in this direction is to seek a linear function of $\alpha_1^T\mathbf{x}$ (Eq. 2.02), of the elements of **x** with maximum variance. Here α_1 is a vector of p constants $\alpha_{11}, \alpha_{12}, .., \alpha_{1p}$ (i.e. $\alpha_{1(1\times p)}^T =< \alpha_{11}, \alpha_{12}, .., \alpha_{1p} >$). Superscript *T* denotes transpose.

$$\alpha_1^T\mathbf{x} = \alpha_{11}x_1 + \alpha_{12}x_2 + \ldots + \alpha_{1p}x_p = \sum_{j=1}^{p} \alpha_{1j}x_j \tag{2.02}$$

As subsequent logical step looking for another linear function α_2^Tx, uncorrelated with α_1^Tx that has a maximum variance, and so on so that the α_k^Tx is the *k*th linear function ($\widehat{\boldsymbol{D}}_k$) that is uncorrelated with previously derived (k – 1) terms; when considered yield p linear functions. Very generally, it is highly likely that much of the variance will be accounted by a few initial linear combinations.

If the majority of the variance gets captured by the first two combinations, the additional advantage of representation of data in two dimensions is possible. Even if the case is not so, consideration of consecutive component's linear function, two at a time, makes two-dimensional representations feasible. Consideration of the number of such representations can be based on predetermined targets on variation explanation.

In this research work, the vector random variable **x** has a known covariance matrix **Σ** (or correlation matrix ***R***, for normalized data). **Σ** would have,

$$\sigma_{ij} = \begin{cases} \text{Variance of } \mathbf{x} & \forall\ i = j \\ \text{Co} - \text{variance of } \mathbf{x} & \forall\ i \neq j \end{cases}$$

In a more realistic case, where **Σ** is unknown, replace **Σ** by sample covariance matrix **S**. It turns out that for k = 1, 2, . . . , p, the *k*th linear function is given by $\widehat{D}_k = \alpha_k^T\mathbf{x}$, where

α_k is an eigenvector of $\mathbf{\Sigma}$ corresponding to its *k*th largest eigenvalue λ_k. Furthermore, if α_k is chosen to have a unit length ($\alpha_k^T \alpha_k = 1$), then var($\widehat{\boldsymbol{D}}_k$) = λ_k, where var($\widehat{\boldsymbol{D}}_k$) denotes the variance of $\widehat{\boldsymbol{D}}_k$.

To derive the form of $\widehat{\boldsymbol{D}}_k$, consider first $\alpha_1^T \mathbf{x} = \widehat{\boldsymbol{D}}_1$. Variance of $\widehat{D}_1$ is,

$$\begin{aligned} E\left(\widehat{\boldsymbol{D}}_1^2\right) &= E(\widehat{\boldsymbol{D}}_1 \times \widehat{\boldsymbol{D}}_1) \\ &= E[(\alpha_1^T.\mathbf{x}) \times (\alpha_1^T.\mathbf{x})^T)] \\ &= \alpha_1^T.E(\mathbf{x}\mathbf{x}^T).\alpha_1 \\ &= \alpha_1^T \mathbf{\Sigma} \alpha_1 \end{aligned} \tag{2.03}$$

The maximization will not stand for finite α_1, so a normalization constraint must be enforced. The constraint is $\|\alpha_1\|$= 1, indicate $\alpha_1^T.\alpha_1 = 1$.

To maximize $\alpha_1^T \Sigma \alpha_1$ subject to $\alpha_1^T.\alpha_1 = 1$, the standard approach is to use the technique of Lagrange multipliers, $\mathcal{L}$ (Shalizi 2013). Maximize

$$\mathcal{L}(\alpha_1, \lambda) = \alpha_1^T \mathbf{\Sigma} \alpha_1 - \lambda(\alpha_1^T.\alpha_1 - 1) \tag{2.04}$$

where λ is a Lagrange multiplier. Differentiating with respect to α_1 gives

$$\mathbf{\Sigma}\alpha_1 - \lambda\alpha_1 = 0 \tag{2.05}$$

or

$$\left(\mathbf{\Sigma} - \lambda \mathbf{I}_p\right)\alpha_1 = 0 \tag{2.06}$$

where $\mathbf{I}_p$ is (p×p) identity matrix. Thus, λ is an eigenvalue of $\mathbf{\Sigma}$ and α_1 is the corresponding eigenvector. To decide which of the p eigenvectors gives $\alpha_1^T \mathbf{x}$ with maximum variance, note that the quantity to be maximized is

$$\alpha_1^T \Sigma \alpha_1 = \alpha_1^T \lambda \alpha_1 = \lambda \alpha_1^T \alpha_1 = \lambda \tag{2.07}$$

so λ must be as large as possible. Thus, α_1 is an eigenvector corresponding to the largest eigenvalue of $\mathbf{\Sigma}$, and var($\alpha_1^T \mathbf{x}$) = $\alpha_1^T \Sigma \alpha_1 = \lambda_1$, the largest eigenvalue.

In general, the *k*th $\widehat{\boldsymbol{D}}_k$ of $\mathbf{x}$ is $\alpha_k^T \mathbf{x}$ and var($\alpha_k^T \mathbf{x}$) = λ_k, where λ_k is the *k*th largest eigenvalue of $\mathbf{\Sigma}$, and α_k is the corresponding eigenvector.

The second $\widehat{\boldsymbol{D}}_2 (= \alpha_2^T \mathbf{x})$, maximizes $\alpha_2^T \mathbf{\Sigma} \alpha_2$ subject to being uncorrelated with $\alpha_1^T \mathbf{x}$, or equivalently subject to cov($\alpha_1^T \mathbf{x}, \alpha_2^T \mathbf{x}$) = 0, where cov(x, y) denoted the covariance between the random variable x and y. But

$$\text{cov}(\alpha_1^T \mathbf{x}, \alpha_2^T \mathbf{x}) = \alpha_1^T \mathbf{\Sigma} \alpha_2 = \alpha_2^T \mathbf{\Sigma} \alpha_1 = \lambda \alpha_2^T \alpha_1 = \lambda \alpha_1^T \alpha_2$$

Thus, any of the equations

$$\alpha_1^T \mathbf{\Sigma} \alpha_2 = 0; \quad \alpha_2^T \mathbf{\Sigma} \alpha_1 = 0; \quad \alpha_2^T \alpha_1 = 0; \quad \alpha_1^T \alpha_2 = 0$$

could be used to specify zero correlation between $\alpha_1^T \mathbf{x}$ and $\alpha_2^T \mathbf{x}$. Applying above condition and normalization constraint ($\|\alpha_2\| = 1$) again, maximize

$$\mathcal{L}(\alpha_1, \lambda, \phi) = \alpha_2^T \mathbf{\Sigma} \alpha_2 - \lambda(\alpha_2^T . \alpha_2 - 1) - \phi \alpha_2^T . \alpha_1 \tag{2.08}$$

where λ, ϕ are Lagrange multipliers. Differentiating with respect to α_2 gives,

$$\mathbf{\Sigma} \alpha_2 - \lambda \alpha_2 - \phi \alpha_1 = 0 \tag{2.09}$$

and multiplication of this equation on the left by α_1^T gives,

$$\alpha_1^T \mathbf{\Sigma} \alpha_2 - \lambda \alpha_1^T \alpha_2 - \phi \alpha_1^T \alpha_1 = 0 \tag{2.10}$$

which, since first two terms are zero and $\alpha_1^T \alpha_1 = 1$, reduces $\phi = 0$. Therefor

$$\mathbf{\Sigma} \alpha_2 - \lambda \alpha_2 = 0 \tag{2.11}$$

or equivalently

$$(\mathbf{\Sigma} - \lambda \mathbf{I}_p) \alpha_2 = 0 \tag{2.12}$$

So λ is once more an eigenvalue of $\mathbf{\Sigma}$, and α_2 the corresponding eigenvector. Again, $\lambda = \alpha_2^T \mathbf{\Sigma} \alpha_2$, so λ is to be as large as possible. Assuming that $\mathbf{\Sigma}$ does not have repeated eigenvalues, a complication, λ cannot equal λ_1. If it did, it follows that $\alpha_1 = \alpha_2$, violating the constraint $\alpha_1^T \alpha_2 = 0$. Hence λ is the second largest eigenvalue of $\mathbf{\Sigma}$, and α_2 is the corresponding eigenvector.

As stated above, it can be shown that for third, fourth, . . . , *p*th linear functions, the vectors of coefficients $\alpha_3, \alpha_4, .., \alpha_p$ are the eigenvectors of $\mathbf{\Sigma}$ corresponding to $\lambda_3, \lambda_4, .., \lambda_p$, the third and fourth largest, . . . , and the smallest eigenvalue, respectively. Furthermore,

$$\text{var}(\alpha_k^T \mathbf{x}) = \lambda_k \quad \text{for } k = 1, 2, 3, \ . \ . \ ., p \tag{2.13}$$

Computation of these linear functions reduce to solution of an eigenvalue–eigenvector problem for a positive-semi-definite symmetric matrix ($\boldsymbol{R}$ or $\mathbf{\Sigma}$). Its general form is,

$$(\mathbf{\Sigma} - \lambda \mathbf{I}_p) \alpha = 0 \tag{2.14}$$

The eigenvalues are arranged in descending order so as to identify the eigenvector contributing maximum variation.

$$\lambda_1 > \lambda_2 > \lambda_3 > \lambda_4 > \ldots > \lambda_{p-1} > \lambda_p \tag{2.15}$$

Data Projection

Consider

$$\widehat{\boldsymbol{D}}_j = \alpha_j^T \mathbf{x} = \mathbf{x}^T \alpha_j \tag{2.16}$$

where $j = 1, 2, \ldots, p$

Now the interest is to synthesize data given as a set of $\widehat{\boldsymbol{D}}_j$

Define $\boldsymbol{A} = [\alpha_1, \alpha_2, \alpha_3, .., \alpha_p]$

and $\widehat{\boldsymbol{D}} = \left[\widehat{D}_1, \widehat{D}_2, \widehat{D}_3, \ldots, \widehat{D}_p\right]^T$

$$\widehat{\boldsymbol{D}} = \left[\alpha_1^T \mathbf{x}, \alpha_2^T \mathbf{x}, \alpha_3^T \mathbf{x}, \ldots, \alpha_p^T \mathbf{x}\right]^T \tag{2.17}$$

$$\widehat{\boldsymbol{D}}_{(p\times n)} = \boldsymbol{A}^T_{(p\times p)} \boldsymbol{X}_{(p\times n)} \tag{2.18}$$

Pre-multiplying both sides by $\boldsymbol{A}$,

$$\boldsymbol{A}\widehat{\boldsymbol{D}} = \boldsymbol{X} \tag{2.19}$$

$$\boldsymbol{X} = \sum_{j=1}^{p} \alpha_j \widehat{\boldsymbol{D}}_j \tag{2.20}$$

Now dimensionality reduction can be forced by selecting initial few eigenvalues, $\lambda_1, \lambda_2, \lambda_3, \lambda_4, \ldots, \lambda_{m-1}, \lambda_m$, and corresponding eigenvectors. Here $m \ll p$. After truncating the insignificant values,

$$\widehat{\boldsymbol{X}} = \sum_{j=1}^{m} \alpha_j \widehat{\boldsymbol{D}}_j \tag{2.21}$$

$$\widehat{\boldsymbol{X}} = [\alpha_1 \quad \alpha_2 \quad \alpha_3 \quad \alpha_4 \quad \ldots \quad \alpha_m] \begin{bmatrix} \widehat{D}_1 \\ \widehat{D}_2 \\ \widehat{D}_3 \\ \widehat{D}_4 \\ \vdots \\ \widehat{D}_m \end{bmatrix} \tag{2.22}$$

$$\widehat{\boldsymbol{X}} = [\widehat{\boldsymbol{A}}][\widehat{\boldsymbol{D}}] \tag{2.23}$$

Eigenvalue decomposition brings out a set of eigenvectors (α) of the covariance matrix (or correlation matrix), and vector capturing maximum variance will have the largest eigenvalue λ. Coefficients of eigenvector speak loading of variables in that dimension. $\sqrt{\lambda}\alpha$ and $\alpha^T \mathbf{x}$ give the projection of variables and individual coordinates on the

corresponding dimension respectively. Since orthogonal dimensions are derived from variables, term $\sqrt{\lambda}\alpha$ is referred to as component(s) and coefficients of projected individual observations as scores (Husson et al. 2017).

POD on a non-square matrix ($\boldsymbol{X}$) is also possible by singular value decomposition (SVD). The basic structure of SVD is

$$\boldsymbol{X} = \boldsymbol{U}\boldsymbol{\Lambda}\boldsymbol{V}^T \tag{2.24}$$

where $\boldsymbol{U}$ and $\boldsymbol{V}$ are right and left singular matrices respectively, which rotate the $\boldsymbol{X}$ matrix. $\boldsymbol{\Lambda}$ contains singular values and speak of magnitude of scale.

2.3 POD FOR PERFORMANCE APPRAISAL OF CONCRETE

Availability of plenty of computational techniques and advancement in computer capabilities have given a chance to study concrete and its cardinal properties in much more detailed manner at both analysis and design stage. Complexity of concrete has not made it possible to predict the relationship between microstructural characteristics and its properties only using analytical models (Boukhatem et al. 2011b).

2.3.1 Computational techniques for handling big data

Decomposition techniques (Jolliffe 2002; Liang et al. 2002), machine learning (ML) algorithms and multivariate statistical approaches have proved themselves to be the best techniques in resolving the big data issues, where generation of analytical models is a difficult task. Computer simulations, artificial neural network (ANN), ML techniques (Boukhatem et al. 2011b) are the current trends in predicting and understanding systems. Atmospheric science (Chávez-Arroyo et al. 2013), weather forecasting (Jaruszewicz and Mandziuk 2002; Ogallo 1989), image processing (Ng 2017) and human behavioural prediction (Raskin and Terry 1988) are the branches of Science that extensively use these techniques to draw conclusions.

Vast data on concrete is available for usage and implementation of computational techniques for development of models and simulations.

2.3.2 Data science in concrete technology

Statistical methods for studies on properties of concrete (Filho et al. 2010) and math models for strength have been proposed adopting ANN in combination with genetic algorithm (GA) considering cement content, cement type, phase composition, chemical

analysis parameters, fineness and soundness of cement, water-cement ratio, aggregate shape and size, fineness modulus of fine aggregates, sand to coarse aggregate ratio, admixture dosage, cube density, curing conditions, slump value, ultrasonic pulse velocity value (Kheder et al. 2003; Lee 2003; Madandoust et al. 2010; Ni and Wang 2000) as variables influencing characteristics of concrete. Regression for tensile strength (Ahmed et al. 2016) and long term strength variation calculations (Aggarwal et al. 2015; Yi et al. 2005), non-linear regression for activation energy and heat of hydration quantification (Folliard et al. 2008; Riding et al. 2012), response surface methodology (RSM) for optimization of silica fume content of ultra-high performance fibre reinforced concrete (Aldahdooh et al. 2013), ANN for determination of dimensional variation due to drying shrinkage (Bal and Buyle-Bodin 2013), multi-variable regression and GA technique for elastic moduli and tensile strength prediction (González-Taboada et al. 2016) and meta-modelling for carbonation front depth calculation (Ta et al. 2016) are few of the research attempts in this direction.

ML techniques are highly efficient in addressing complex physical and chemical phenomenon of deterioration of reinforced concrete over conventional prediction models (Taffese and Sistonen 2017). For addressing durability and serviceability issues in existing structures state of the art of data acquisition and processing facilities have popularised ML techniques. Stochastic approaches have also been employed in life cycle assessment (Pan et al. 2017; Trejo et al. 2017).

Concrete technology provides huge opportunities for employment and exploitation of big data analytics (Newlands 2019).

2.3.3 Analytical tools in concrete performance appraisal

Principal component analysis (PCA), factor analysis, cluster analysis, ANN, GA, fuzzy logics have all been considered and adopted in performance appraisal of concrete to analyse experimental data, noise reduction of data acquired, prediction and projection math modelling, durability studies and failure forensics.

2.3.3.1 Historical monument forensics

There are some structural investigations of historical monuments which have used PCA techniques to draw inferences.

For classification of mortars from Byzantine and Ottoman monuments (Moropoulou et al. 2003) into distinct groups based on physicochemical characteristic tests, feature extraction of mortars of churches St. Lorenzo (Milan) and St. Abbondio (Como) (Rampazzi et al. 2006) with the aid of chemo-metric analysis, the method of PCA has been employed. Further, score and loading plots of PCA has been utilized along with least square regression to predict binder-aggregate ratio and to differentiate hydraulic and aerial binders (Rampazzi et al. 2006).

Using cluster analysis and PCA, similar work has been reported for Quadrangular tower of the Balivi Complex in Aosta (Italy) (Arizio et al. 2013). Decision to choose number of specimens for mortar characterization and number of tests for determination of binder fraction and sulphate fraction had been made based on these techniques. Some statistical studies on characterization of monumental structures are available.

PCA has been adopted to correlate variables for checking composition of hardened concrete samples from a narrow-gauge railway viaduct in Braine-l'Alleud (Belgium), built in 1904 by Hennebique company (Hellebois et al. 2013). This study emphasises the need for extensive representative data in failure forensics.

2.3.3.2 Experimental data analysis

Math modelling for varieties of concrete has been attempted to develop statistical prediction models (Chou et al. 2011). ANN (Boukhatem et al. 2012; Kellouche et al. 2017), data mining (Chou et al. 2015), RSM (Aldahdooh et al. 2013), regression (Aggarwal et al. 2015) and other statistical techniques have been used as tools to estimate the strength of concrete, having different variable sets from the experiments. Only basic descriptive statistical inferences have been used (Filho et al. 2010) for evaluation and comparison of self-compacting concrete properties variability with code recommendations.

The efficacy of modelling with dimensionality reduction technique has been demonstrated by a study on concrete with different mineral admixtures (Boukhatem et al. 2011a, 2012).

Improved predictability has been reported when ANN is used for slump and strength modelling, multiple regression for computing shear strength, in combination with PCA.

PCA has also been incorporated in assessing performance of application sealants and fillers in asphalt concrete pavement cracks (Li et al. 2017).

Combined PCA and self-organization feature map (SOFM) – a hybrid model to determine the pull-off adhesion between concrete layers, has reduced the number of input variables as well as improved the precision of prediction (Sadowski et al. 2015).

PCA and PLS-DA (partial least square-discriminant analysis) have been used to build hyperspectral image technology model to detect presence of mortar paste attached to recycled aggregate surface (Bonifazi et al. 2018).

PCA has been employed to interpret experimental data, and recognised relationships have been confirmed (Manoj and Babu Narayan 2019; Manoj and Narayan 2021).

2.3.3.3 Output analysis of acoustic emission test

PCA and K mean clustering have been adopted in environmental noise removal and suppression in AE (structural health monitoring) data of long time corrosion monitoring of a pre-damaged post-tensioned concrete beam (Calabrese et al. 2012). PCA to reduce the dimensionality of AE data in CFRP-retrofitted RC slabs (Degala et al. 2009), to characterise the acoustic behaviour of concrete made with crumb rubber waste (Ghizdăveț et al. 2016) and cluster analysis to group the AE data of hydration of cement (Thirumalaiselvi and Sasmal 2019) has also been attempted.

2.3.3.4 Damage analysis

POD, a generalized method of PCA, has been effectively employed in damage detection and analysis (Al-Ghalib and Mohammad 2016; Gryllias et al. 2009; Santos et al. 2016). The power of PCA has been exploited in development of damage indices for quantification of concrete structure conditions. In terms of the existence of damage and its corresponding severity, different rebar conditions have been classified with the assistance of PCA (Lu et al. 2013). It has also been used in identifying the correlation between the considered damage parameters and microstructural feature assessment (Gulotta et al. 2015).

2.3.3.5 Durability

Efforts have been made towards development of regression models with PCA for physical properties and durability characteristics of different cement mortars (Falchi et al. 2015), assessment of durability and service life of reinforced concrete structures by

utilisation of ML techniques (Taffese and Sistonen 2017) and PCA based evaluation of sealants and fillers for cracks in asphalt concrete pavements (Li et al. 2017).

The need for standardised testing of input parameters has being accentuated for reliable service life prediction of RC structures considering corrosion aspect (Trejo et al. 2017). Studies on durability aspects using POD method are found to be limited.

A beginning has been made in understanding and implementing the usage potential of data analytics in Concrete technology. There also is a tremendous need and scope for employment of POD in reorganising, rationalising available data for formulation of math models in concrete technology.

2.4 ESSENCE OF LITERATURE REVIEW

From the literature review, it is evident that decomposition techniques are,

a) Very useful to understand the compatibility of new materials in restoration of historical structures (for reconstruction of original material).
b) Helpful in relating results drawn with microstructural properties (SEM) of mixes.
c) Valuable in drawing inference on causal-effect relations of material behaviour.
d) Useful to develop models to evaluate performance characteristics of different varieties of concrete.
e) Suitable in acoustic emission test noise removal and suppression.

Dependence, interdependence and independence of variables can very clearly be understood, vital variables can be identified and system's behaviour can be modelled by limiting consideration to variables that significantly influence the behaviour without compromise on prediction capability/loss of information by utilizing POD.

2.5 RESEARCH MOTIVATION

Concrete has come a long way from its days of plain cement concrete through reinforced concrete, pre-stressed concrete, structural light weight concrete, high-density concrete, high strength concrete, regulated sleeping concrete, high-performance concrete, self-compacting concrete, fibre reinforced concrete . . .. The attributes still are challenging for understanding and attainment of contemplated characteristics as the number of variables that dictate the performance are too many. POD should help the analyst in this onerous task and should serve as a decision-making tool.

2.6 RESEARCH GAPS

Based on review of literature, following research gaps have been identified.

a) Hierarchizing the influence of variables on wet and set concrete properties has hardly been attempted.
b) POD is of utility as an immensely powerful tool in hierarchizing, that needs attention of concrete technologists.
c) Whole-to-part and part-to-whole exploration of complex concrete data, utilizing POD technique can help in recognising and understanding unknown cause-effect relations and gaining valuable insights. This possibility needs consideration and exploitation.
d) Assessment of existing models of concrete performance and their refinement has tremendous scope for utilization of POD.

2.7 RESEARCH OBJECTIVES

The present research aims at,

1. Decomposing and hierarchizing the parameters affecting workability, strength, durability of concrete.
2. Utilizing POD in performance appraisal.
3. Application in selection of appropriate math models suitable for projection of performance with available dataset.

2.8 SCOPE

This research is an attempt to investigate

a) Utilization of POD to identify significant parameters affecting concrete performance.
b) Possible dimensionality reduction and proposition of performance index based on vital variables identified.
c) POD application in refinement to concrete modelling techniques in performance based design.

2.9 SUMMARY

A detailed account of relevant literature has been presented and the research gaps, objectives and scope have been outlined in this chapter.

CHAPTER 3

POD – FOR REORGANISATION, RATIONALISATION AND REDUCTION OF DIMENSIONALITY

3.1 OVERVIEW

This chapter covers in detail the methodology adopted to accomplish set objectives. Fig. 3.01 provides sequential steps to be followed while performing POD (Jolliffe 2002; Liang et al. 2002).

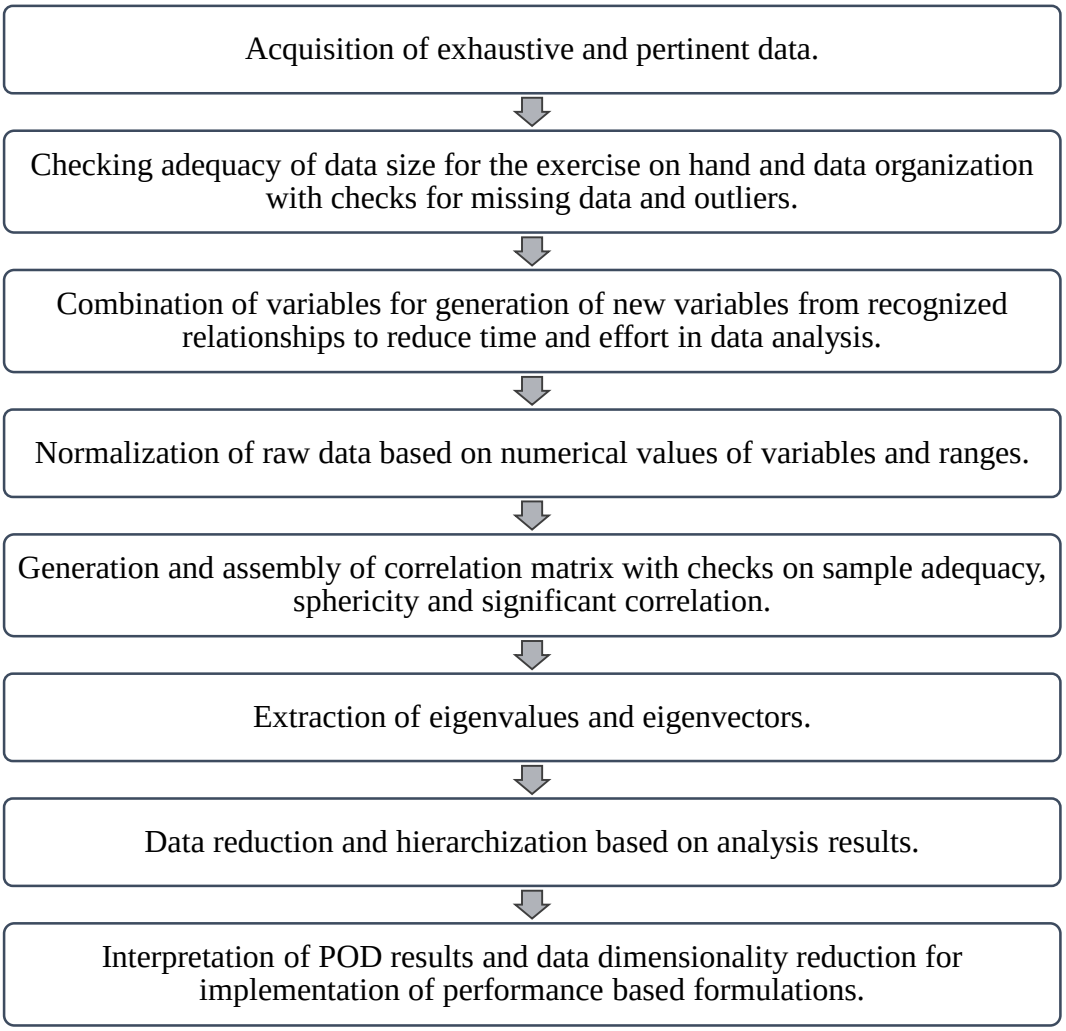

Figure 3.01 Steps in POD

3.2 DESCRIPTION OF METHODOLOGY

Following sub-sections elaborate the sequential steps provided in Fig. 3.01.

3.2.1 Data acquisition

Relevant data acquisition is the first step in POD. Preferably datasets should be exhaustive, encompassing a large number of observations for variables to capture cause-effect relations. For the present investigation, details of data employed are given in Table 3.01.

Table 3.01 Sources of data sets analysed by POD in the present investigation

Sl.No.	Source	Source type	Description
01.	Pradeep et al. (2012)	Thesis	Experimental data on concrete 28 days compressive strength and slump characteristics.
02.	Yaragal et al. (2010)	Journal article	Studies on normal strength concrete cubes subjected to elevated temperatures.
03.	Lavanya (2018)	Thesis	An experimental investigation on properties of high strength self-compacting concrete mixes.
04.	Rejilin (2018)	Thesis	Strength and durability properties of geo-polymer concrete
05.	Dhir et al. (2010)	Technical report	Innovative cement combinations for concrete performance.
06.	Poole (2007)	Thesis	Modeling temperature sensitivity and heat evolution of concrete.

3.2.2 Testing and data re-organisation

3.2.2.1 *Data structure*

Checking data structure and classification of variables to quantitative and qualitative subsets are the initial steps in data reorganisation.

3.2.2.2 *Missing values*

POD demands completeness in data matrix before testing and generation of correlation values. Variables with incomplete observations and missed values have been excluded from the analysis.

3.2.2.3 *Outlier detection*

Outliers are identified from boxplots (Krzywinski and Altman 2014). In this investigation for all the datasets, no exclusion of outliers has been attempted to make

comparisons of interpretations from the current investigation with findings of the studies from which data has been sourced.

3.2.2.4 *Bartlett sphericity test*

'Bartlett sphericity test' (Bartlett 1950; Tobias and Carlson 1969) is used as a measure of the extent of deviation from the reference situation – determinant of correlation matrix being 1, to foresee the possibility of dimensionality reduction. Though not essential, sphericity test can suggest the scope and extent of dimensionality reduction possible. The test statistic under H_0 is,

$$\chi^2 = -\left(N - 1 - \frac{2P + 5}{6}\right) \times |\boldsymbol{R}| \tag{3.01}$$

following an χ^2 distribution with a [$P \times (P - 1) / 2$] degree(s) of freedom. The Null hypothesis, H_0 = Determinant is 1, indicate '$\boldsymbol{R}$ 'is an identity matrix or off-diagonal terms are zero, meaning variables are unrelated and unsuitable for structure detection.

3.2.2.5 *Descriptive statistics*

Arithmetic mean (average), standard deviation, minimum and maximum values have been looked into to understand data. A data matrix plot is also included for the first dataset to visualize the scatter.

3.2.3 Variables generation

Variables have been combined for generation of new variables from recognized and established relationships to reduce data analysis efforts.

3.2.4 Data normalization

To avoid bias, mean centring and variance scaling normalisation (Eq. 3.02) has been performed, since datasets include a heterogeneous mixture of variables with different measuring units and scales.

$$z_{ij} = \left(\frac{x_{ij} - \bar{x}_j}{\sigma_j}\right) \tag{3.02}$$

where,

z_{ij}= Normalized value of variable

x_{ij}= Original variable value

$\bar{x}_j$= Variable mean

σ_j= Standard deviation of variable

$$\sigma_j = \sqrt{\frac{1}{N}\sum_{i=1}^{N}\left(x_{ij} - \bar{x}_j\right)^2} \tag{3.03}$$

N = Total number of observations

3.2.5 Correlation matrix generation

Correlation matrix can be used to analyse dependence, interdependence and independence between variables. Eq. 3.04, gives expression to compute correlation between any two variables.

$$r_{ij} = \frac{N\sum\left(x_i x_j\right) - \left(\sum x_i\right)\left(\sum x_j\right)}{\sqrt{\left[N\Sigma x_i^2 - (\Sigma x_i)^2\right]\left[N\Sigma x_j^2 - \left(\Sigma x_j\right)^2\right]}} \tag{3.04}$$

where r_{ij} is correlation value between i^{th} and j^{th} variables.

Correlation coefficient indicates nature and degree of linear relationship between two variables considered.

To decide *significance of correlation*, two-tail T-test has been used. Consider,

Null hypothesis, H_0: $r = 0$

Alternate hypothesis, H_1: $r \neq 0$

Null hypothesis indicates correlation value is not significantly different from zero, and there is no significant linear relationship between variables tested. Alternate hypothesis indicates correlation value is significantly different from zero, and there is a significant linear relationship between variables tested.

Based on the number of observations (N), significant correlation values can be found from the T-test statistic (Eq. 3.05) for prefixed significance level norms or a minimum value of |±0.7| (Jeffers 1967) is considered for identifying important correlation. For the test, the level of significance (α) has been set to 95%. Degree of freedom (DF) for two–tail T–test is (N – 2).

$$t_{\alpha,N-2} = \frac{r\sqrt{N-2}}{\sqrt{1-r^2}} \tag{3.05}$$

On rearranging,

$$\text{Significant correlation, } r = \sqrt{\frac{t_{\alpha,N-2}^2}{t_{\alpha,N-2}^2 + N - 2}} \tag{3.06}$$

Table 3.02 Critical correlation values

N	$r_{significant}$	$r_{critical}$
6	0.81	0.81
7	0.75	0.75
8	0.71	0.71
9	0.67	0.70
≥10	≤0.63	0.70

Higher among the value computed and literature suggested minimum value is deemed to be critical correlation. Critical absolute correlation values calculated from both the criterion are listed in Table 3.02. The critical correlation is one of the norm considered in identifying significant variables affecting target characteristics.

3.2.6 Orthogonal decomposition

POD is performed on the correlation matrix ($\boldsymbol{R}$) to obtain a set of eigenvalues and eigenvectors (λ_j, v_j). Eigenvectors obtained are the linear combination of initial variables. Eigenvalues (λ_j) account the amount of variation explained by each dimension and eigenvectors indicate direction of components.

$$(\boldsymbol{R} - \lambda \mathbf{I}_P)v = 0 \tag{3.07}$$

Coefficients of eigenvector are indicators of influence of variables (vector loading), and those variables with large absolute magnitude are deemed as significant.

3.2.7 Dimensionality reduction

Dimensionality reduction of data employs scree plot (elbow plot) and Pareto chart. Percentage variation captured by *j*th component is calculated as,

$$\frac{\lambda_j}{\sum_{j=1}^{P} \lambda_j} \times 100 \tag{3.08}$$

where λ_j is the jth eigenvalue and p is the total number of components.

Number of components to be included for performance appraisal is judiciously decided by prefixing the percentage variation to be captured by the components considered.

3.2.8 POD results interpretation

Variable coordinates of new orthogonal space constructed by principal components/ dimensions (D_j) are computed as a product of square root of eigenvalue and corresponding eigenvector.

$$D_j = \sqrt{\lambda_j} v_j \tag{3.09}$$

Plotting orthogonal components D_j, two at a time against each other, gives "component plot", which is of immense help in identifying, classifying important and unimportant variables and their effect on target characteristics. Further analysis can be limited to reduced dimensions. "Component plot" is also sometimes called "correlation plot".

Quality of representation of a variable on a component can be measured by the distance between the point within the space and the projection on the component of interest (Husson et al. 2017). In reality, it is preferred to calculate the percentage of contribution of variables on components. Square of component coefficients quantify the quality of representation (Q_j) of variables in a specific component. These can also be graphically presented, as exemplified in Fig. 4.03.

High Q_j values represent a good representation of variables on that component, and such variables are close to the circumference of the component plot (see Fig. 4.08). Variables away from circumference and near the centre of component plot depict that such variables do not contribute significantly to variation in those dimensions and possibly be well defined in dimensions that are not under consideration. The contribution of a variable to a specific component variation (in percentage) is given by,

$$\text{Variable Contibution} = \frac{Q_j}{\sum_{j=1}^{P} Q_j} \times 100 \tag{3.10}$$

Generally, variables that are highly correlated with first two components (i.e. D_1 and D_2) are the most important in explaining variability in data decomposed.

3.2.9 Performance index and charts for design

Orthogonal components can be used to develop mathematical models for prediction of characteristics of concrete. In this work, one such model has been proposed to quantify performance level indicator for the target characteristic. Design charts have been developed and proposed based on the performance index.

3.3 WORKING ENVIRONMENT

In the present investigation, all data analyses by POD have been performed in "RStudio".

3.4 SUMMARY

In this chapter, details on data collection, organization, testing, decomposition and dimensionality reduction have been explained comprehensively.

CHAPTER 4
POD APPLICATIONS IN VARIED CONTEXTS – ANALYSIS, RESULTS AND DISCUSSION

4.1 GENERAL

Amenability of POD in a wide and varied range of situations of data handling has been attempted and details of analysis, interpretation of analysis results, utility in addressing the specific situation have been described in the following sections.

Understanding workability and strength characteristics, performance appraisal of concrete at elevated temperatures, evaluation of high strength self-compacting concrete, assessment of long term behavioural aspects of geo-polymer concrete in aggressive environment, performance-based design of concrete by innovative cement combinations and comparison of models for early-age cracking of concrete, have been considered as specific cases for investigation.

4.2 CONCRETE WORKABILITY AND STRENGTH CHARACTERISTICS

As a first exercise of POD in establishing dependence, interdependence and independence of variables in influencing workability and strength characteristics, an available dataset has been subject to analysis.

4.2.1 Data – Source and pre-processing

1. Source: Pradeep et al. (2012)

Mix design details are pertaining to experimentations at National Institute of Technology Karnataka, Surathkal. Variables considered in the mix design and testing have been listed in Table 4.01.

2. Total number of variables: 10 Quantitative + 5 Qualitative = 15 Variables.

Among ten quantitative variables, original variables are compressive strength, slump, cement content, water content, fine aggregate and coarse aggregate. The remaining four variables are synthetic variables generated to assist interpretation of analysis results. Variation of compressive strength and slump have been investigated with reference to other listed variables.

Table 4.01 List of variables considered in data on concrete workability and strength characteristics

Quantitative variables	Symbols	Qualitative variables (Class)
1. Compressive strength	CS	1. Name of observations
2. Slump	Sl	2. Strength category (Cat_Str)
3. Cement	C	(*Low* (*LS*), *medium* (*MS*),
4. Water/Cement	W/C	*high* (*HS*))
5. Water	W	3. Strength (*0-20, 20-30, 30-40, 40-50 MPa*)
6. Fine aggregate	FA	
7. Coarse aggregate	CA	4. Slump (*Very low*, *low*, *medium*, *high*, *very high*)
8. Fine aggregate/Cement	FA/C	
9. Coarse aggregate/Cement	CA/C	5. Cement (*Low*, *medium, high*)
10. Cement/(Total aggregate)	C/(FA+CA)	

3. Total number of observations (Individuals)**:** 97

4. Matrix size of quantitative data: 97×10

5. Missing values: This dataset has no missing values.

6. Bartlett sphericity test

χ^2 = 2628.95

DF = 45

Probability value $\cong 2.22\times10^{-16} < 0.05$

Reject the null hypothesis. Dataset is not spherical and is accepted for analysis by POD.

7. Descriptive statistics: Table 4.02 describes the basic statistics of variables considered in the experiments conducted on concrete compressive strength and slump.

4.2.2 Correlation matrix and data matrix plot

1. Standardization of data

Mean centring and variance scaling normalisation has been performed before deriving correlation matrix. Table 4.03 presents correlation matrix of the dataset. Coefficient of correlation matrix reveals the measure of linear dependency of each variable with another.

Table 4.02 Descriptive statistics of data on concrete workability and strength characteristics

Variables	Units	Mean	SD	Minimum	Maximum
CS	N/mm^2	35.86	7.69	17.30	46.70
Sl	mm	54.19	29.49	10.00	120.00
C	kg/m^3	391.46	43.87	259.00	470.00
W/C	Ratio	0.49	0.05	0.40	0.60
W	lt/m^3	188.08	10.15	155.40	198.00
FA	kg/m^3	616.91	79.47	456.50	707.62
CA	kg/m^3	1178.71	101.52	1056.02	1335.60
FA/C	Ratio	1.60	0.29	1.10	2.64
CA/C	Ratio	3.07	0.56	2.27	5.04
C/(FA+CA)	Ratio	0.22	0.03	0.13	0.27

Table 4.03 Correlation matrix of data on concrete workability and strength characteristics

$\mathbf{x}_i$	CS	Sl	C	W/C	W	FA	CA	FA/C	CA/C	C/(FA+CA)
CS	1	0.22	0.69	-0.65	0.31	-0.07	-0.27	-0.52	-0.58	0.70
Sl	0.22	1	0.21	0.09	0.68	0.73	-0.80	0.31	-0.51	0.26
C	0.69	0.21	1	-0.91	0.55	0	-0.41	-0.70	-0.90	0.98
W/C	-0.65	0.09	-0.91	1	-0.16	0.26	0.15	0.79	0.71	-0.88
W	0.31	0.68	0.55	-0.16	1	0.47	-0.66	-0.13	-0.73	0.54
FA	-0.07	0.73	0	0.26	0.47	1	-0.75	0.69	-0.31	-0.01
CA	-0.27	-0.80	-0.41	0.15	-0.66	-0.75	1	-0.21	0.74	-0.50
FA/C	-0.52	0.31	-0.70	0.79	-0.13	0.69	-0.21	1	0.45	-0.69
CA/C	-0.58	-0.51	-0.90	0.71	-0.73	-0.31	0.74	0.45	1	-0.92
C/(FA+CA)	0.70	0.26	0.98	-0.88	0.54	-0.01	-0.50	-0.69	-0.92	1

Note: Significant correlation values ≥ |±0.7|, have been shown with coloured boxes.

Data matrix plot shown in Fig. 4.02 helps understand correlations between variables graphically. The plot provides a graphical explanation for dependence, interdependence and independence.

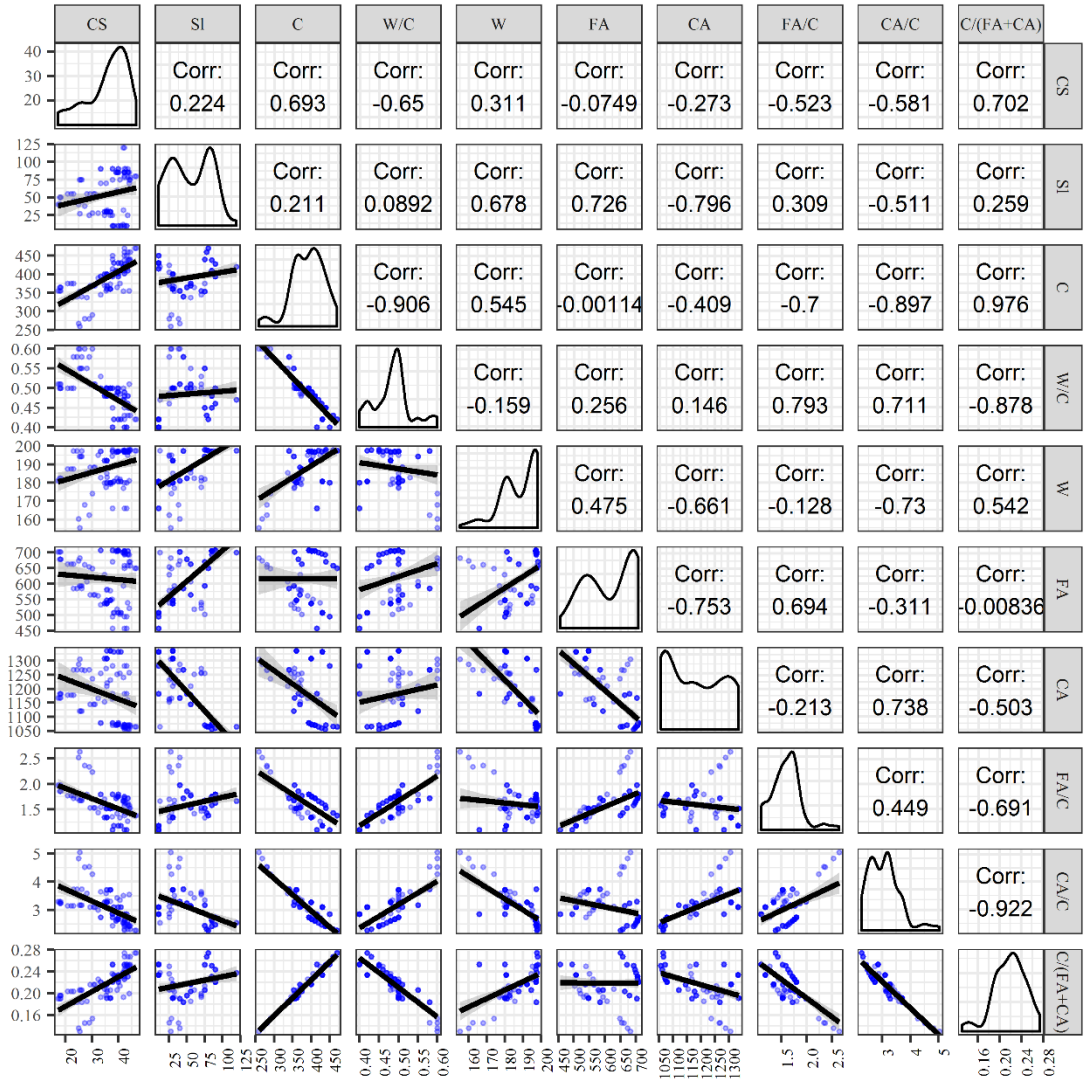

Figure 4.01 Data matrix plot

Correlation values in Table 4.03 (or data matrix plot in Fig. 4.01) indicate, 28 days' compressive strength of concrete is most strongly correlated to cement to aggregate ratio and next to cement content. In contrast, for slump, the strong correlations are with fine and coarse aggregate quantities.

4.2.3 Performing orthogonal decomposition of correlation matrix of experimental data on concrete compressive strength and slump characteristics

Eigenvalues and eigenvectors obtained after decomposition have been given in Tables 4.04 and 4.05, respectively. Along with component eigenvalues, Table 4.04 include details on percentage variation explained by each component and cumulative variation explained by the successive components.

Table 4.04 Eigenvalues of data on concrete workability and strength characteristics

Dimensions	1	2	3	4	5	6	7	8	9	10
λ_i	5.36	3.24	0.54	0.48	0.21	0.14	0.03	0.00	0.00	0.00
Var. %	53.61	32.38	5.35	4.85	2.10	1.42	0.27	0.01	0.01	0.00
Cum. Var. %	53.61	85.99	91.34	96.19	98.29	99.70	99.98	99.99	100	100

From Table 4.04, it is observable that eigenvalue for first component is highest, and explanation is around 54% of variation in the data. Dimensions 1 and 2 together explain about 86 % of variation in the data, signifying that with only 14% information loss, a 10-dimensional problem can be reduced to a 2–dimensional problem. Further addition of subsequent dimensions does not contribute to information extraction vitally; instead, it intricates the visualisation. It can also be seen from Fig. 4.02 that the gradient of the line has a dramatic change beyond Component 3. Beyond 3rd dimension, the slope is insignificant, suggesting that first 2 components explain major part of data variation.

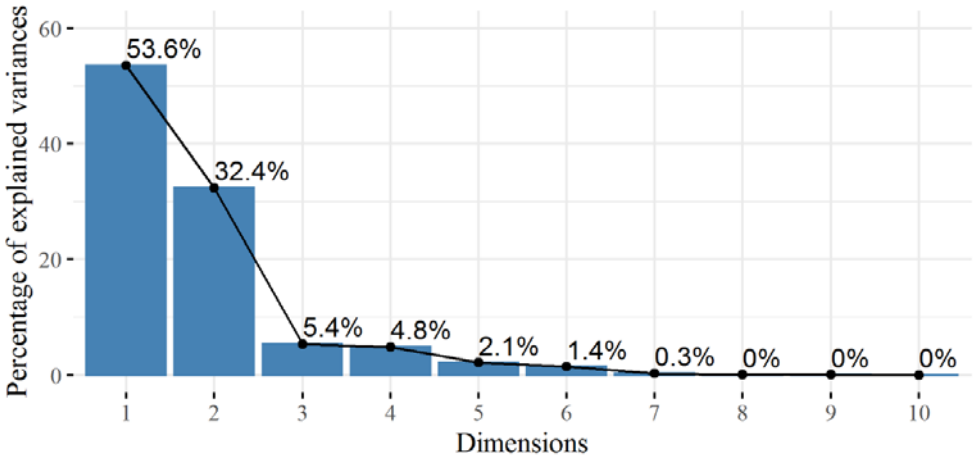

Figure 4.02 Scree plot

The eigenvectors (which are unit vectors) tabulated in Table 4.05 give direction of components in transformed orthogonal space. Coefficients of eigenvector indicate loading of each variable to variation in that component. Eigenvalues and vectors can be put together as components.

Table 4.05 Eigenvectors of data on concrete workability and strength characteristics

$\mathbf{x}_i$	v_1	v_2	v_3	v_4	v_5	v_6	v_7	v_8	v_9	v_{10}
CS	0.32	-0.13	0.62	0.62	0.24	-0.19	-0.09	-0.03	0.01	0.01
Sl	0.19	0.44	0.03	0.36	-0.55	0.57	0.05	-0.02	-0.01	0.01
C	0.41	-0.13	-0.04	-0.16	0.23	0.25	0.42	-0.23	0.34	-0.58
W/C	-0.34	0.29	-0.21	0.35	-0.01	-0.36	0.25	-0.21	0.62	0.08
W	0.30	0.26	-0.63	0.35	0.42	-0.09	-0.02	0.10	-0.37	-0.04
FA	0.08	0.51	0.22	-0.28	0.45	0.22	-0.18	0.39	0.35	0.20
CA	-0.27	-0.39	-0.13	0.21	0.36	0.60	0.00	-0.24	0.08	0.39
FA/C	-0.25	0.43	0.31	-0.15	0.23	-0.01	0.34	-0.51	-0.46	0.03
CA/C	-0.42	-0.08	0.11	0.20	0.07	0.12	0.50	0.64	-0.16	-0.25
C/(FA+CA)	0.42	-0.11	-0.01	-0.14	-0.11	-0.13	0.59	0.13	0.00	0.63

Component coordinates D_j and quality of representation of variables Q_j values of concrete workability and strength data are presented in Tables 4.06 and 4.07 respectively.

Table 4.06 Component coordinates of data on concrete workability and strength characteristics

$\mathbf{x}_i$	D_1	D_2	D_3	D_4	D_5	D_6	D_7	D_8	D_9	D_{10}
CS	0.73	-0.23	0.46	0.43	0.11	-0.07	-0.01	0.00	0.00	0.00
Sl	0.45	0.79	0.02	0.25	-0.25	0.22	0.01	0.00	0.00	0.00
C	0.95	-0.23	-0.03	-0.11	0.11	0.09	0.07	-0.01	0.01	-0.01
W/C	-0.79	0.52	-0.15	0.25	0.00	-0.13	0.04	-0.01	0.02	0.00
W	0.68	0.48	-0.46	0.24	0.19	-0.03	0.00	0.00	-0.01	0.00
FA	0.17	0.92	0.16	-0.20	0.21	0.08	-0.03	0.01	0.01	0.00
CA	-0.63	-0.71	-0.09	0.15	0.17	0.23	0.00	-0.01	0.00	0.00
FA/C	-0.57	0.78	0.22	-0.11	0.10	0.00	0.06	-0.02	-0.01	0.00
CA/C	-0.97	-0.15	0.08	0.14	0.03	0.04	0.08	0.02	0.00	0.00
C/(FA+CA)	0.97	-0.19	-0.01	-0.10	-0.05	-0.05	0.10	0.00	0.00	0.01

Table 4.07 Quality of representation of data on concrete workability and strength characteristics

$\mathbf{x}_i$	D_1	D_2	D_3	D_4	D_5	D_6	D_7	D_8	D_9	D_{10}
CS	0.53	0.05	0.21	0.19	0.01	0.01	0.00	0.00	0.00	0.00
Sl	0.20	0.62	0.00	0.06	0.06	0.05	0.00	0.00	0.00	0.00
C	0.91	0.05	0.00	0.01	0.01	0.01	0.00	0.00	0.00	0.00
W/C	0.62	0.27	0.02	0.06	0.00	0.02	0.00	0.00	0.00	0.00
W	0.47	0.23	0.21	0.06	0.04	0.00	0.00	0.00	0.00	0.00
FA	0.03	0.85	0.03	0.04	0.04	0.01	0.00	0.00	0.00	0.00
CA	0.39	0.50	0.01	0.02	0.03	0.05	0.00	0.00	0.00	0.00
FA/C	0.32	0.60	0.05	0.01	0.01	0.00	0.00	0.00	0.00	0.00
CA/C	0.94	0.02	0.01	0.02	0.00	0.00	0.01	0.00	0.00	0.00
C/(FA+CA)	0.94	0.04	0.00	0.01	0.00	0.00	0.01	0.00	0.00	0.00

Graphical presentation of quality of representation can be seen in Fig. 4.03, from which it is perceived that most of the variables are well represented in first two dimensions.

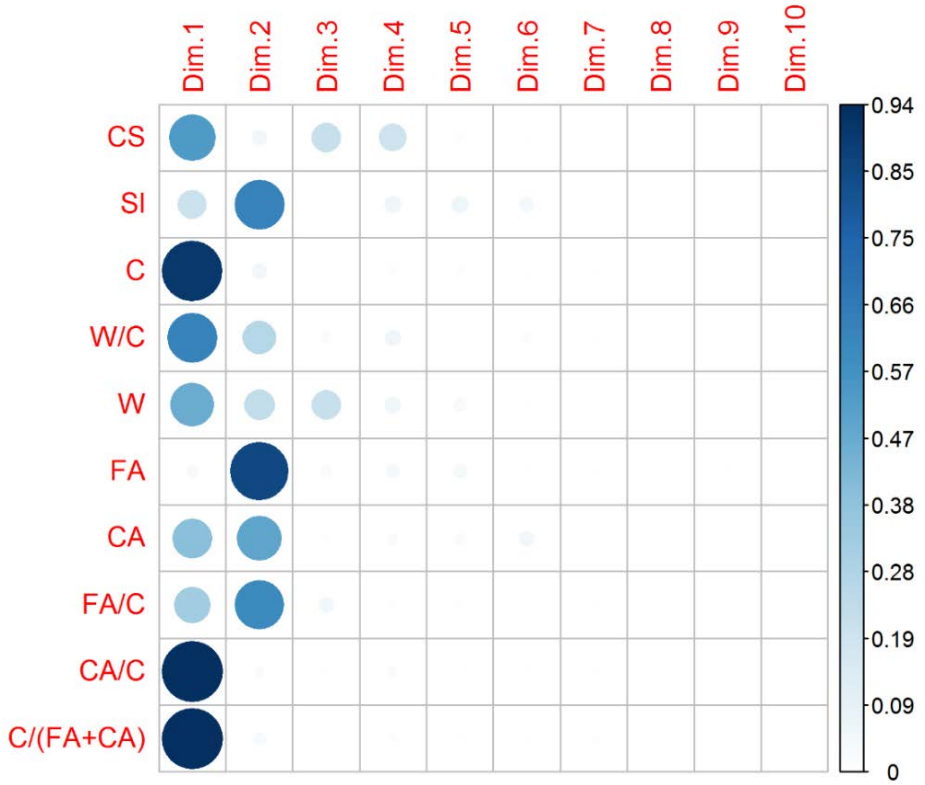

Figure 4.03 Quality of representation

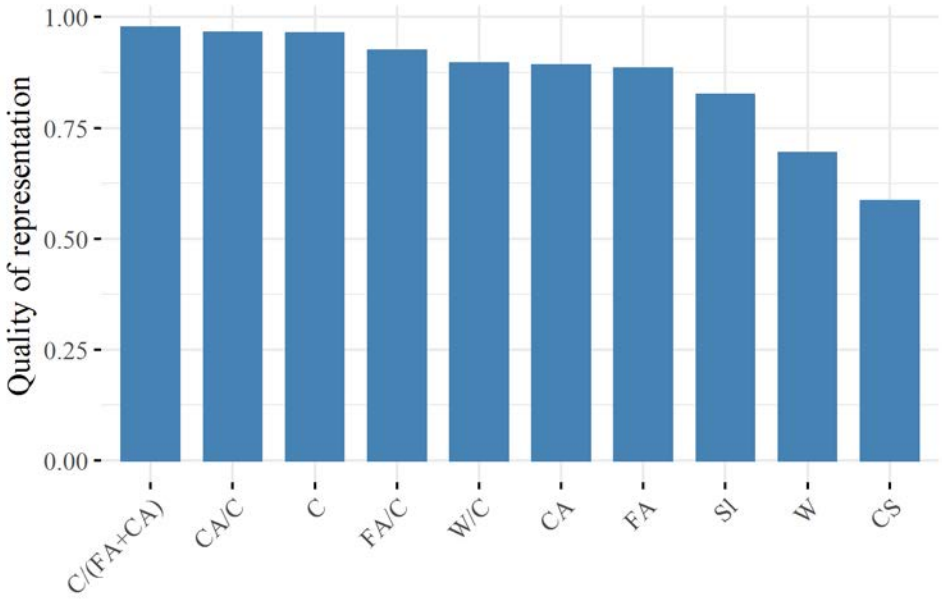

Figure 4.04 Combined quality of representation of variables in dimensions 1 & 2

The combined quality of representation as presented in bar plot – Fig. 4.04, points out that all the variables represent more than 50% of their variation in first two components and representation of variables is good enough.

Table 4.08 Percentage variable contribution

$\mathbf{x}_i$	D_1	D_2	D_3	D_4	D_5	D_6	D_7	D_8	D_9	D_{10}
CS	9.95	1.58	38.94	38.90	5.99	3.76	0.79	0.06	0.01	0.01
Sl	3.75	19.26	0.08	13.30	30.58	32.67	0.30	0.05	0.01	0.00
C	16.96	1.64	0.14	2.48	5.33	6.09	17.28	5.47	11.34	33.27
W/C	11.64	8.37	4.45	12.53	0.01	12.69	6.35	4.38	38.88	0.70
W	8.71	6.99	39.29	11.97	17.70	0.72	0.03	1.03	13.41	0.13
FA	0.57	26.35	4.91	7.95	20.58	5.03	3.41	15.05	12.36	3.81
CA	7.30	15.43	1.60	4.53	13.05	35.94	0.00	5.98	0.71	15.46
FA/C	6.01	18.57	9.45	2.36	5.13	0.00	11.75	25.89	20.77	0.07
CA/C	17.59	0.65	1.14	4.02	0.48	1.35	25.42	40.43	2.52	6.39
C/(FA+CA)	17.51	1.15	0.01	1.96	1.14	1.73	34.67	1.66	0.00	40.16

Variables contribution in accounting for the variability in a particular component, expressed as percentages, is tabulated in Table 4.08. Graphically contribution of variables has been presented in Fig. 4.05. Such plots are essential if dimensions have to be studied exclusively.

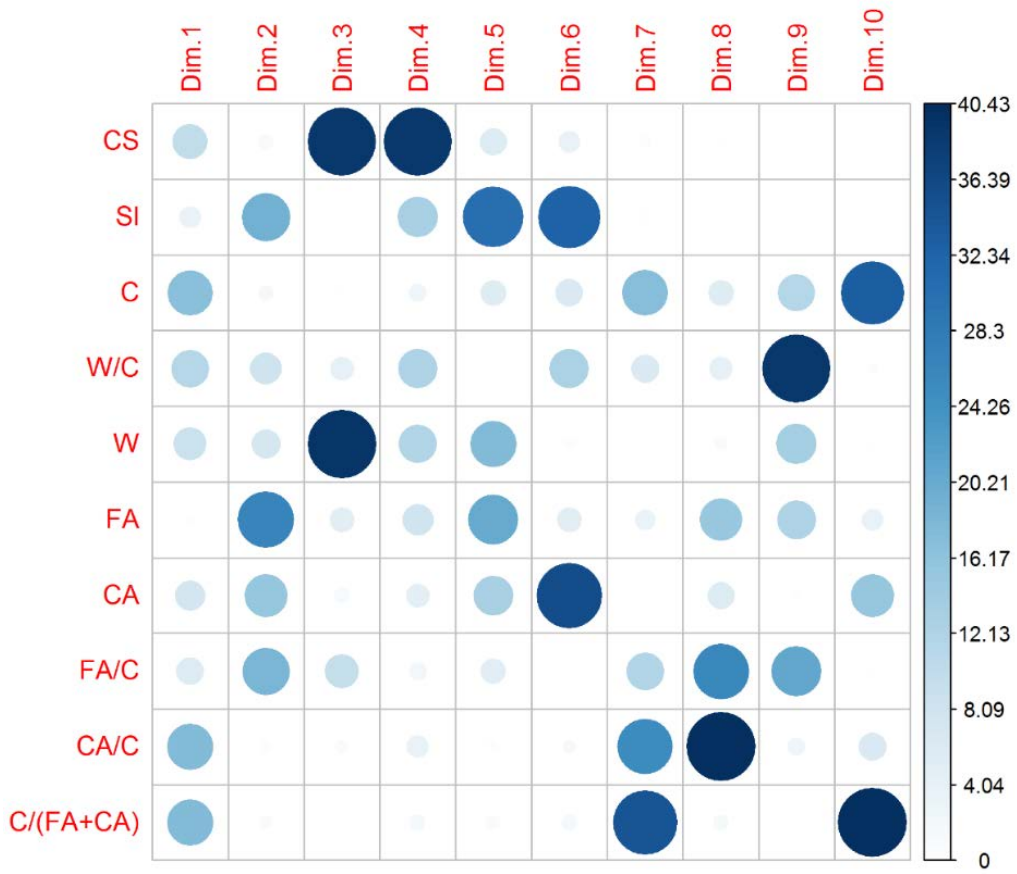

Figure 4.05 Percentage variable contribution of data on concrete workability and strength characteristics

It is seen in Fig. 4.05 that most of the variation in 1st dimension (≈54% of total variation) is contributed from all variables except FA, FA/C and Sl. In 2nd dimension, Slump and fine aggregate content contribute highest to variation in the component (Variation in 2nd dimension is about 33%), but in contrary compressive strength, cement, CA/C and CA/(FA+CA) contribute insignificantly. In 3rd dimension, compressive strength and water content have the highest say (Total variation in 3rd component is about 5%).

From Fig. 4.05, it may seem that compressive strength is not sufficiently well represented as much as other variables in first two dimensions. Hence its variable contribution is further investigated with the help of variance contribution bar plots for first two dimensions separately.

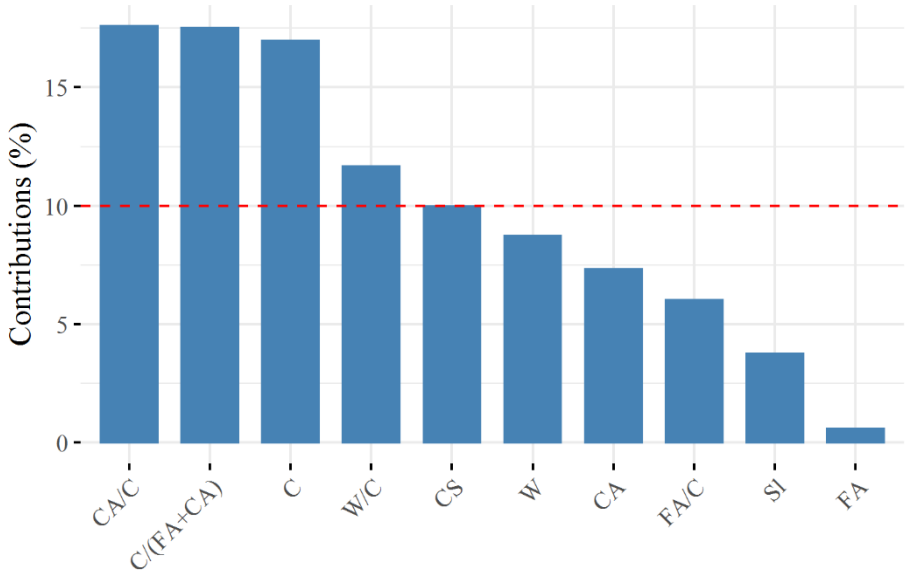

Figure 4.06 Contribution of variables to dimension 1 of data on concrete workability and strength characteristics

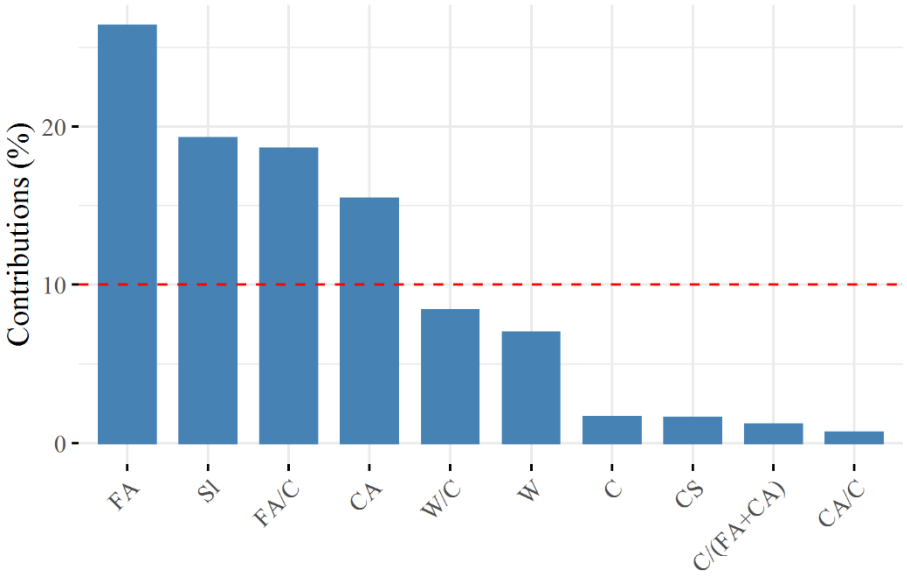

Figure 4.07 Contribution of variables to dimension 2 of data on concrete workability and strength characteristics

Figs. 4.06 and 4.07 depict that compressive strength is fairly contributing ($\geq(1/N)\times100\%$) to the variation in first dimension, not to the second. It is to be remembered the first component itself encompasses a significant part of the total variation, i.e. about 54%. Hence contribution of compressive strength to first two components is assumed to be fair.

Overall variation captured beyond the second component is less than 14% altogether. Further study has been limited to dimensions 1 and 2.

Component Plot

Meeting all conditions of dimensionality reduction (by any of the methods: Elbow in scree plot, desired cut-off percentage and number of component retention (preferably 2)), and analysis of contribution and quality of representation plots, the dataset has been reduced to two dimensions. Fig. 4.08 presents correlation plot generated for the first two components considered.

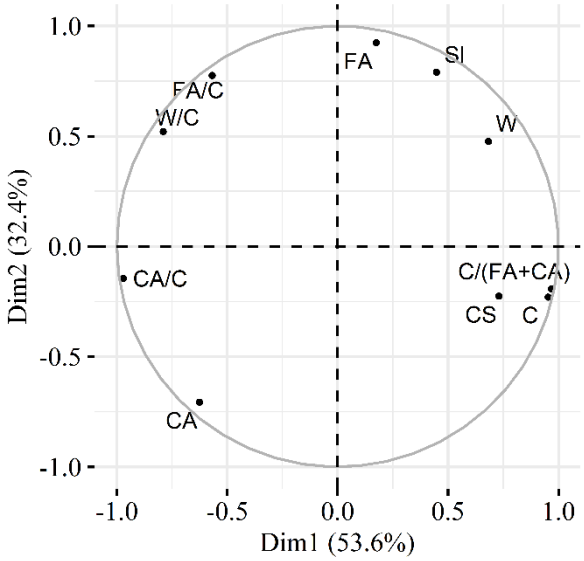

Figure 4.08 Correlation plot of variables in dimensions 1 and 2

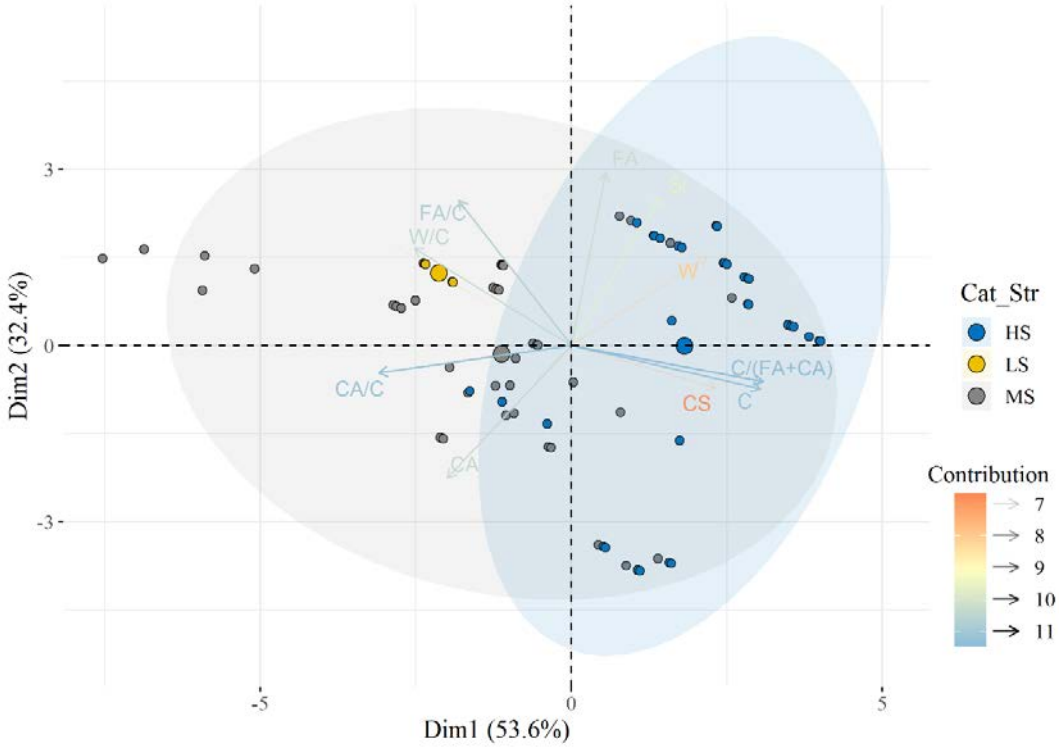

Figure 4.09 Bi-plot of data on concrete workability and strength characteristics

Projection of individual observations on principal component plane give their representation in that plane and is called score plot. Correlation circle superimposed on score plot results in bi-plot. Fig. 4.10 shows bi-plot for the concrete data analysed. Here, confidence (95%) ellipses are drawn based on strength categorical variables.

4.2.4 Interpretation of POD results of data on concrete workability and strength characteristics

Analysis of POD results for the data indicates,

a) Increase in compressive strength with cement content and ratio of cement to aggregate.
b) Decrease in strength with increase in water to cement ratio. This result is consistent with the recognised Abram's law.
c) Strength is negatively correlated to fine aggregate to cement content and coarse aggregate to cement content ratios.
d) Slump as an indicator of workability is directly influenced by water and fine aggregate content as intuitively expected.
e) Higher coarse aggregate content makes the mix harsher and hence reduces the slump.

Based on critical correlation values and component plot of the first two dimensions, significant variables affecting 28 day's compressive strength and slump have been identified and listed in Table 4.09.

Table 4.09 Significant variables affecting strength and slump characteristics identified from data on concrete workability and strength characteristics

Target characteristics	Significant variables
CS	C/(FA+CA), C, W/C
Sl	CA, FA, W

Text code: Navy blue colour indicates positive correlation;
Red colour indicates negative correlation.

Note: It may seem obvious that the component plot encompasses most of the analysis results of quality of representation and variable contribution. So obtaining a correlation plot becomes a principal step in POD. In cases considered next, only essential results are presented along with correlation plot(s).

4.3 NORMAL STRENGTH CONCRETE PERFORMANCE AT ELEVATED TEMPERATURES

Performance appraisal of concrete at elevated temperatures has always been an interesting and challenging exercise. Utility of POD in this regard has been investigated.

4.3.1 Data – Source and pre-processing

1. Source: Yaragal et al. (2010)

Available data (Yaragal et al. 2010) on concrete exposed to elevated temperature has been gathered for analysis by POD. Concrete grade (CG), cement content (C), fine aggregate (FA), coarse aggregate (CA – 12 mm and 20 mm passing), crushed rock fines content (CRF), water content (W), admixture dosage (A), gel space ratio (GSR), water to cement ratio (W/C), cement to aggregate ratio (C/(FA+CA)), slump (Sl), 28 days cube strength (CS28 *T*°C), residual compressive strength (RCS) and weight loss (WL_T) after exposure to elevated temperature (T) are available as variables in the data set.

Table 4.10 List of variables in data on concrete exposed to elevated temperature

Variables	Symbols	Variables	Symbols
01. Weight loss after exposure to elevated temperature	WL_T	08. Water	W
02. Residual compressive strength	RCS	09. Fine aggregates	FA
03. 28 days cube compressive strength at elevated temperature T°C	CS28*T*°C	10. Coarse aggregate (12 mm downsize)	CA12
04. Slump	Sl	11. Coarse aggregate (20 mm downsize)	CA20
05. Concrete grade	CG	12. Cement to aggregate ratio	C/(FA+CA)
06. Cement	C	13. Crushed rock fines	CRF
07. Water/Cement	W/C	14. Admixture dosage (High range water reducing admixture)	SP
		15. Gel space ratio	GSR

2. Total number of variables: 15 Quantitative + 0 Qualitative = 15 Variables (refer Table 4.10). Dataset has been used as available, without generating any new synthetic variables. Interaction of residual compressive strength and weight loss after exposure to elevated temperature with variables available have been studied employing POD.

3. Total number of observations (Individuals)**:** 48

4. Matrix size of quantitative data: 48×15

5. Missing values: Dataset collected has no missing values.

6. Bartlett sphericity test

$\chi^2 = 10920.34$

DF = 105

Probability value $\cong 2.22\times10^{-16} < 0.05$

Reject the null hypothesis. Data is not spherical and is accepted for analysis by POD.

7. Descriptive statistics

Basic statistical details of concrete subject to elevated temperatures have been provided in Table 4.11.

Table 4.11 Descriptive statistics of concrete subject to elevated temperature

Variables	Units	Mean	SD	Minimum	Maximum
WL_T	%	3.45	2.22	0.05	7.26
RCS	Ratio	0.66	0.26	0.18	1.09
CS28*T*°C	N/mm^2	27.82	12.06	8.00	49.78
Sl	mm	73.33	18.14	50.00	100.00
CG	kg/m^3	32.50	8.63	20.00	45.00
C	kg/m^3	366.67	60.60	280.00	454.00
W/C	Ratio	0.45	0.07	0.37	0.56
W	kg/m^3	160.83	5.36	156.00	170.00
FA	kg/m^3	485.83	29.13	434.00	512.00
CA12	kg/m^3	297.50	21.12	286.00	344.00
CA20	kg/m^3	740.33	4.80	735.00	747.00
C/(FA+CA)	Ratio	0.20	0.04	0.14	0.26
CRF	kg/m^3	323.50	29.17	293.00	376.00
SP	%	2.65	0.57	1.98	3.72
GSR	Ratio	0.86	0.08	0.74	0.95

4.3.2 Correlation matrix

Z-score standardisation (normalisation) has been carried out to normalise the data before computing correlation matrix.

Correlation of WL_T and RCS with other Variables

Correlation coefficients of weight loss with other variables at different exposure temperature levels are as in Table 4.12, and correlation coefficients of RCS are reported in Table 4.13.

Inference from correlation coefficient matrices for various temperature ranges of exposure

Inferences can be drawn from the correlation coefficient matrices for WL_T and RCS at different ranges of exposure temperatures.

Table 4.12 Correlation of weight loss with variables at different temperature levels

x_i	Exposure Temperature (°C)							
	100	**200**	**300**	**400**	**500**	**600**	**700**	**800**
RCS	0.30	-0.27	-0.65	-0.92	-0.86	-0.86	-0.78	-0.89
CS28*T*°C	-0.47	-0.30	0.70	0.95	0.76	0.35	0.66	0.57
Sl	0.73	0.35	-0.59	-0.64	-0.64	-0.61	-0.30	-0.53
CG	-0.64	-0.23	0.79	0.90	0.84	0.87	0.77	0.85
C	-0.67	-0.24	0.78	0.86	0.81	0.84	0.72	0.82
W/C	0.79	0.39	-0.77	-0.81	-0.86	-0.83	-0.72	-0.83
W	0.39	0.56	0.22	0.34	-0.02	0.19	0.29	0.20
FA	0.50	0.09	-0.67	-0.77	-0.63	-0.70	-0.53	-0.65
CA12	0.23	-0.14	-0.75	-0.56	-0.50	-0.54	-0.72	-0.58
CA20	0.24	0.03	-0.55	-0.20	-0.35	-0.24	-0.27	-0.16
C/(FA+CA)	-0.67	-0.24	0.79	0.86	0.81	0.83	0.71	0.81
CRF	0.92	0.63	-0.57	-0.72	-0.84	-0.77	-0.50	-0.72
SP	-0.53	-0.18	0.64	0.85	0.74	0.82	0.72	0.81
GSR	-0.79	-0.38	0.78	0.82	0.86	0.84	0.71	0.82

Note: Significant correlation values ≥ |±0.7|, have been shown with coloured boxes.

Influence of variables on WL_T and RCS for exposure temperatures less than 300 °C

Usage of CRF increases the water demand and water-cement ratio. For 100 °C and 200 °C, the correlation coefficients of W/C and WL_T are positive, indicating higher water to cement ratios result in higher weight loss for exposure of concrete up to 200 °C. The correlation coefficients of WL_T are negative at this temperature range with GSR, C/(FA+CA), C and CG, suggesting higher these variables are WL_T going to be less.

The effect of temperature on strength at exposure up to 200 °C is insignificant as indicated by low correlation coefficients between RCS and CS28*T*°C. Variables C, C/(FA+CA), GSR, CG and SP show a strong negative correlation with RCS. Positive correlation of RCS with FA and W/C signifies the importance of these variables in strength retention. Influence of CRF on RCS is less than that on WL_T.

Table 4.13 RCS correlation with variables at different temperature levels

x_i	Exposure Temperature (°C)							
	100	**200**	**300**	**400**	**500**	**600**	**700**	**800**
WL_T	0.30	-0.27	-0.65	-0.92	-0.86	-0.86	-0.78	-0.89
CS28*T*°C	-0.40	-0.05	-0.47	-0.78	-0.55	0.09	-0.43	-0.64
Sl	0.56	0.55	0.77	0.73	0.44	0.70	0.46	0.84
CG	-0.85	-0.68	-0.86	-0.94	-0.86	-0.98	-0.85	-0.94
C	-0.86	-0.72	-0.86	-0.93	-0.84	-0.98	-0.84	-0.93
W/C	0.76	0.66	0.70	0.87	0.88	0.96	0.81	0.88
W	-0.65	-0.43	-0.74	-0.38	-0.18	-0.32	-0.46	-0.29
FA	0.82	0.69	0.97	0.85	0.60	0.84	0.71	0.88
CA12	0.72	0.68	0.42	0.51	0.84	0.76	0.90	0.40
CA20	-0.05	0.15	-0.25	-0.02	0.41	0.24	0.34	0.01
C/(FA+CA)	-0.85	-0.72	-0.86	-0.92	-0.83	-0.97	-0.84	-0.93
CRF	0.49	0.41	0.59	0.80	0.64	0.78	0.48	0.89
SP	-0.88	-0.63	-0.94	-0.95	-0.76	-0.92	-0.78	-0.93
GSR	-0.76	-0.66	-0.72	-0.88	-0.86	-0.96	-0.80	-0.89

Note: Significant correlation values ≥ |±0.7|, have been shown with coloured boxes.

Influence of variables on WL_T and RCS for exposure temperature range 300 °C to 600 °C

In temperature range 300 °C and 600 °C, WL_T is poorly correlated to water content, suggesting water loss happening at lower temperature levels than 300 °C. High positive correlation of WL_T with cement content and CG and negative correlation with RCS are indicative of the vulnerability of higher grades of concrete.

Higher admixture dosage leads to lower RCS, and higher fines content helps in strength retention at elevated temperature exposures.

Influence of variables on WL_T and RCS for exposure temperature above 600 °C

Higher grades of concrete suffer more WL_T for exposure temperatures above 600 °C. FA and CRF contribute largely to strength retention characteristics.

For all levels of exposure temperatures, low correlation coefficients between CA20, WL_T and RCS indicate that coarse aggregate has less influence on these variations.

4.3.3 Performing orthogonal decomposition for concrete subject to elevated temperature data

First two eigenvalues extracted from POD and the percentage of total variation explained are given in Table 4.14. The first 2–dimensions capture more than 80% of the variation in the data. First and second component coefficients are as given in Table 4.15 and Table 4.16, respectively.

Table 4.14 Eigenvalues of concrete subject to elevated temperature data

Exposure Temperature (°C)	**100**	**200**	**300**	**400**	**500**	**600**	**700**	**800**
1st eigenvalue	10.30	9.60	10.50	10.90	10.60	10.30	10.40	10.60
% variation contribution	68.90	64.20	70.00	72.90	70.80	68.50	69.00	70.50
2nd eigenvalue	2.30	2.30	2.40	2.10	2.30	2.10	2.20	2.20
% variation contribution	15.70	15.30	16.30	14.00	15.30	14.00	14.60	14.40
Cumulative variance %	84.60	79.50	86.30	86.90	86.10	82.50	83.60	84.90

Vector loadings represent the strength of a variable in a particular dimension. They quantify the contribution of variables to variation of data in the axis under consideration. For the analysis performed, vector loadings for all temperature ranges are presented in Fig. 4.10(a–h).

Table 4.15 Coefficients of first component, D_1

x_i	Exposure Temperature (°C)							
	100	**200**	**300**	**400**	**500**	**600**	**700**	**800**
WL_T	-0.70	-0.27	0.82	0.91	0.87	0.87	0.76	0.85
RCS	-0.82	-0.69	-0.87	-0.94	-0.85	-0.97	-0.85	-0.96
CS28*T*°C	0.76	0.70	0.73	0.85	0.80	0.02	0.73	0.64
Sl	-0.86	-0.86	-0.85	-0.84	-0.84	-0.84	-0.82	-0.84
CG	0.99	0.99	1.00	1.00	1.00	1.00	1.00	1.00
C	1.00	1.00	1.00	0.99	0.99	1.00	1.00	0.99
W/C	-0.97	-0.96	-0.95	-0.95	-0.97	-0.97	-0.96	-0.96
W	0.30	0.32	0.34	0.33	0.29	0.31	0.34	0.31
FA	-0.92	-0.93	-0.93	-0.92	-0.90	-0.91	-0.91	-0.91
CA12	-0.59	-0.59	-0.61	-0.59	-0.60	-0.61	-0.63	-0.59
CA20	-0.14	-0.13	-0.15	-0.14	-0.17	-0.15	-0.16	-0.15
C/(FA+CA)	1.00	1.00	1.00	0.99	0.99	1.00	1.00	0.99
CRF	-0.89	-0.88	-0.86	-0.87	-0.88	-0.87	-0.85	-0.88
SP	0.95	0.95	0.95	0.96	0.94	0.95	0.95	0.95
GSR	0.98	0.97	0.96	0.96	0.98	0.98	0.97	0.97

Table 4.16 Coefficients of second component, D_2

x_i	Exposure Temperature (°C)							
	100	**200**	**300**	**400**	**500**	**600**	**700**	**800**
WL_T	0.51	0.75	-0.33	-0.05	-0.25	-0.12	-0.26	-0.12
RCS	-0.38	-0.36	-0.45	-0.11	0.35	0.10	0.27	-0.11
CS28*T°C*	-0.13	-0.09	-0.29	-0.09	0.24	-0.02	0.18	-0.29
Sl	-0.04	0.02	-0.19	-0.19	-0.30	-0.23	-0.34	-0.25
CG	0.05	0.03	0.00	0.00	0.03	0.02	0.02	0.01
C	0.04	0.03	0.01	0.00	0.04	0.03	0.02	0.02
W/C	0.22	0.23	0.24	0.25	0.21	0.23	0.20	0.22
W	0.92	0.92	0.75	0.74	0.71	0.74	0.58	0.69
FA	-0.34	-0.30	-0.35	-0.35	-0.41	-0.38	-0.38	-0.37
CA12	0.19	0.03	0.46	0.50	0.53	0.49	0.63	0.52
CA20	0.81	0.60	0.96	0.96	0.93	0.95	0.93	0.97
C/(FA+CA)	0.04	0.02	0.01	0.00	0.04	0.03	0.03	0.02
CRF	0.28	0.37	0.12	0.12	0.04	0.09	-0.04	0.06
SP	0.30	0.23	0.28	0.27	0.30	0.29	0.27	0.28
GSR	-0.19	-0.20	-0.20	-0.21	-0.17	-0.19	-0.16	-0.18

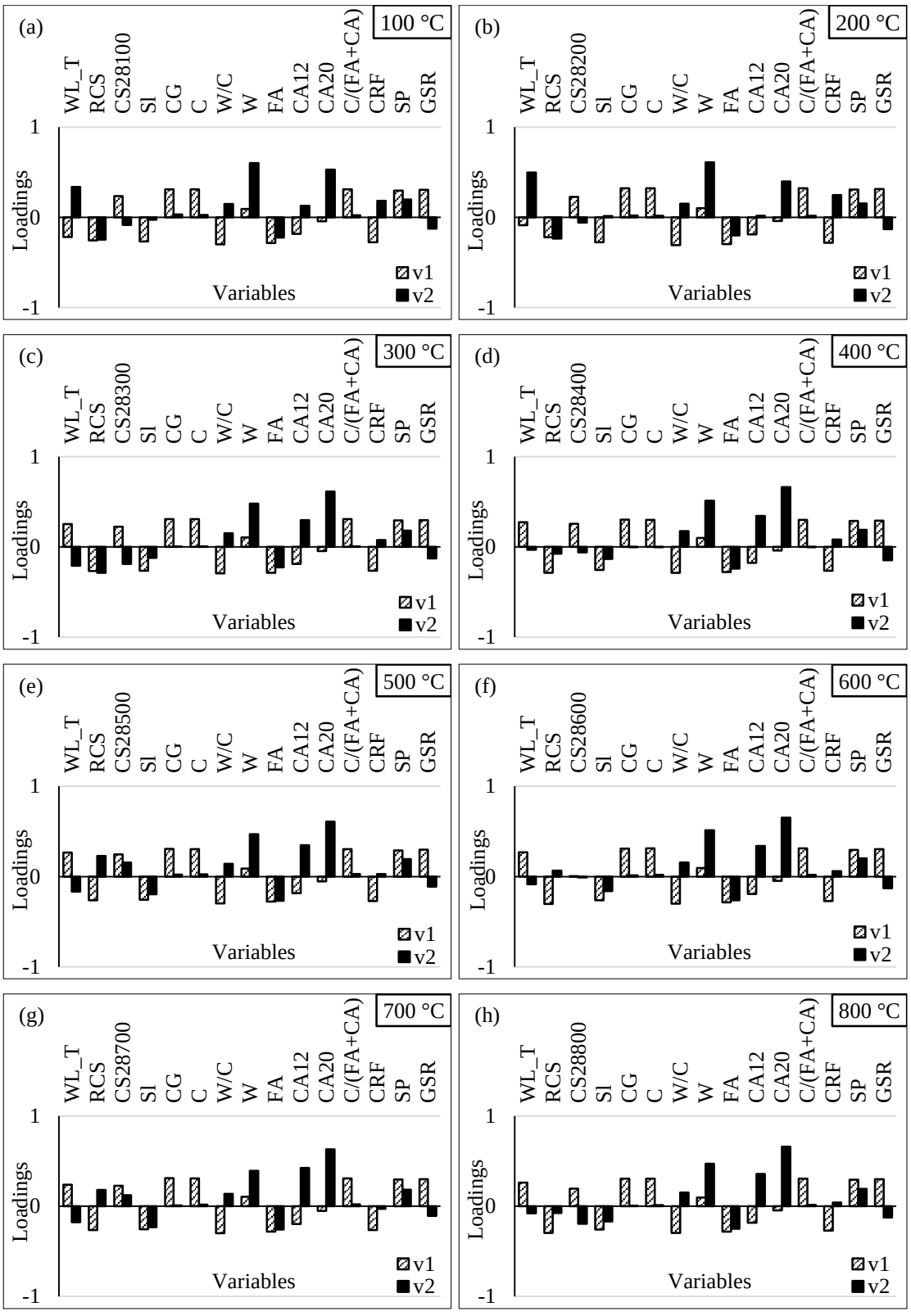

Figure 4.10 Vector loadings at exposure temperature (a) 100 °C (b) 200 °C (c) 300 °C (d) 400 °C (e) 500 °C (f) 600 °C (g) 700 °C and (h) 800 °C

Inferences from POD results for various temperature ranges of exposure

CA20 is loaded in second dimension, and CA12 is loaded in higher dimensions indicating their influence on WL_T and RCS is negligible for the type of aggregate in question.

Variables interaction for exposure temperatures up to 200 °C

CRF and other fines holding more water lead to variation of WL_T up to exposure temperature 100 °C. For exposure temperatures up to 200 °C, first two axes consideration is necessary to address influence of water on WL_T.

Higher fine content and W/C contribute to strength retention on exposure to temperature up to 200 °C. Higher strength and admixture dosage affects strength retention characteristics adversely.

Variables interaction for exposure temperature range from 300 °C to 800 °C

For exposure temperature range between 300 °C and 800 °C, the loading plots are similar; hence variables have same influence on WL_T and RCS.

More fines in mix lead to less WL_T, and higher the strength of concrete, higher is WL_T at elevated temperatures. It is also evident from the loading plots that WL_T and RCS have vector loadings of opposite signs, indicating the influence of variables is opposite in nature. Even in this temperature range of exposure, the beneficial effect of fines in strength retention and the adverse effect of high cement content is clearly seen.

Component plots

The data set in all has 15 components/variables. The components at eight temperature exposure levels namely 100 °C, 200 °C, 300 °C, 400 °C, 500 °C, 600°C, 700 °C and 800 °C, are as shown in Fig. 14.11(a–h).

The first two components for these temperatures explain about 85%, 80%, 86%, 87%, 86%, 83%, 84% and 85% of the variation in the data respectively.

4.3.4 POD results interpretation – concrete subject to elevated temperature data

From component plots, it is evident that variables influencing a characteristic cluster together. Hence, grouping of variables is possible for further dimensionality reduction.

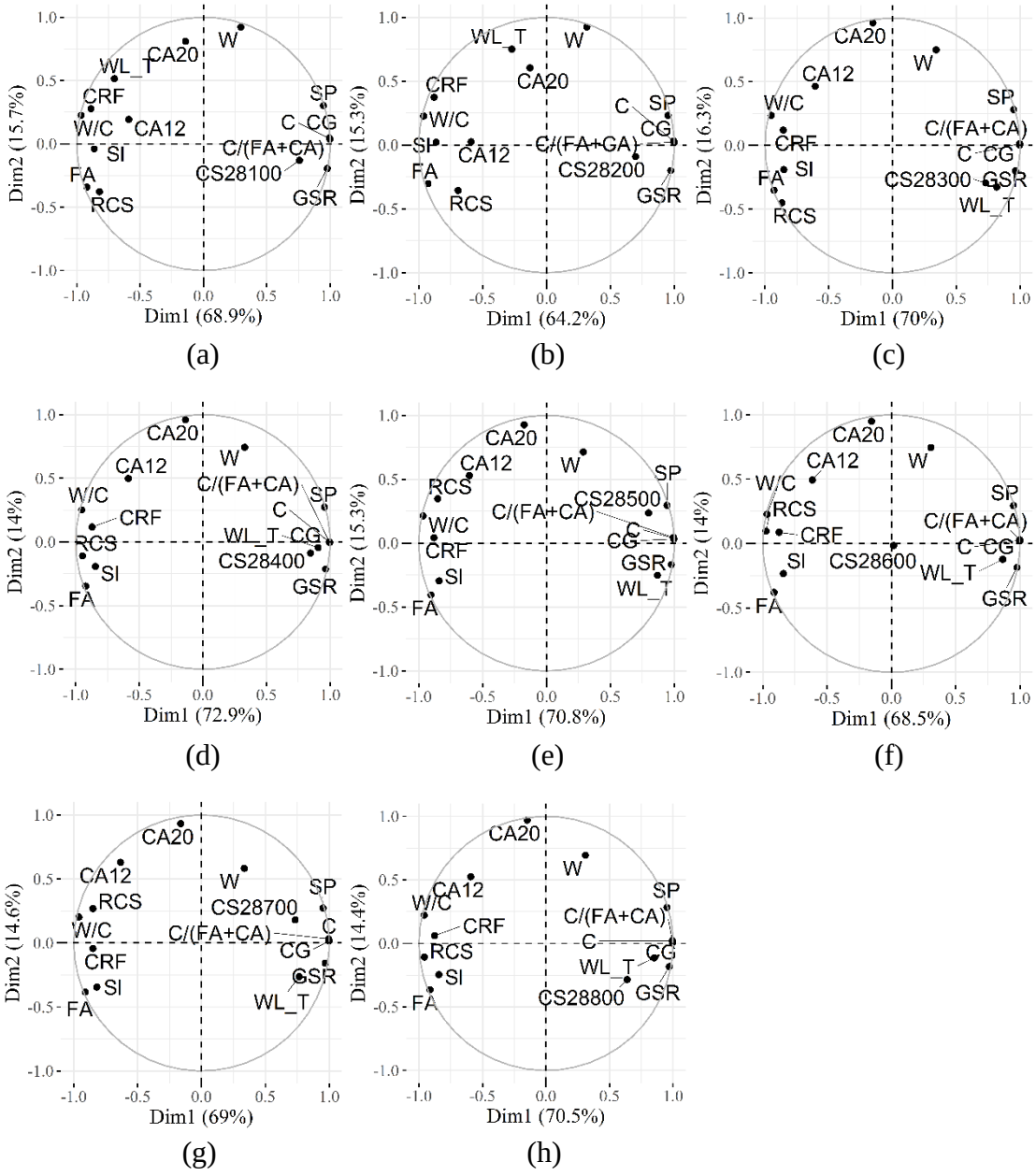

Figure 4.11 Component plots for concrete at temperature (a) 100 °C (b) 200 °C (c) 300 °C (d) 400 °C (e) 500 °C (f) 600 °C (g) 700 °C and (h) 800 °C

For exposure temperature up to 200 °C W/C and CRF are variables strongly influencing WL_T. In this range influence of W, CA(20mm), CRF, WL_T on RCS is very less, and these variables need not be accounted in residual strength predictions.

Component plots for exposure temperatures from 300 °C to 800 °C do not show much difference. Hence, a single model may be operational for temperatures above 300 °C, to study WL_T and RCS. In this range, as W, CA12 and CA20 have no much vector loadings, their inclusion in prediction model is unnecessary.

From component plots, it is also clear that W/C and GSR lead to almost same correlation coefficients with opposite sign and hence any one can be treated as a variable of interest at the expense of other.

It is to be appreciated that a 15–dimensional problem can be reduced to 2–dimensions that explains about 80–87% of the inherent variation. Key variables affecting RCS and WL_T have been identified and listed in Table 4.17.

Table 4.17 Significant variables affecting RCS and weight loss for concrete subject to elevated temperatures

Exposure Temperature (°C)	**WL_T**	**RCS**
100	CRF, W/C, GSR	SP, C, C/(FA+CA), CG, FA, W/C, GSR, $CA12^{-}$
200	–	C, C/(FA+CA), FA, $CA12^{-}$, CG, SP^{+}
300	CG, C/(FA+CA), C, GSR, W/C, CA12, CS28300, CRF^{+}	FA, SP, C, C/(FA+CA), CG, GSR^{-}, W^{-}, W/C^{-}
400	CS28400, CG, C, C/(FA+CA), SP, GSR, W/C, FA, CRF	SP, CG, C, C/(FA+CA), GSR, W/C, FA, CRF, CS28400
500	GSR, W/C, CG, CRF, C, C/(FA+CA), $CS28500^{-}$, SP^{-}	W/C, CG, GSR, C, CA12, C/(FA+CA), SP^{-}
600	CG, GSR, C, C/(FA+CA), W/C, SP^{-}, CRF, FA^{-}	CG, C, C/(FA+CA), GSR, W/C, SP^{-}, FA^{-}, CRF, CA12
700	CG, C, W/C, SP^{-}, CA12, GSR, C/(FA+CA) , CRF^{+}	CA12, CG, C, C/(FA+CA), W/C, GSR, SP, FA, CRF^{+}
800	CG, W/C, C, GSR, SP^{-}, C/(FA+CA), CRF	CG, C, C/(FA+CA) , SP, GSR, CRF, W/C, FA

Text code: Navy blue colour indicates positive correlation; Red colour indicates negative correlation. Superscript '+' or '–' denote variables that are added or fit for removal based on study of component plots.

4.4 PERFORMANCE APPRAISAL OF HIGH STRENGTH SELF–COMPACTING CONCRETE

Amenability of POD in selecting suitable ingredients and appropriate mix design of high strength self-compacting concrete for accomplishment of targeted performance levels has been explored.

4.4.1 Data – Source and pre-processing

1. Source: Lavanya (2018)

Table 4.18 Data variable list of experimental investigation on properties of high strength SCC mixes

Variables	Symbols	Variables	Symbols
1. Slump spread	SlS	13. Water absorption	Wabs
2. Slump flow time to spread 50 cm diameter	SlS50	14. Sorption	SRP28
3. V Funnel test concrete flow time to flow 10 cm	VT10	15. Rapid chloride penetration test value	RCPT28
4. V Funnel test concrete flow time to flow 50 cm	VT50	16. Weight loss due to acid attack	WL_AA
5. Blocking ratio from L box test	LB(H2/H1)	17. Weight loss due to sulphate attack	WL_SA
6. Passing ability from U box test	UB(H2/H1)	18. Weight loss due to corrosion	WL_Cor
7. Cube compressive strength at 28 days	CS28	19. Fly ash	F
8. Cube compressive strength at 90 days	CS90	20. Ground granulated blast furnace slag	GGBS
9. Split tensile strength value	STS28	21. Silica fumes	SF
10. Flexural strength	FlS28	22. Fine aggregate	FA
11. Elastic modulus	E	23. Water to cement ratio	W/C
12. Poisson’s ratio	PR	24. Water	W

Dataset on use of mineral admixture for replacement of fine aggregate in self-compacting concrete of M60 grade has been studied utilizing POD. The dataset includes

variables namely, water to cement ratio (W/C), water content (W), fine aggregate (FA), slump spread (SlS), slump flow time to spread 50 cm diameter (SlS50), V funnel test concrete flow time to flow 10 cm (VT10) and 50 cm (VT50), blocking ratio from L box test (LB(H2/H1)), passing ability from U box test (UB(H2/H1)), cube compressive strength at 28 (CS28) and 90 days (CS90), split tensile strength value (STS28), flexural strength (FlS28), elastic modulus (E), Poisson's ratio (PR), water absorption (Wabs), sorption (SRP28), rapid chloride penetration test value (RCPT28), weight loss due to acid arrack (WL_AA), sulphate solution (WL_SA) and corrosion (WL_Cor).

2. Total number of variables: 24 (Quantitative) (Refer Table 4.18)
Different percentage (5 – 25 %) of fine aggregate (FA) has been replaced with fly ash (F), ground granulated blast furnace slag (GGBS) and silica fumes (SF). In all mixes, cement content (C), coarse aggregate content (CA) and super-plasticizer dosage are kept constant and are equal to 550 kg/m^3 and 589 kg/m^3 and 11 kg/m^3 respectively.

3. Total number of observations (Individuals)**:** 24

4. Matrix size of quantitative data: 24×24

5. Missing values: Observations with missing values have been removed before finalising the data matrix.

6. Bartlett sphericity test
$\chi^2 = 1165.24$
DF = 276
Probability value $\cong 2.22\times10^{-16} < 0.05$
Reject the null hypothesis. Data is not spherical and is accepted for analysis by POD.

7. Descriptive statistics: Statistical information of collected SCC data has been displayed in Table 4.19.

Table 4.19 Descriptive statistics of SCC data

Variables	Units	Mean	SD	Minimum	Maximum
W/C	Ratio	0.34	0.04	0.30	0.40
W	kg/m^3	185.63	20.27	165.00	220.00
FA	kg/m^3	810.32	47.12	730.40	867.40
F	kg/m^3	57.08	68.98	0.00	182.6.00
SF	kg/m^3	22.83	44.66	0.00	137.00
GGBS	kg/m^3	22.83	44.66	0.00	137.00
SlS	mm	714.13	88.3	624.00	886.00
SlS50	s	4.66	1.82	2.30	7.30
VT10	s	7.95	1.17	6.00	10.00
VT50	s	13.63	2.01	10.00	18.00
LB(H2/H1)	Ratio	0.86	0.03	0.80	0.89
UB(H2/H1)	Ratio	22.71	2.31	20.00	28.00
CS28	N/mm^2	61.89	3.67	55.60	68.75
CS90	N/mm^2	71.17	2.62	66.74	75.95
STS28	N/mm^2	5.12	0.6	3.70	6.20
FlS28	N/mm^2	7.69	0.85	6.20	9.30
E	N/mm^2	44519.83	4915.26	35670.00	53940.00
PR	Ratio	0.11	0.00	0.11	0.12
Wabs	Percentage	3.04	0.19	2.64	3.30
SRP28	$mm/\sqrt{s}$	0.03	0.01	0.02	0.04
RCPT28	C	567.88	151.95	365.00	840.00
WL_AA	Percentage	2.91	0.34	2.40	3.50
WL_SA	Percentage	3.08	0.23	2.64	3.52
WL_Cor	Percentage	3.5	0.35	2.94	4.27

Table 4.20 Correlation matrix for concrete with fine aggregate replaced by fly ash, GGBS and silica fume

Cases	**Fly ash**				**GGBS**				**Silica fume**			
Variables	W/C	W	FA	F	W/C	W	FA	GGBS	W/C	W	FA	SF
SlS	0.99	0.99	-0.05	0.05	0.75	0.75	0.50	-0.50	0.20	0.20	0.97	-0.97
SlS50	-0.62	-0.62	-0.33	0.33	-0.86	-0.86	0.37	-0.37	-0.19	-0.19	-0.90	0.90
VT10	-0.59	-0.59	-0.72	0.72	-0.95	-0.95	-0.30	0.30	-0.60	-0.60	-0.74	0.74
VT50	-0.70	-0.70	-0.44	0.44	-0.76	-0.76	-0.52	0.52	-0.70	-0.70	0.36	-0.36
LB(H2/H1)	0.00	0.00	-0.56	0.56	-0.52	-0.52	-0.21	0.21	0.87	0.87	0.00	0.00
UB(H2/H1)	-0.85	-0.85	0.48	-0.48	-0.93	-0.93	0.23	-0.23	-0.96	-0.96	0.24	-0.24
CS28	-0.70	-0.70	0.62	-0.62	-0.82	-0.82	-0.53	0.53	0.19	0.19	-0.85	0.85
CS90	-0.48	-0.48	-0.85	0.85	-0.39	-0.39	-0.90	0.90	-0.50	-0.50	-0.86	0.86
STS28	-0.77	-0.77	0.56	-0.56	-0.73	-0.73	-0.63	0.63	-0.67	-0.67	-0.68	0.68
FlS28	-0.83	-0.83	0.54	-0.54	-0.66	-0.66	-0.70	0.70	-0.69	-0.69	-0.66	0.66
E	-0.82	-0.82	0.55	-0.55	-0.66	-0.66	-0.69	0.69	-0.69	-0.69	-0.67	0.67
PR	-0.58	-0.58	0.04	-0.04	-0.83	-0.83	0.41	-0.41	-0.61	-0.61	0.58	-0.58
Wabs	0.15	0.15	-0.06	0.06	0.84	0.84	-0.28	0.28	0.18	0.18	-0.40	0.40
SRP28	-0.45	-0.45	0.18	-0.18	0.75	0.75	-0.39	0.39	0.35	0.35	-0.52	0.52
RCPT28	-0.48	-0.48	0.22	-0.22	0.85	0.85	-0.35	0.35	0.29	0.29	-0.66	0.66
WL_AA	-0.21	-0.21	0.14	-0.14	0.88	0.88	-0.36	0.36	0.46	0.46	-0.49	0.49
WL_SA	-0.25	-0.25	0.18	-0.18	0.81	0.81	-0.44	0.44	0.55	0.55	-0.37	0.37
WL_Cor	0.19	0.19	0.20	-0.20	0.86	0.86	-0.38	0.38	0.59	0.59	-0.42	0.43

4.4.2 Correlation matrix

Data has been normalised before the application of POD. Table 4.20 presents correlation matrix, giving values of degrees of dependence of target characteristics on input variables.

It is evident that fly ash content is highly correlated to cube compressive strength at 28 & 90 days and V funnel concrete flow time (VT10) to flow 100 mm.

Cube compressive strength at 90 days, split tensile strength, flexural strength and modulus of elasticity are greatly affected by GGBS content.

Use of silica fume as a replacement to fine aggregate influences compressive strength at 28 & 90 days, split tensile strength, flexural strength and elastic modulus. Fine aggregate content replacement by silica fume reduces slump spread as indicated by negative correlation value.

4.4.3 Performing orthogonal decomposition of SCC data

POD technique is applied to the chosen dataset; results are obtained and presented in Tables 4.21 and 4.22.

Table 4.21 Eigenvalues of SCC data

Cases	Fly ash			GGBS			Silica fume		
Dimensions	1	2	3	1	2	3	1	2	3
λ_i	9.31	5.58	5.33	13.40	6.59	1.03	10.45	8.30	2.29
Var. %	42.30	25.40	24.20	60.90	29.90	4.70	47.50	37.70	10.40
Cum. Var. %	42.30	67.70	91.90	60.90	90.80	95.50	47.50	85.20	95.60

Component plots

Fig. 4.12 presents component plots for first two dimensions obtained for the data on replacement of fine aggregates with fly ash, GGBS and silica fumes of SCC.

From Table 4.22 and Fig. 4.12 (a), it is seen that fly ash replacement to fine aggregates majorly influence L box test blocking ratio, V funnel test flow time, water absorption and weight loss due to acid exposures & corrosion of reinforcement.

Use of GGBS as a replacement to FA largely affects 90 days' cube compressive strength, flexural strength and modulus of elasticity, as seen in Fig. 4.12 (b).

Table 4.22 Component coordinates for SCC with fine aggregates replaced by fly ash, GGBS and silica fume

Cases	Fly ash			GGBS				Silica fume		
Variables	D_1	D_2	D_3	Variables	D_1	D_2	D_3	Variables	D_1	D_2	D_3
W/C	-0.91	0.04	0.38	W/C	-0.98	0.06	-0.05	W/C	0.10	-0.95	-0.28
W	-0.91	0.04	0.38	W	-0.98	0.06	-0.05	W	0.10	-0.95	-0.28
FA	0.29	-0.62	0.70	FA	-0.08	-0.97	0.20	FA	-0.89	-0.22	0.37
F	-0.29	0.62	-0.70	GGBS	0.08	0.96	-0.20	SF	0.89	0.22	-0.37
SlS	-0.94	0.04	0.30	SlS	-0.76	-0.53	-0.36	SlS	-0.88	-0.39	0.24
SlS50	0.63	0.58	-0.30	SlS50	0.85	-0.38	0.11	SlS50	0.95	0.30	0.03
VT10	0.41	0.65	-0.63	VT10	0.95	0.24	0.08	VT10	0.47	0.79	-0.31
VT50	0.58	0.38	-0.62	VT50	0.82	0.43	-0.31	VT50	-0.28	0.51	0.74
LB(H2/H1)	-0.13	0.58	-0.39	LB(H2/H1)	0.55	0.30	0.73	LB(H2/H1)	0.01	-0.78	-0.54
UB(H2/H1)	0.90	-0.36	0.00	UB(H2/H1)	0.85	-0.29	0.01	UB(H2/H1)	-0.31	0.86	0.34
CS28	0.81	-0.49	0.18	CS28	0.85	0.47	-0.15	CS28	0.91	-0.10	-0.02
CS90	0.20	0.51	-0.74	CS90	0.49	0.82	-0.24	CS90	0.73	0.65	-0.17
STS28	0.90	-0.33	0.09	STS28	0.79	0.59	0.06	STS28	0.58	0.78	-0.08
FlS28	0.92	-0.38	0.05	FlS28	0.72	0.69	0.03	FlS28	0.56	0.79	-0.04
E	0.92	-0.38	0.06	E	0.73	0.68	0.06	E	0.56	0.80	-0.05
PR	0.35	-0.57	-0.67	PR	0.82	-0.48	-0.14	PR	-0.81	0.56	-0.09
Wabs	0.10	0.77	0.53	Wabs	-0.86	0.42	0.12	Wabs	0.76	-0.26	0.53
SRP28	0.70	0.53	0.45	SRP28	-0.77	0.54	0.15	SRP28	0.84	-0.39	0.37
RCPT28	0.73	0.48	0.44	RCPT28	-0.86	0.47	0.08	RCPT28	0.92	-0.29	0.22
WL_AA	0.49	0.63	0.57	WL_AA	-0.87	0.47	0.07	WL_AA	0.79	-0.50	0.28
WL_SA	0.53	0.59	0.59	WL_SA	-0.81	0.56	0.06	WL_SA	0.71	-0.61	0.33
WL_Cor	0.13	0.61	0.75	WL_Cor	-0.86	0.48	0.02	WL_Cor	0.72	-0.63	0.24

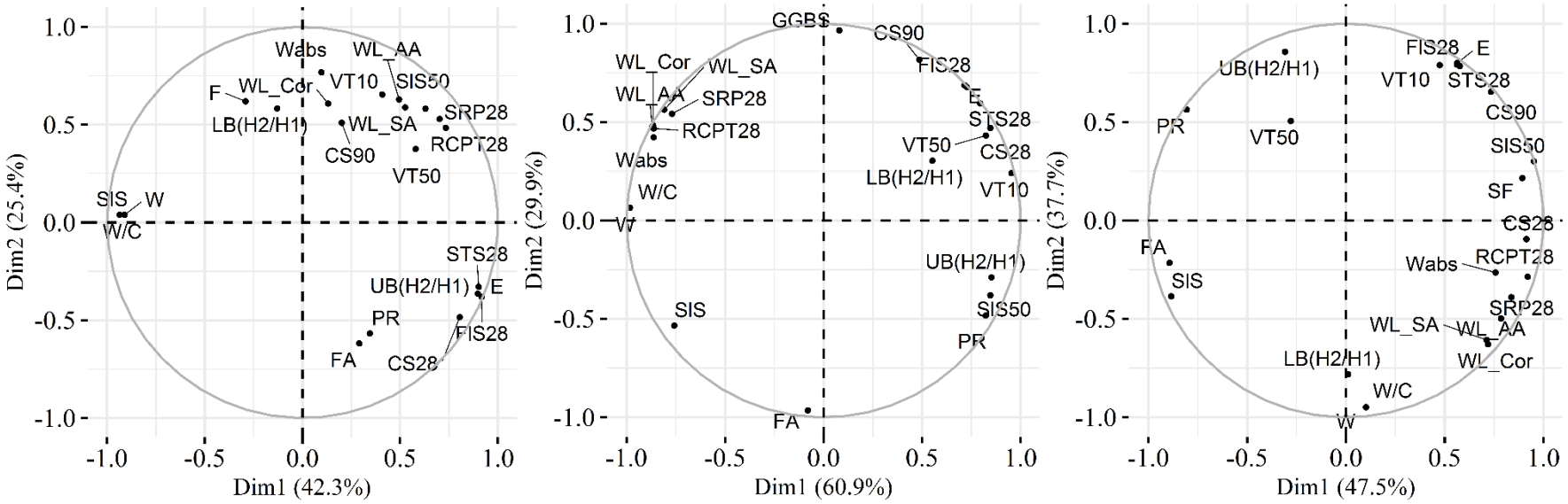

(a) (b) (c)

Figure 4.12 Component plots (a) SCC with fly ash replacement to fine aggregates (b) SCC with GGBS replacement to fine aggregates (c) SCC with silica fumes replacement to fine aggregates.

SF replacement increases early age and long term strengths. From Fig. 4.12 (c), it is evident that replacement of SF has major effect on durability aspects when compared to fly ash and GGBS replacement to fine aggregates. Use of silica fume reduces the slump flow and Poisson's ratio of SCC.

List of significant variables affecting characteristics of SCC has been tabulated in Table 4.23.

Table 4.23 Significant variables affecting characteristics of SCC with fly ash, GGBS and silica fumes replacement to fine aggregates

Target Characteristics	Fly ash	GGBS	Silica fume
SlS	W/C, W	W/C, W	FA, SF
SlS50	–	W/C, W	FA, SF
VT10	FA, F	W/C, W	FA, SF
VT50	W/C, W	W/C, W	W/C, W
LB(H2/H1)	–	–	W/C, W
UB(H2/H1)	W/C, W	W/C, W	W/C, W
CS28	W/C, W	W/C, W	FA, SF
CS90	FA, F	FA, GGBS	FA, SF
STS28	W/C, W	W/C, W	–
FlS28	W/C, W	FA, GGBS	–
E	W/C, W	–	–
PR	–	W/C, W	–
Wabs	–	W/C, W	–
SRP28	–	W/C, W	–
RCPT28	–	W/C, W	–
WL_AA	–	W/C, W	–
WL_SA	–	W/C, W	–
WL_Cor	–	W/C, W	–

Text code: Navy blue colour indicate positive correlation; Red colour indicate negative correlation.

4.5 STRENGTH AND DURABILITY OF GEO-POLYMER CONCRETE

Strength and durability characteristics of geo-polymer concrete have been studied with the aid of POD for an available dataset. Analysis, results, interpretation of POD outcomes and appreciation of behavioural aspects of GPC in aggressive environments have been highlighted.

4.5.1 Data – Source and pre-processing

1. Source: Rejilin (2018)

Available data set on geo-polymer concrete cured at ambient temperature has been taken up to study the interaction of concrete variables with its cardinal properties. Data consists of three cases of blends without fibre (FC, FG, GC) and three cases with fibre (FRFC, FRFG, FRGC).

Fine aggregate (630 kg/m^3), coarse aggregate (1800 kg/m^3), NaOH (57.15 kg/m^3), Na_2SiO_3 (142.85 kg/m^3), Gujcon CRF fibres (7 g/m^3) and total fines quantity (400 kg/m^3) are adopted and maintained constant for all combination of concrete mixes.

The data available as variables considered for the study are in Table 4.24.

Table 4.24 Geo-polymer concrete data variable list

Variables	Symbols	Variables	Symbols
1. Cement	C	7. Split tensile strength at 7 days	STS7
2. Fly ash	F	8. Split tensile strength at 28 days	STS28
3. Ground granulated blast furnace slag	GGBS	9. Modulus of elasticity	E
4. Slump	Sl	10. Weight loss due to acid attack	WL_AA
5. Compressive strength at 7 days	CS7	11. Strength loss due to acid attack	CSL_AA
6. Compressive strength 28 days	CS28	12. Strength loss due to thermal shock	CSL_TS
		13. Strength loss due to exposure to fire	CSL_Fire

2. Total number of variables: 13 Quantitative

3. Total number of observations (Individuals)**:** 60

4. Matrix size of quantitative data: 60×13

5. Missing values: Collected data has no missing value.

6. Bartlett sphericity test

$\chi^2 = 3112.59$

DF = 78

Probability value $\cong 2.22\times10^{-16} < 0.05$

Reject the null hypothesis. Data is not spherical and is accepted for analysis by POD

7. Descriptive statistics: Refer to Table 4.25 for basic statistical details of GPC data.

Table 4.25 Descriptive statistics of GPC data

Variables	Units	Mean	SD	Min	Max
C	kg/m^3	164	167.28	0	400
F	kg/m^3	176	166.12	0	400
GGBS	kg/m^3	60	96.78	0	400
Fibres	g/m^3	3.5	3.53	0	7
Sl	mm	69.48	18.24	20	89
CS7	N/mm^2	36.9	20.18	8.13	76.33
CS28	N/mm^2	51.42	23.23	10.59	96.53
STS7	N/mm^2	3.13	1.74	0.35	6.73
STS28	N/mm^2	4.53	1.83	0.72	7.97
E	N/mm^2	35.07	7.66	15.48	48.84
WL_AA	Percent	1.22	0.43	0.48	2.3
CSL_AA	Percent	3.35	2	0.18	7.55
CSL_ TS	Percent	1.91	1.43	0.09	5.7
CSL_ Fire	Percent	3.13	2.05	0.27	8.49

4.5.2 Correlation matrix

Data has been normalised before the POD application.

Since there are six cases in collected GPC data, it would result in six correlation matrices. Also, from previous analyses it is apparent that the relationship between variables will be well captured and projected in first few components; correlation matrix values have not been presented for the chosen set of data.

4.5.3 Performing orthogonal decomposition for GPC data

The normalised dataset correlation matrices have been subject to eigenvalue decomposition, and results are presented in Tables 4.26 and 4.27.

Table 4.26 Eigenvalues of GPC data

Cases	**FC**	**FRFC**	**FG**	**FRFG**	**GC**	**FRGC**
λ_1	7.83	8.70	10.46	10.38	7.87	7.23
Var. %	65.20	72.50	87.20	86.60	65.60	60.30
λ_2	2.87	2.65	0.90	0.86	3.86	4.51
Var. %	23.90	22.10	7.50	7.20	32.30	37.60
Cum. Var. %	89.10	94.60	94.70	93.80	97.80	97.90

Table 4.27 First two components of FC, FRFC, FG, FRFG, GC, FRGC mix concrete data without and with fibres

Cases	FC		FRFC			FG		FRFG			GC		FRGC	
Variables	D_1	D_2	D_1	D_2		D_1	D_2	D_1	D_2		D_1	D_2	D_1	D_2
C	0.55	0.80	0.46	-0.88	F	-0.98	-0.06	-0.98	0.05	C	0.51	0.86	0.62	0.78
F	-0.55	-0.80	-0.46	0.88	GGBS	0.98	0.06	0.98	-0.05	GGBS	-0.51	-0.86	-0.62	-0.78
Sl	-0.76	-0.63	-0.55	0.83	Sl	-0.92	-0.14	-0.95	-0.22	Sl	0.57	0.82	0.64	0.76
CS7	0.98	-0.09	0.98	0.11	CS7	0.96	0.16	0.98	-0.02	CS7	0.97	0.20	0.99	-0.01
CS28	0.95	-0.24	0.97	0.17	CS28	0.97	0.14	0.99	-0.03	CS28	0.99	0.03	0.97	-0.21
STS7	0.95	-0.28	0.98	0.01	STS7	0.99	0.09	0.97	0.23	STS7	0.98	0.02	0.99	-0.06
STS28	0.96	-0.14	0.96	0.11	STS28	0.97	0.14	0.95	0.21	STS28	0.99	-0.07	0.98	-0.21
E	0.97	-0.13	0.98	0.07	E	0.97	0.20	0.96	0.23	E	0.99	0.08	1.00	-0.05
WL_AA	-0.98	-0.14	-0.98	0.10	WL_AA	-0.94	-0.22	-0.91	-0.22	WL_AA	-0.46	0.85	-0.66	0.72
CSL_AA	-0.77	0.49	-0.86	-0.37	CSL_AA	-0.82	0.48	-0.85	0.49	CSL_AA	-0.89	0.41	0.41	0.89
CSL_ TS	-0.69	0.43	-0.88	-0.31	CSL_ TS	-0.88	0.38	-0.86	0.05	CSL_ TS	-0.89	0.41	-0.67	0.70
CSL_ Fire	0.04	0.76	-0.87	-0.35	CSL_ Fire	-0.79	0.57	-0.77	0.61	CSL_ Fire	-0.61	0.78	-0.39	0.91

As per Table 4.26, twelve-dimensional data set can be reduced to 2-dimensions as the first two axes account for about 90% of variation.

Coordinate information of components in reduced dimensional space has been organised in Table 4.27. The coefficients reveal orientation of variables to lie in a specific dimension.

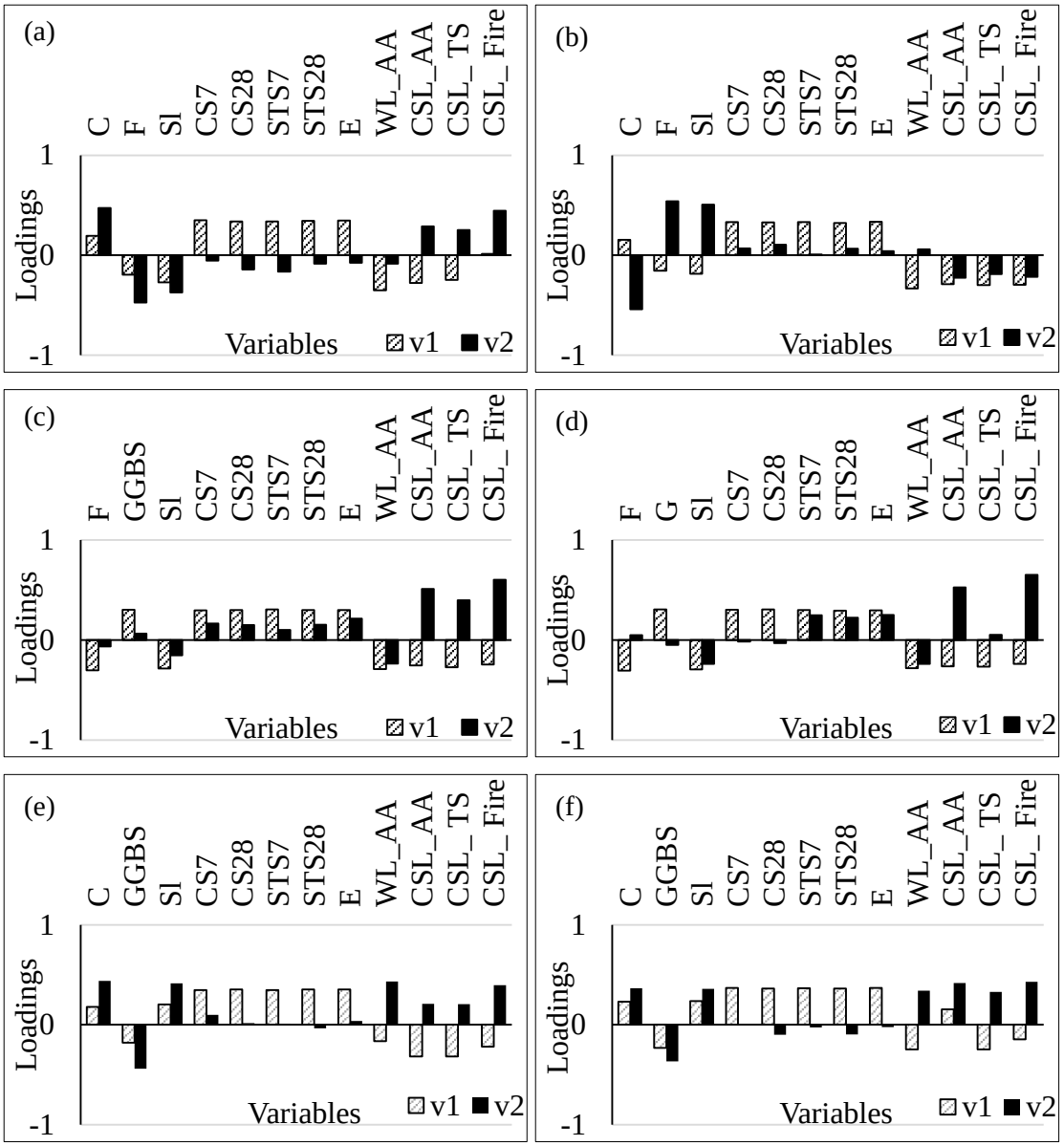

Figure 4.13 Vector loadings (a) FC (b) FRFC (c) FG (d) FRFG (e) GC (f) FRGC

Vector loadings shown in Fig. 4.13 give an idea of amount of contribution of variables to each dimension and nature of contribution.

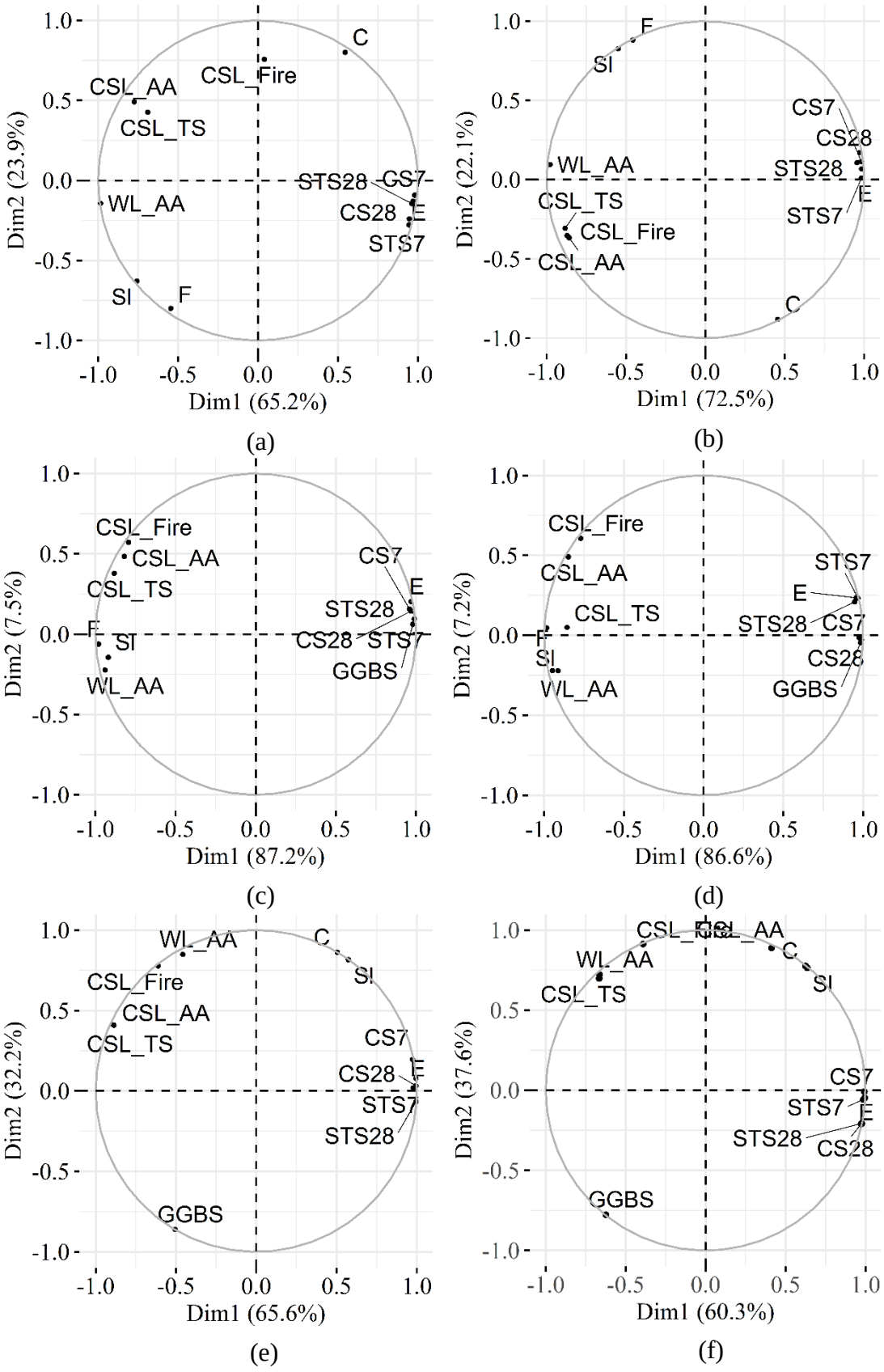

Figure 4.14 Component plot (a) FC (b) FRFC (c) FG (d) FRFG (e) GC (f) FRGC

Component Plots

Fig. 4.14 shows component plots that are of utility in identifying prime variables influencing targeted concrete characteristics. This exercise immensely helps in discarding variables that do not affect target characteristics. Such elimination vastly reduces time and efforts in modelling and simulations.

It is observable from correlation plots (Fig. 4.14a & 4.14b) of cement-fly ash based mixes that WL_AA, CSL_AA and CSL_TS are negatively correlated to strength of concrete. In mixes without fibres, CSL_Fire is not well correlated with any other variables considered. With addition of fibres, CSL_Fire is negatively correlated to strength variables. Slump is strongly and positively correlated to fly ash content.

As observed from Figs. 4.14c and 4.14d, in FG and FRFG mixes also, slump increases as fly ash content increases. Strength parameters are positively correlated to GGBS and negatively correlated to fly ash contents. WL_AA, CSL_AA, CSL_TS and CSL_Fire are more in mixes with higher fly ash quantities. Addition of fibres does not show much change in nature of variables interaction.

Figs. 4.14e and 4.14f show that usage of fibres in cement-GGBS based mixes has highest influence on CSL_AA. In mixes without fibres CSL_AA has negative correlation with strength whereas in mixes with fibres CSL_AA has high positive correlation with cement content. Slump increases with an increase in OPC content. Weight loss due to acid exposure and strength loss due to thermal shock & exposure to fire are negatively correlated to 28 days' compressive strength.

4.6 PERFORMANCE-BASED DESIGN OF CONCRETE BY INNOVATIVE CEMENT COMBINATIONS

Innovative cement combinations are being tried for accomplishment of economic growth with due concern to environment. To pick the most appropriate combination for a given situation, POD can be a valid decision-making tool. Arrival at the judicious combination by way of determining performance index has been elaborated.

4.6.1 Data – Source and pre-processing

1. Source: Dhir et al. (2010)

Available data set "Innovative cement combinations for concrete performance" has been studied using POD technique. Data set of 159 observations and 58 variables reduced to matrix of 159×35 size after removing variables with missing values and this matrix further categorised into 13 case-specific combinations (see Table 4.32). Ordinary Portland cement – CEMI (PC) based unary mixes, flyash (F), ground granulated blast-furnace slag (GGBS), silica fume (SF), metakaolin (MK) and limestone (LS) based binary and ternary mixes had been formulated and experimentally studied (Dhir et al. 2010). Along with available data on quantities of these mineral admixtures, their corresponding percentages in total fines content (T_fines) are also taken as variables (PCp, Fp, GGBSp, SFp, MKp, LSp) to assist the data analysis.

As reported, 0.35, 0.50 and 0.65 water binder ratios W/B (by weight) and 470, 330 and 255 kg/m^3 binder contents were adopted. Superplasticizer was used to maintain nominal slump of 75±25 mm, (British Standards Institution 2000). A water content of 165 kg/m^3 was maintained across all mixes. Fine aggregate (FA), 10 mm downsize coarse aggregate (CA5_10), 20 mm downsize coarse aggregate (CA10_20) contents ranged between 434–867.40 kg/m^3, 286–385 kg/m^3 and 725–765 kg/m^3 respectively.

Compressive strength of 100 mm cubes at 3, 7, 28, 90, 180 days (CS3, CS7, CS28, CS90, CS180), expected time to achieve 10 N/mm^2 strength (ET_10MPa), initial surface absorption (ISAT28, ISAT180), sorptivity (SRP28, SRP180), water penetration (WP28, WP180), air permeability (AP28, AP180) at 28 and 180 days, carbonation depth (Car8w, Car20w) at 8 and 20 weeks and embodied carbon dioxide (Emb_CO2) are available as data on target performances. Blaine fineness and particle density test results reported are as mentioned in Table 4.29.

Table 4.28 Data variable list of innovative cement combinations for concrete performance

Sl No.	Variables	Symbols	Units	N	Mean	SD	Min.	Max.
01.	Portland cement (CEMI)	PC	kg/m^3	159	184.18	106.54	25.00	475.00
02.	Fly ash	F	kg/m^3	159	36.45	57.02	0.00	255.00
03.	Ground granulated blast-furnace slag	GGBS	kg/m^3	159	97.70	109.28	0.00	420.00
04.	Lime stone	LS	kg/m^3	159	16.92	35.64	0.00	165.00
05.	Metakaolin	MK	kg/m^3	159	10.25	18.65	0.00	70.00
06.	Silica fume	SF	kg/m^3	159	5.69	12.37	0.00	50.00
07.	Fine aggregate or sand	FA	kg/m^3	159	743.71	78.77	625.00	845.00
08.	Coarse aggregates (5–10mm size)	CA5_10	kg/m^3	159	374.65	5.37	355.00	385.00
09.	Coarse aggregates (10–20mm size)	CA10_20	kg/m^3	159	751.91	9.57	725.00	765.00
10.	Total fines	T_Fines	kg/m^3	159	351.19	91.09	245.00	480.00
11.	Portland cement (percentage)	PCp	%	159	52.42	26.12	9.09	100.00
12.	Fly ash (percentage)	Fp	%	159	10.51	15.76	0.00	55.38
13.	Ground granulated blast-furnace slag (percentage)	GGBSp	%	159	27.69	29.23	0.00	90.91
14.	Limestone (percentage)	LSp	%	159	4.81	9.75	0.00	36.36
15.	Metakaolin (percentage)	MKp	%	159	2.94	5.15	0.00	16.00
16.	Silica fume (percentage)	SFp	%	159	1.63	3.38	0.00	10.64
17.	Water to binder ratio	W/B	Ratio	159	0.50	0.12	0.34	0.67
18.	Cube compressive strength at 3 days	CS3	MPa	159	18.46	12.60	2.00	56.00

Sl No.	Variables	Symbols	Units	N	Mean	SD	Min.	Max.
19.	Cube compressive strength at 7 days	CS7	MPa	159	27.79	15.50	5.00	70.00
20.	Cube compressive strength at 28 days	CS28	MPa	159	41.26	17.73	10.00	86.00
21.	Cube compressive strength at 90 days	CS90	MPa	159	49.94	18.76	14.50	94.00
22.	Cube compressive strength at 180 days	CS180	MPa	159	54.46	19.08	17.00	96.00
23.	Initial surface absorption test at 28 days	ISAT28	$(\times 10^{-2})$ ml/m^2 s	159	49.42	14.91	27.50	102.00
24.	Initial surface absorption test at 180 days	ISAT180	$(\times 10^{-2})$ ml/m^{2}s	159	35.91	13.21	14.90	87.00
25.	Sorptivity at 28 days	SRP28	$(\times 10^{-4})$ mm/$\sqrt{s}$	159	269.25	94.06	95.00	620.00
26.	Sorptivity at 180 days	SRP180	mm/$\sqrt{s}$	159	195.86	77.38	70.00	465.00
27.	Water penetration at 28 day curing	WP28	mm	159	32.35	20.48	5.00	110.00
28.	Water penetration at 180 day curing	WP180	mm	159	17.20	11.35	2.00	70.00
29.	Intrinsic air permeability at 28 days curing	AP28	$(\times 10^{-17})$ m^2	159	5.54	5.91	0.99	30.00
30.	Intrinsic air permeability at 180 days curing	AP180	$(\times 10^{-17})$m^2	159	4.62	5.21	0.56	25.10
31.	Embodied CO_2 per kg	EmbCO2	kg/m^3	159	0.84	0.49	0.25	2.60
32.	Expected time to reach 10 MPa cube strength	ET_10MPa	h	159	61.57	91.68	4.40	672.00
33.	Accelerated carbonation depth at 8 weeks	Car8w	mm	141	18.71	11.33	1.50	50.00
34.	Accelerated carbonation at depth 20 Weeks	Car20w	mm	141	25.01	13.44	4.00	52.00
35.	Non-steady state chloride migration for 28 days cured concrete	Cl_Mig28	$(\times 10^{-12})$ m^2/s	32	12.13	8.64	2.30	33.90

Sl No.	Variables	Symbols	Units	N	Mean	SD	Min.	Max.
.36.	Non steady state chloride migration for 90 days cured concrete	Cl_Mig90	($\times 10^{-12}$) m^2/s	22	10.12	9.15	1.40	29.50
37.	Chloride migration for 180 days cured concrete	Cl_Mig180	($\times 10^{-12}$) m^2/s	22	7.84	7.48	0.70	23.80
38.	Heat of hydration – rate of evolution	HoH_RoE	W/kg	28	2.69	0.83	1.39	4.06
39.	Time to reach maximum rate of HoH	HoH_T	h	28	9.22	1.70	7.40	13.60
40.	Total heat evolved in 72 h	HoH_Tot	KJ/kg	28	207.07	45.82	128.00	268.00
41.	Quantity of $CaOH_2$ at 28 days	CaOH2_28	% Cement Mass	29	11.97	5.35	4.20	22.90
42.	Quantity of $CaOH_2$ at 180 days	CaOH2_180	% Cement Mass	25	11.49	6.22	3.40	24.10
43.	Superplasticizer dosage	SP	% of Cement	159	0.32	0.13	0.14	0.76
44.	Embodied CO_2 at 3 days cube strength	Emb.CO2_CS3	MPa	39	15.64	3.26	9.80	22.90
45.	Embodied CO_2 at 180 days cube strength	Emb.CO2_CS1	MPa	39	54.34	5.13	43.50	66.00
46.	Embodied CO_2	Emb.CO2_Per2	kg/m^3	39	177.26	43.43	102.00	277.00
47.	Initial surface absorption test at 28 days	ISTA10_28	$ml/(m^2.s)$	39	45.30	7.48	32.70	63.60
48.	Initial surface absorption test at 180 days	ISTA10_180	$ml/(m^2.s)$	39	31.24	6.09	19.70	45.60
49.	Water penetration at 28 day curing	WP_40MPa_28	mm	39	27.54	10.30	12.30	55.00
50.	Water penetration at 180 day curing	WP_40MPa_18	mm	39	13.31	4.18	7.00	24.00
51.	Sorptivity at 28 days	SRP_40MPa28	($\times 10^{-4}$) $mm/\sqrt{s}$	39	235.62	49.02	108.00	342.00
52.	Sorptivity at 180 days	SRP_40MPa180	($\times 10^{-4}$) $mm/\sqrt{s}$	39	172.49	41.95	75.00	271.00
53.	Intrinsic air permeability at 28 days curing	IA_40MPa28	($\times 10^{-17}$) m^2	39	3.90	2.79	1.07	11.61

Sl No.	Variables	Symbols	Units	N	Mean	SD	Min.	Max.
54.	Intrinsic air permeability at 180 days curing	IA_40MPa180	($\times 10^{-17}$) m^2	39	3.10	2.27	0.89	8.90
55.	Accelerated carbonation depth at 8 weeks	Carb40MPa8w	mm	39	17.67	5.60	9.50	29.00
56.	Accelerated carbonation depth at 20 weeks	Carb40MPa20w	mm	39	24.94	7.07	14.00	42.00
57.	Non steady state chloride migration for 28 days cured concrete	Cl40MPa28	($\times 10^{-12}$) m^2/s	32	12.33	10.06	2.00	44.10
58.	Non steady state chloride migration for 180 days cured concrete	Cl40MPa180	($\times 10^{-12}$) m^2/s	13	11.76	10.44	2.10	32.80

Table 4.29 Reported values of Blaine fineness and particle density

Property	PC		F	GGBS	MK	LS	SF
Blaine fineness, m^2/kg	410	370	10.2	450	12400	1550	24000
Particle density, g/cm^3	3.14	3.14	2.20	2.91	2.59	2.63	2.10

2. Total number of variables: 58 Quantitative (Table 4.28)

3. Observations (Individuals): 159

4. Quantitative data size: 159 × 58

5. Missing values: Collected data has many missing values. Variables with missing values are excluded from POD analysis. Data without missing values reduces to a matrix of 159 × 33 size.

6. Bartlett sphericity test

$\chi^2 = 13708.26$

DF = 528

Probability value $\cong 2.22 \times 10^{-16} < 0.05$

Reject the null hypothesis. Data is not spherical and is accepted for analysis by POD.

7. Descriptive statistics

Statistical information of binary and ternary blend mix concrete data is given in Table 4.28.

Data has been classified (Table 4.30) based on mix ingredients and are analysed separately to understand variable interaction across the type of mixes.

Table 4.300 Innovative cement combinations for concrete performance data classification chart

	Combination	Notation	N	P
Ternary Blends	PC + F + GGBS	PFG	15	29
	PC + F + LS	PFL	9	29
	PC + F + MK	PFM	15	29
	PC + F + SF	PFS	12	29
	PC + GGBS + LS	PGL	21	27
	PC + GGBS + MK	PGM	21	27
	PC + GGBS + SF	PGS	15	27
Binary Blends	PC + F	PF	9	27
	PC + GGBS	PG	12	25
	PC + LS	PL	9	27
	PC + MK	PM	9	27
	PC + SF	PS	6	27
Cement based Mix	PC	P	6	24

Z-score standardization has been carried out to normalize the data.

4.6.2 Correlation matrix

Obtained correlation matrices of different combinations of mix have been subject to POD analysis.

4.6.3 Performing orthogonal decomposition for innovative cement combinations for concrete performance data

Table 4.31 Eigenvalues

Cases	λ_1	Var. %	λ_2	Var. %	Cum. Var %
PFG	20.39	70.31	5.05	17.42	87.73
PFL	20.87	71.97	5.01	17.29	89.26
PFM	18.19	62.74	7.30	25.16	87.89
PFS	18.75	64.65	6.87	23.69	88.34
PGL	16.97	62.83	6.87	25.43	88.27
PGM	16.43	60.85	7.18	26.59	87.44
PGS	16.67	61.75	7.51	27.80	89.54
PF	19.40	71.85	5.83	21.61	93.46
PG	17.09	68.36	6.23	24.91	93.27
PL	21.62	80.07	4.05	14.99	95.06
PM	20.92	77.50	3.47	12.84	90.33
PS	21.36	79.12	3.44	12.74	91.86
P	21.36	89.00	1.61	6.72	95.72

Eigenvalues obtained are listed in Table 4.31. The first two dimensions have been investigated for targeted performance appraisal of concrete with an emphasis on significant variables, as these dimensions explain about 87% of the inherent variation. Component plots have been presented in Fig. 4.15.

Cause-effect relation has been inferred from the correlation coefficients. Variables interaction have been analyzed using correlation values and component plots.

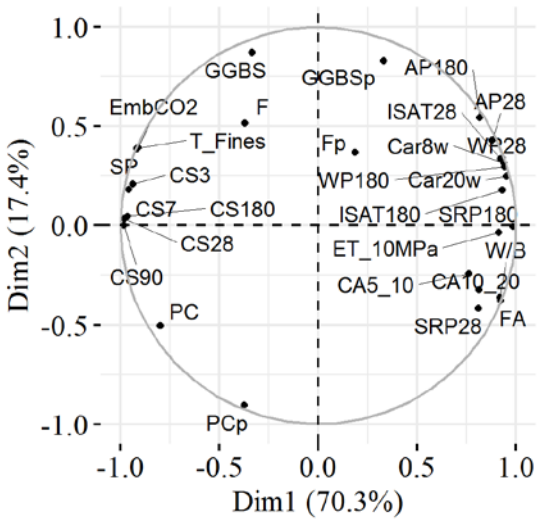

(a) PFG

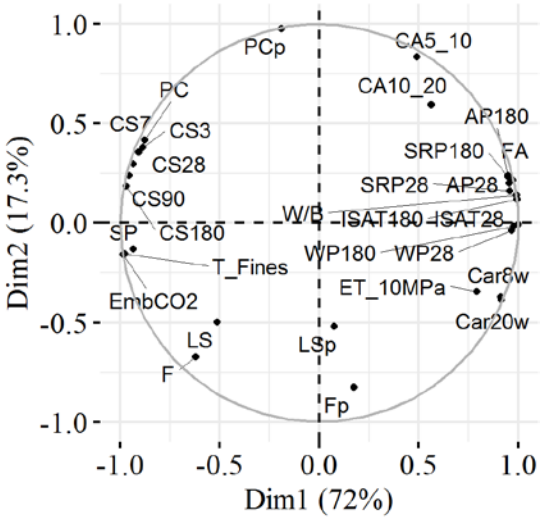

(b) PFL

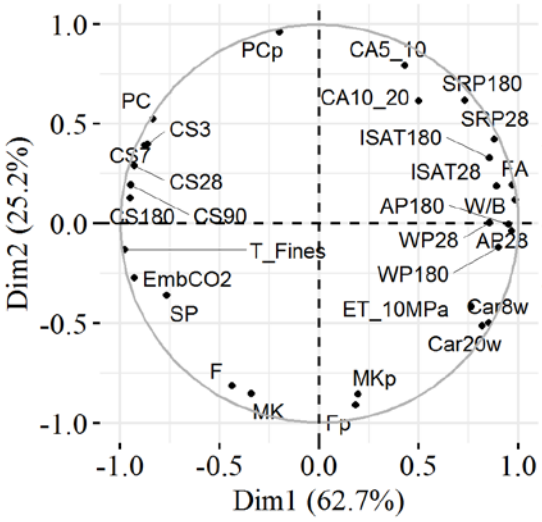

(c) PFM

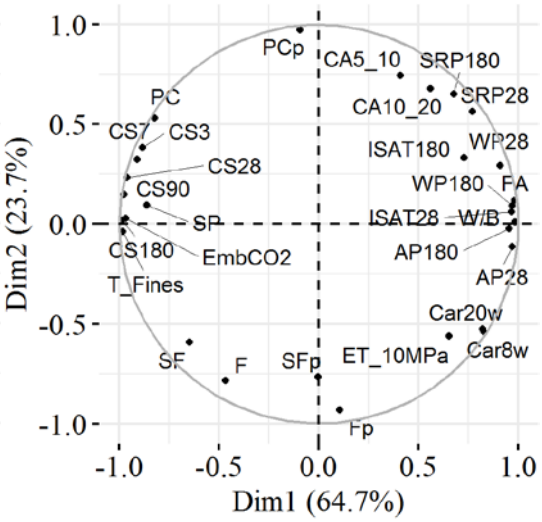

(d) PFS

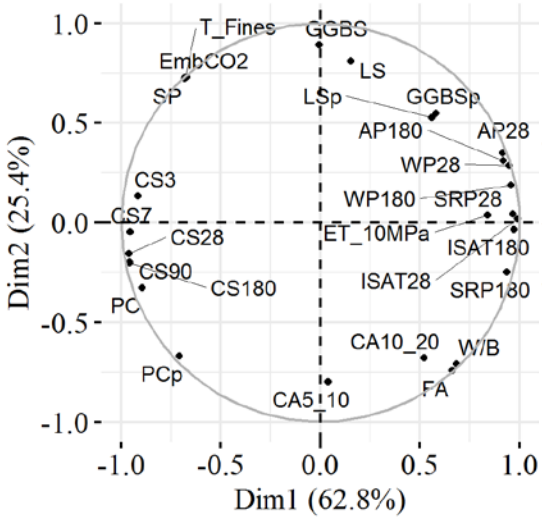

(e) PGL

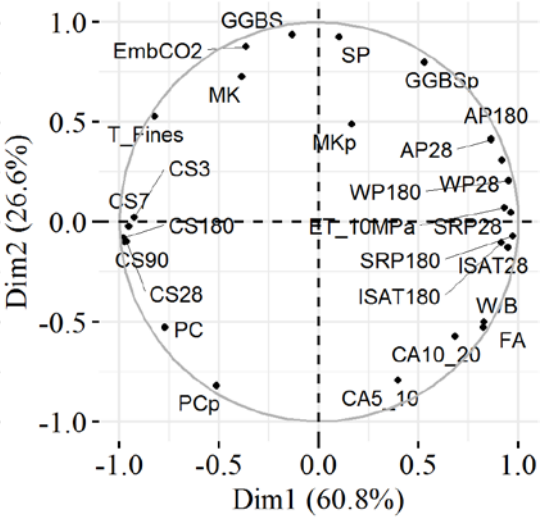

(f) PGM

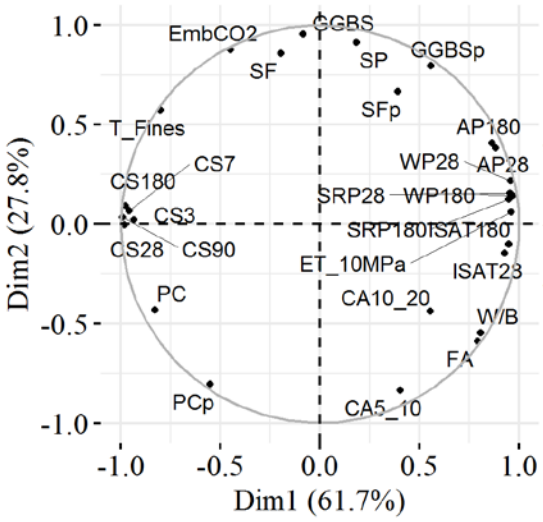

(g) PGS

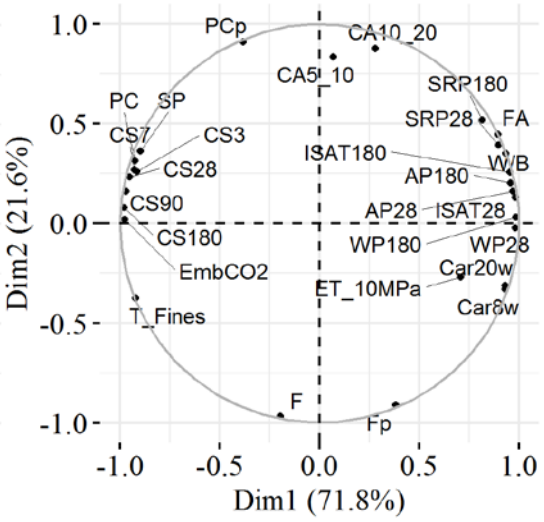

(h) PF

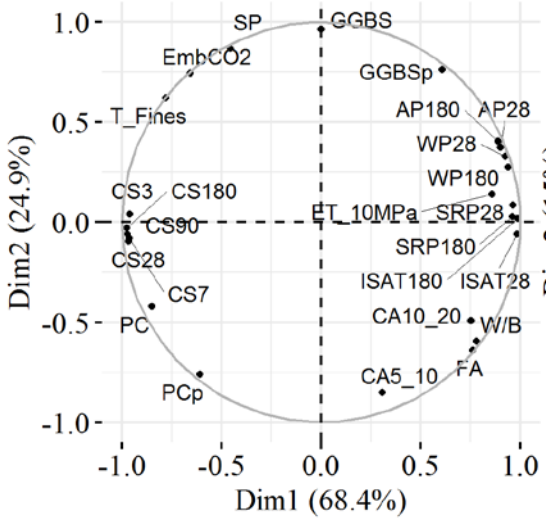

(i) PG

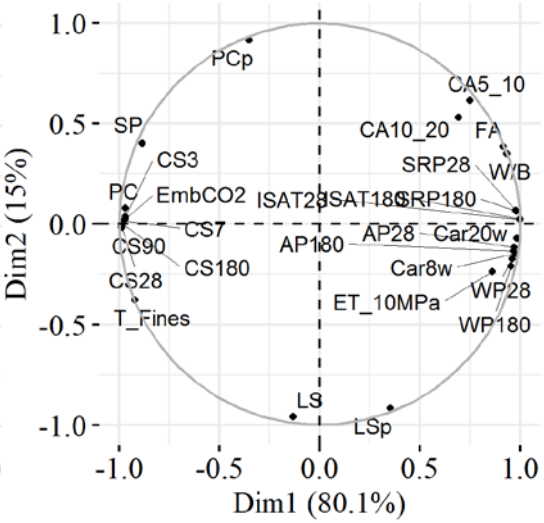

(j) PL

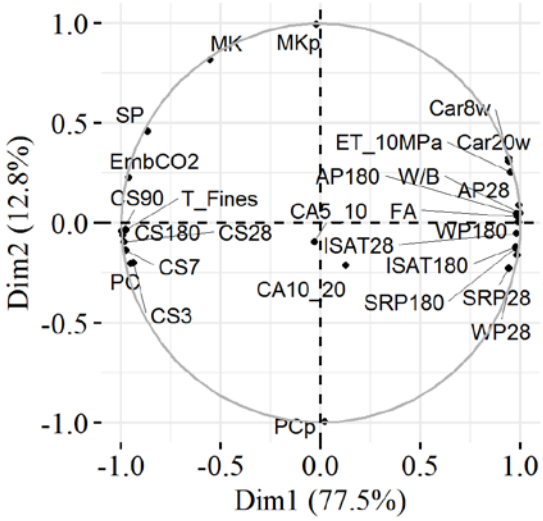

(k) PM

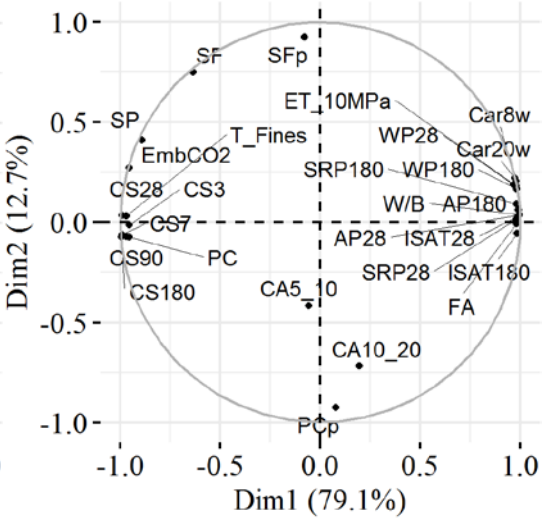

(l) PS

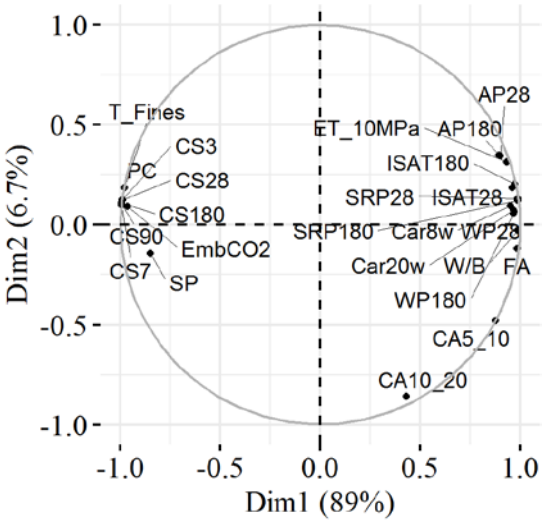

(m) P

Figure 4.15 Correlation plots for innovative cement combinations for concrete performance data

4.6.4 Inferences from component plots

For all concrete formulations

POD accomplishes dimensionality reduction of data by explaining that, 87% of the variation is explained by first two components and limiting consideration of these two components with just 13% loss of information, reduces time and effort. Component plots in addition to helping in dimensionality reduction enhance visualization and understanding of variable interaction.

Observation of component plots helps in segregating cement mixes from binary and ternary as variables are concentrated around 1st dimension for PC (Fig. 4.15 m) and not so for binary (Fig. 4.15 h – l) and ternary (Fig. 4.15 a – g).

As 1st component explains the maximum variation strength characteristics in almost all plots and ISAT28, ISAT180, SRP28, SRP180, WP28, WP180, AP28, AP180, Car8w, Car20w in majority of the plots lie around 1st axis indicating variation due to mix proportions.

Correlation plots suggest that variables affecting strength and adsorption, permeation and carbonation are at loggerheads. Cement content and strength have a positive correlation, whereas cement content and ISAT28, ISAT180, SRP28, SRP180, WP28, WP180, AP28, AP180, Car8w, Car20w have a negative correlation. Sorption, surface

adsorption, water & air permeability and carbonation characteristics are positively correlated to W/B ratio and fine aggregate contents. Super-plasticiser used enhances workability, contribute to strength enhancement and durability. Embodied CO_2 is positively correlated to OPC, T_Fines and SP contents. Maximum size of coarse aggregate has not significantly affected concrete characteristics in comparison to other variables.

Specific trends observed for blends

Binary Blends

Figs. 4.20 (k) and 4.20 (l), component plots for PM and PS blends show strength increase with increase in metakaolin and silica fume contents whereas increase in GGBS reduces strength as indicated by Fig. 4.15 (i). Addition of fly ash or limestone has not changed strength characteristics much (Fig. 4.15 (h) and 4.15 (j)). This difference is due to the higher fineness of silica fume and metakaolin in comparison to GGBS, flyash and limestone. Higher GGBS contents lead to increased permeability which adversely affects durability, and this aspect is highlighted by Fig. 4.15 (i).

Ternary Blends

Component plots for all fly ash based ternary blends (Figs. 4.15 a, b, c & d) indicate positive correlation of strength with variables, suggesting accomplishment of higher strength as possible with blends. However, corresponding weak correlation in GGBS based ternary mixes (Figs. 4.15 e, f & g) suggest futility of such blending exercise. Component plots also provide indications to the order for discrimination of these blends. A deviation in direct inverse relation of strength and W/B is observed for GGBS blends except for PFG case, needs further probing to account for the deviation.

On the whole fly ash based ternary blends have performed better than GGBS.

4.6.5 Identification of significant variables for possible dimensionality reduction

Significant variables identified based on significant correlation values and examination of component plots have been summarised in Table 4.32. Based on the need and objective of works at site, variables recognised can be fine-tuned to obtain targeted performance levels.

Text code: Navy blue colour indicate positive correlation; Red colour indicate negative correlation.

Table 4.32 List of significant variables for cement, binary and ternary blend concrete mixes

Performance Characteristics	Cases			
	PFG	**PFL**	**PFM**	**PFS**
EmbCO2	T_Fines, SP, FA, W/B, CA10_20, CA5_10	W/B, FA, T_Fines, SP, PC	FA, T_Fines, W/B, SP	SP, T_Fines, W/B, FA, PC
CS3	T_Fines, SP, FA, W/B, CA10_20, CA5_10, PC	PC, T_Fines, W/B, FA, SP	PC, T_Fines, W/B, FA	PC, T_Fines, W/B, FA, SP
CS7				
CS28				
CS90				
CS180				
ET_10MPa	W/B, FA, SP, T_Fines, CA5_10	SP, PC, W/B	PC, W/B, T_Fines	PC, W/B
ISAT28	PC, W/B, FA, SP, T_Fines	W/B, FA, T_Fines, SP, PC	W/B, FA, T_Fines, SP	W/B, FA, T_Fines, SP, PC
ISAT180	W/B, FA, PC, SP, T_Fines			SP, SF, FA, W/B, T_Fines
SRP28	W/B, FA, SP, T_Fines, CA10_20, CA5_10	W/B, SP, FA, T_Fines, F, PC	FA, W/B, T_Fines, SP, F	F, SF, CA10_20, CA5_10, FA, W/B, T_Fines
SRP180	W/B, FA, SP, T_Fines, PC, CA10_20		F, FA, W/B, T_Fines, SP, MK, CA5_10	F, SF, CA10_20, CA5_10, FA, W/B

WP28	PC, W/B, FA, SP, T_Fines	SP, W/B, FA, T_Fines, PC	W/B, T_Fines, FA, SP, PC	FA, W/B, T_Fines, SP
WP180			W/B, T_Fines, FA, PC	W/B, FA, T_Fines, SP, PC
AP28	PC, PCp, GGBSp		W/B, FA, T_Fines, PC, SP	
AP180				
Car8w	PC, W/B, FA, SP, T_Fines	PC, W/B, T_Fines, FA, SP	PC, W/B, T_Fines, FA	PC, W/B, T_Fines, FA, SP
Car20w				

Table 4.32 List of significant variables for cement, binary and ternary blend concrete mixes (Continued)

Performance Characteristics	**Cases**			
	PGL	**PGM**	**PGS**	**PG**
EmbCO2	T_Fines, SP, FA, W/B, CA10_20, CA5_10	GGBS, SP, CA5_10, FA, CA10_20, T_Fines, W/B, MK	CA5_10, FA, T_Fines, GGBS, W/B, SF, SP, CA10_20	FA, T_Fines, SP, W/B, CA10_20, CA5_10, GGBS
CS3	PC, T_Fines, SP, W/B, FA	PC, T_Fines, FA, W/B, CA10_20	PC, T_Fines, W/B, FA	PC, CA10_20, T_Fines, W/B, FA
CS7	PC, GGBSp, LSp			
CS28	PC, PCp, GGBSp, LSp			
CS90				
CS180				
ET_10MPa	PC, GGBSp, LSp	W/B, FA, T_Fines	W/B, PC, T_Fines, FA	

ISAT28	PC, T_Fines, W/B, SP	FA, T_Fines	W/B, FA, T_Fines	PC, W/B, FA, T_Fines, CA10_20
ISAT180				
SRP28	PC, W/B, SP	W/B, FA, T_Fines	PC, W/B	
SRP180	W/B, FA, SP, T_Fines, PC			
WP28	PC, PCp, GGBS, LSp	PC, GGBSp, PCp	PC, W/B	PC, PCp, GGBSp
WP180				
AP28	PC, PCp, GGBS, LSp	PC, GGBSp, PCp	PC, GGBS, PCp	
AP180				

Table 4.32 List of significant variables for cement, binary and ternary blend concrete mixes (Continued)

Performance Characteristics	**Cases**				
	PF	**PL**	**PM**	**PS**	**P**
EmbCO2	PC, SP, T_Fines, W/B, FA	PC, SP, T_Fines, W/B, FA, CA10_20, CA5_10	T_Fines, FA, W/B, SP, PC, MK	FA, T_Fines, W/B, SP, PC, SF	PC, T_Fines, FA, SP, W/B, CA5_10
CS3	PC, SP, T_Fines, W/B, FA	PC, T_Fines, FA, W/B, SP, CA5_10, CA10_20	W/B, PC, T_Fines, FA, SP	W/B, FA, T_Fines, PC, SP	PC, T_Fines, FA, W/B, CA5_10, SP
CS7					
CS28					
CS90					
CS180					
ET_10MPa	PC, SP, W/B	SP, PC, W/B	W/B, FA, PC, T_Fines, SP	W/B, FA, T_Fines, PC, SP	W/B, FA, PC, T_Fines, SP

ISAT28	W/B, FA, T_Fines, PC, SP	PC, W/B, T_Fines, FA, SP, CA5_10	W/B, FA, T_Fines, SP, PC	W/B, FA, T_Fines, PC, SP	W/B, FA, T_Fines, PC, SP, CA5_10
ISAT180	W/B, FA, T_Fines, PC				
SRP28	W/B, FA, T_Fines	W/B, FA, T_Fines, PC, SP, CA5_10	W/B, SP, FA, T_Fines, PC, MK		W/B, FA, T_Fines, PC, CA5_10, SP
SRP180					
WP28	W/B, SP, T_Fines, PC, FA,	SP, PC, W/B, FA, T_Fines	W/B, FA, T_Fines, PC, SP	W/B, FA, PC, T_Fines, SP	
WP180					
AP28	W/B, FA, T_Fines, PC, SP	PC, SP, W/B, FA, T_Fines	W/B, FA, T_Fines, PC, SP	W/B, FA, T_Fines, PC, SP	SP, W/B, FA, PC, T_Fines
AP180					
Car8w	PC, SP, W/B, T_Fines, FA	PC, SP, W/B, FA, T_Fines	W/B, PC, FA, T_Fines,	W/B, FA, PC, T_Fines, SP	W/B, FA, T_Fines, PC, CA5_10, SP
Car20w					

4.7 DESIGN AIDS FROM POD

4.7.1 Performance index

A Performance index has been developed and proposed to quantify relative performance of mixes with significant variables identified from POD. Component weights have been multiplied by scaled variable values, to quantify positive and negative effects as Q_P and Q_N, respectively. Ratios of normalised positive and negative effects give relative performance indices. The general form of performance index proposed is detailed in Eq. 4.01.

$$PI_x = \frac{Q_P/Q_{P,max}}{Q_N/Q_{N,min}} \quad (4.01)$$

where,

Q_P, Q_N : Quantity of Positive and Negative effects which are computed using Eq. 4.02.

$$Q_{Effect,x} = \left(\frac{1}{m}\sum_{k=1}^{m} D_{1,y_k}\ \frac{y_k}{y_{k,ref}}\right) \times D_{1,x} + \left(\frac{1}{m}\sum_{k=1}^{m} D_{2,y_k}\ \frac{y_k}{y_{k,ref}}\right) \times D_{2,x} \qquad (4.02)$$

$Q_{P,max}$: Maximum value of Q_P computed

$Q_{P,min}$: Minimum value of Q_N computed

m : Number of significant variables

D : Component weight

y_k : Important variables affecting target characteristics, as listed in Table 4.32.

y_{ref} : Reference maximum value of the variable in dataset (Table 4.33)

Table 4.33 Reference maximum values

Variables	Reference Values (kg/m^3)	Variables	Reference Values (%)	Variables	Reference Values
PC	475	PC_p	100	T_Fines	480 kg/m^3
F	255	F_p	55	W/B	0.67
GGBS	420	$GGBS_p$	90.91	CA5_10	385 kg/m^3
SF	50	SF_p	10.6	CA10_20	765 kg/m^3
MK	70	MK_p	36.36	FA	845 kg/m^3
LS	165	LS_p	10	SP	0.76 (% of PC)

High performance index will be obtained for formulations for which positive attributes are maximum and negative are minimum.

4.7.2 Design charts

For all concrete formulations, indices obtained have been mapped against corresponding concrete performance characteristics as reported in data (Fig. 4.16). Blue, yellow and red ellipses are the regions of 95% CI for 0.35, 0.50 and 0.65 W/B ratios respectively.

From performance indices and also from Fig. 4.16, for the data analysed fly ash based mixes have exhibited their superiority over GGBS based mixes in satisfaction of performance basis.

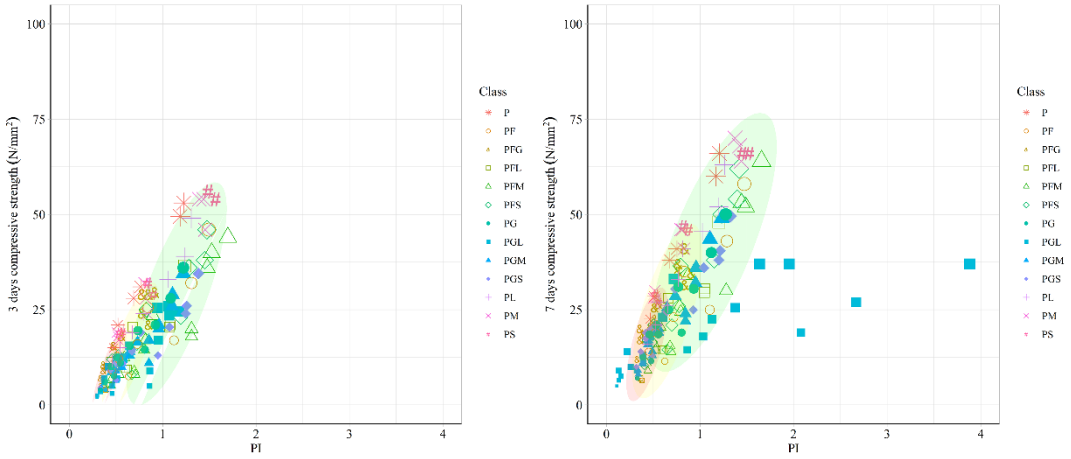

(a) 3 day's compressive strength

(b) 7 day's compressive strength

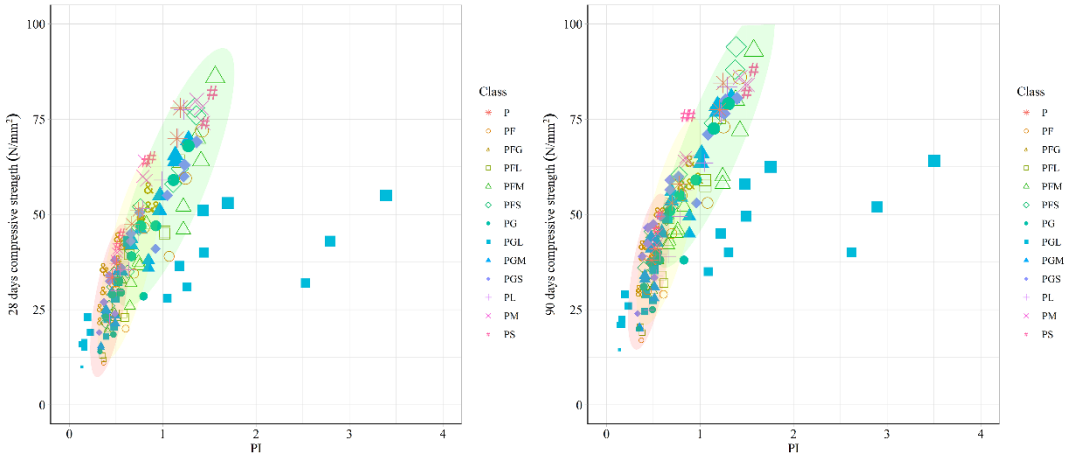

(c) 28 day's compressive strength

(d) 90 day's compressive strength

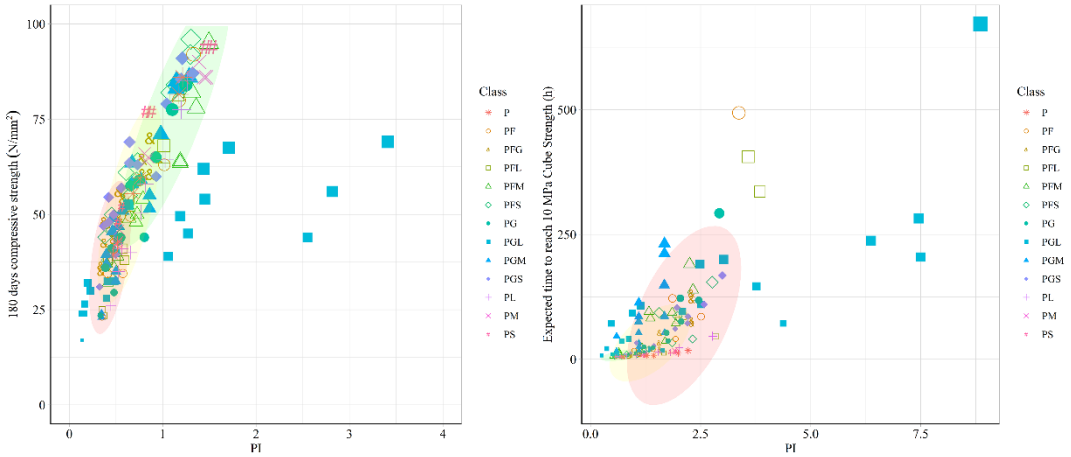

(e) 180 day's compressive strength (f) Expected time to reach 10 MPa cube strength

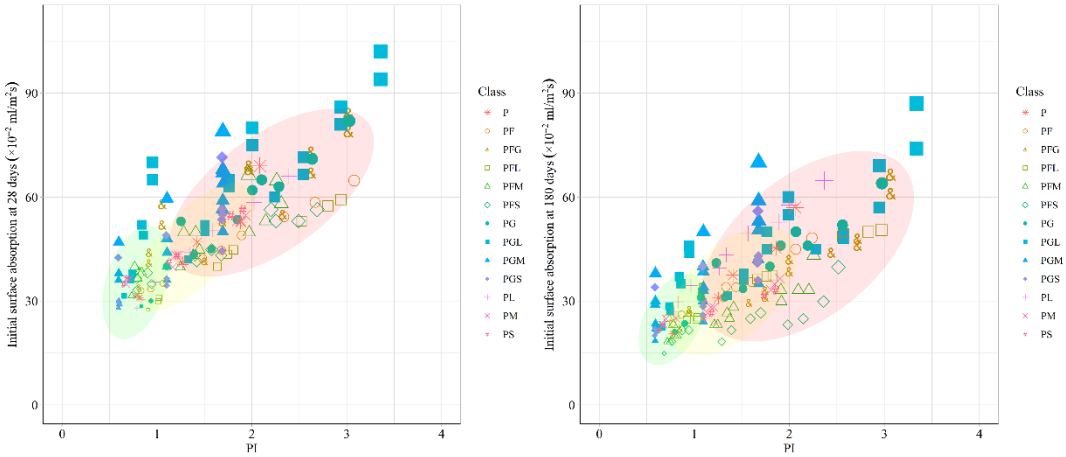

(g) Initial Surface Adsorption at 28 days (h) Initial Surface Adsorption at 180 days

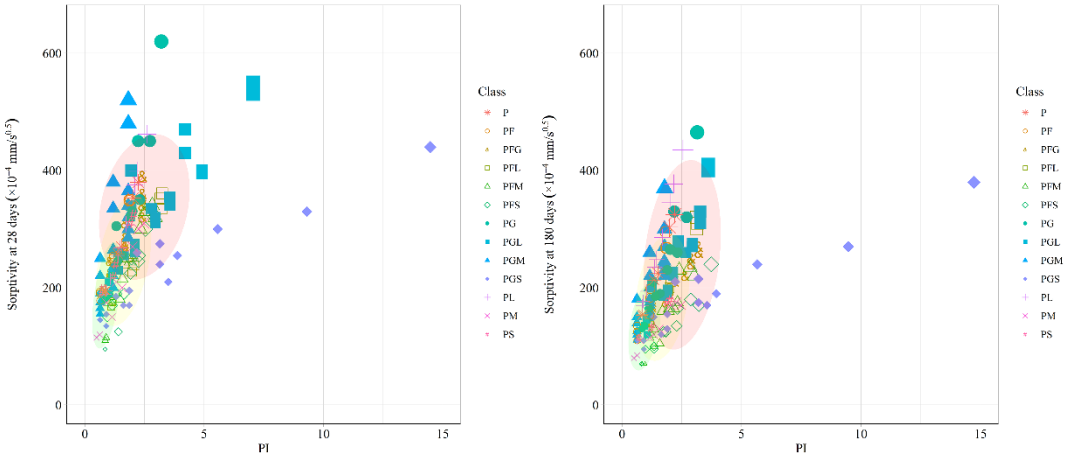

(i) Sorptivity at 28 days (j) Sorptivity at 180 days

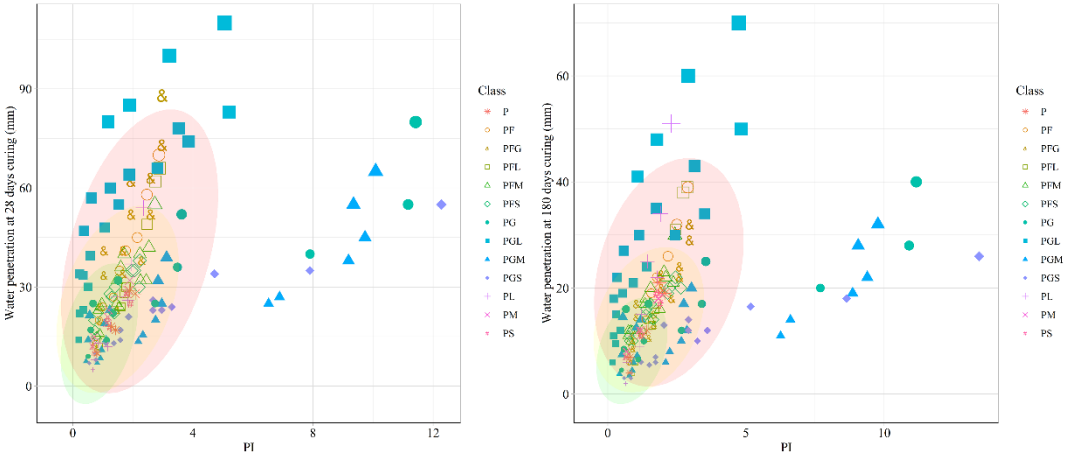

(k) Water penetration at 28 days curing (l) Water penetration at 180 days curing

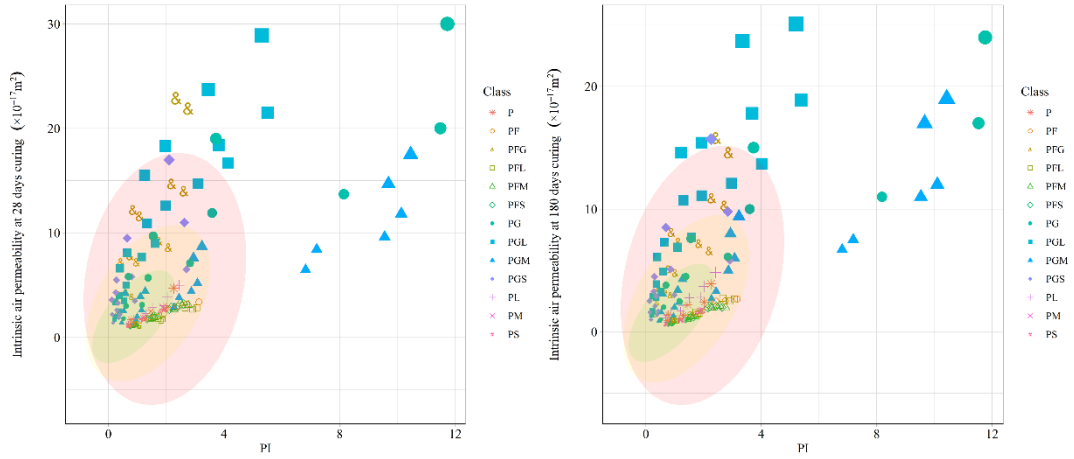

(m) Intrinsic air permeability at 28 days curing (n) Intrinsic air permeability at 180 days curing

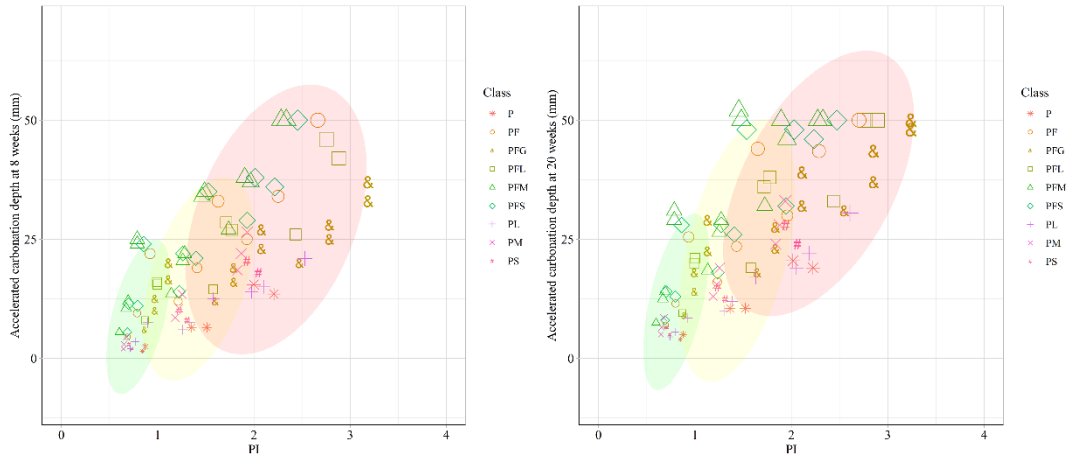

(o) Accelerated Carbonation depth at 8 weeks (p) Accelerated Carbonation depth at 20 weeks

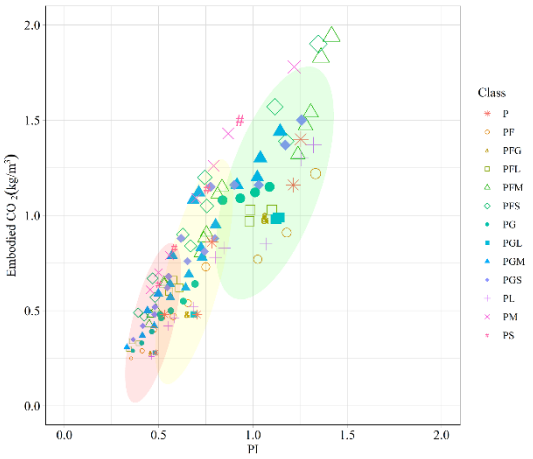

(q) Embodied CO_2

Figure 4.16 Performance design charts

4.8 UTILITY OF POD IN COMPUTATIONAL MECHANICS

Cracking is inherent to concrete, triggered by heat released during hydration, shrinkage, insolation, thermal-hygral-structural loadings and many other causes. The extent of early-age cracking is one of the prime factors that decide the strength and durability of concrete. Quantification of heat release during hydration of cement and its rate is an important step in developing models to simulate early age cracking. Using Arrhenius equation, three-parameter exponential hydration-maturity relationship and equation of heat release rate, Schindler suggested an expression to compute heat release with time, as in Eq. 4.03 (Riding et al. 2012; Schindler et al. 2002; Schindler and Folliard 2005).

$$Q_h(t) = H_u C_c \left(\frac{\tau}{t_e}\right)^{\beta} \left(\frac{\beta}{t_e}\right) \alpha_u \, e^{\left(-\frac{\tau}{t_e}\right)^{\beta}} e^{\frac{E_a}{R}\left(\frac{1}{T_r}-\frac{1}{T_c}\right)} \tag{4.03}$$

Q_h is heat release with time, H_u total heat available for reaction (J/g), C_c is cementitious material content (g/m^3), t_e (h) is the equivalent age for a material hydrating at reference temperature T_r(K), R is the universal gas constant (8.314 J/mol/K), T_c is the temperature of the concrete (K), and E_a is the apparent activation energy (J/mol), which depends on composition and proportioning of the cementitious materials.

τ is the hydration time parameter (h), β is the hydration slope parameter, and α_u is the ultimate degree of hydration in the three-parameter model for degree of hydration. The τ term represents the time delay from mixing until setting, β represents the slope of the S-shaped curve, and α_u is the total amount of cement that has reacted at $t = \infty$ where $\alpha_u = 0$ for no hydration and $\alpha_u = 1$ is for complete hydration. The terms β, τ and α_u themselves depend on composition and proportioning of cementitious materials. To determine β, τ and α_u many multi-variate non-linear regression expressions are established through experimentations on mixes with a wide range of compositions. Past works have used the technique of ANOVA in selection/exclusion of variables and combination of selected variables.

Poole (2007) chooses two Bogue compounds C_3A, C_4AF and Blaine fineness (F_b) as suggested by Schindler et al. (2002) model and additionally gypsum content and water-cement ratio for modeling apparent activation energy to arrive at Eq. 4.04 based on Bogue calculations and Eq. 4.05 based on Reitveld analysis.

$$E_a = 31400\left(\left(p_{C_3A} + p_{C_4AF}\right) p_{Gypsum}\right)^{0.13} Blaine^{-0.07}\, W/C^{-0.05} \quad (4.04)$$

$$E_a = 37800\left(\left(p_{C_3A}\right)(CaSO_4.xH_2O + K_2SO_4)\right)^{0.05} Blaine^{-0.03} W/C^{-0.04} \quad (4.05)$$

Available datasets used to develop Eqs. 4.04 and 4.05 are analyzed by POD and results obtained are presented in Figs. 4.17 and 4.18 respectively.

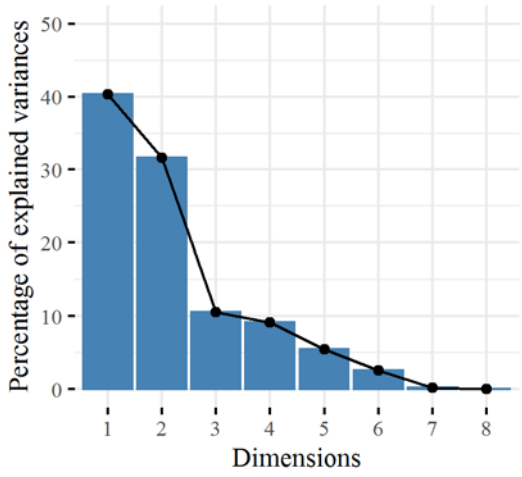

(a) Scree plot

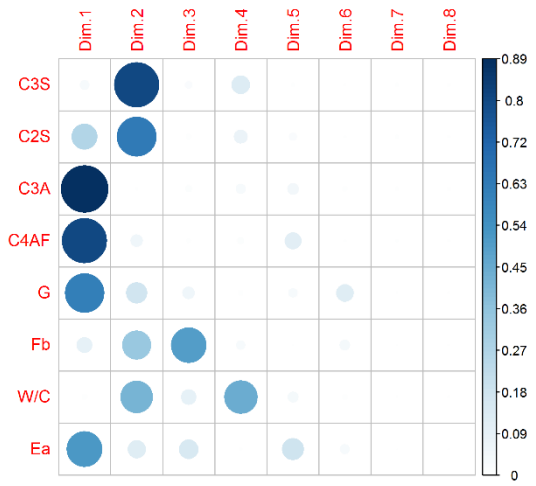

(b) Quality of representation

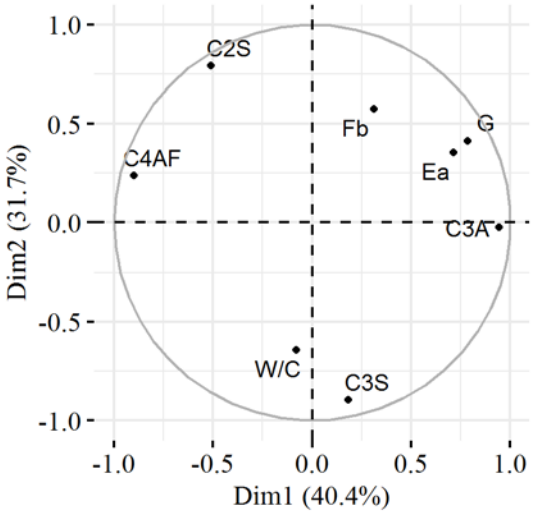

(c) Component plot

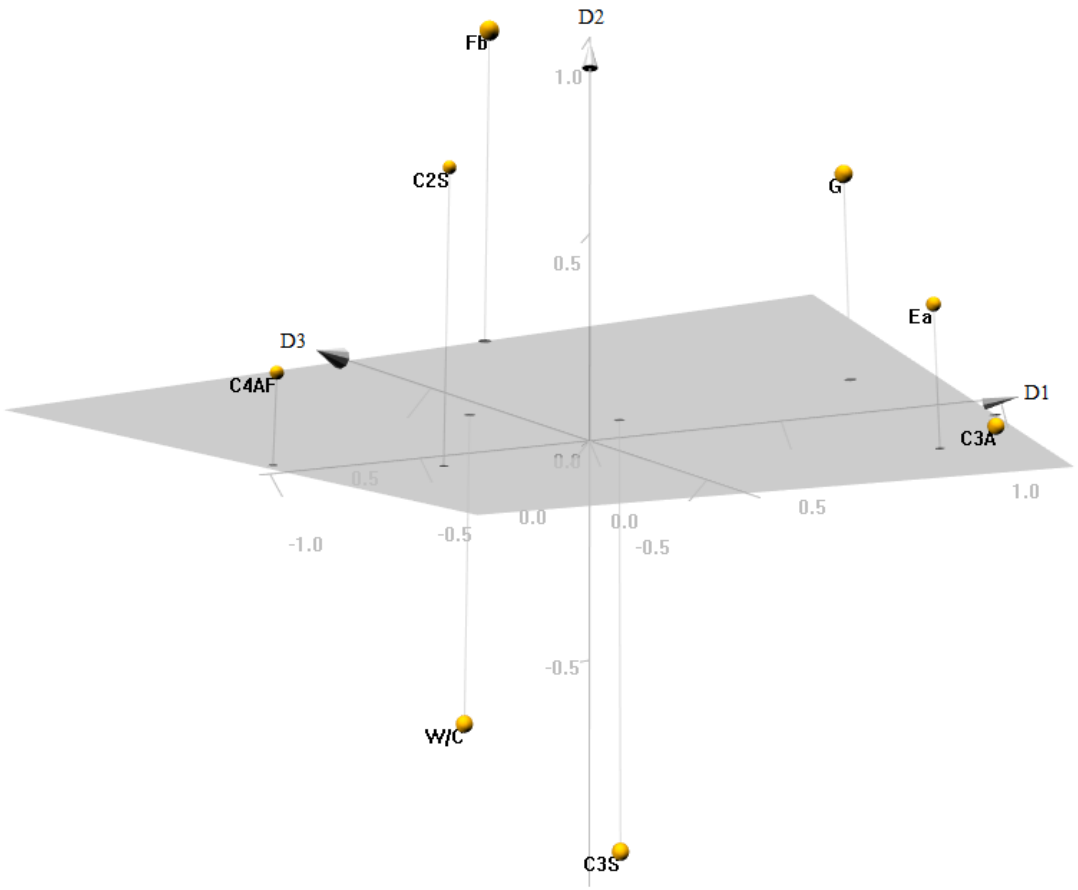

(d) 3D component plot

Figure 4.17 POD results for Poole data used for modelling Eq. 4.04

As evident from Fig. 4.17 (a), first two components explain about 70% of total variation in the data. Also, as per Fig. 4.17 (b), the target variable E_a is well represented in first dimension. From component plot as presented in Fig. 4.17 (c), it is clear that prime variables to be considered in modeling E_a are C_3A, C_4AF, gypsum content and Blaine fineness. Variables W/C, C_3S and C_2S do not significantly affect E_a. This result is consistent with variables selected by Poole in modeling Eq. 4.04.

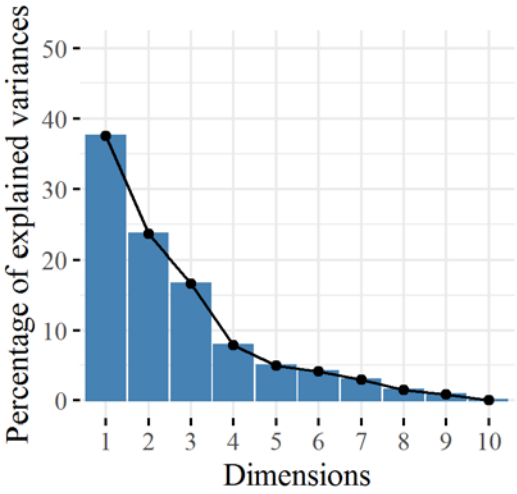

(a) Scree plot

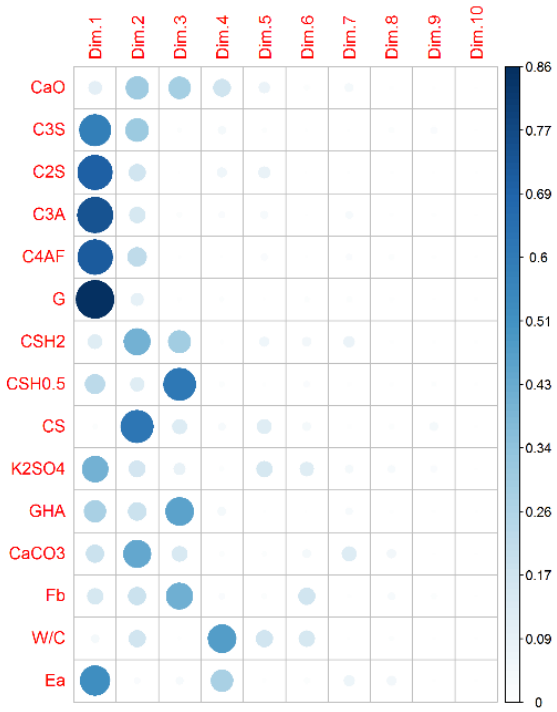

(b) Quality of representation

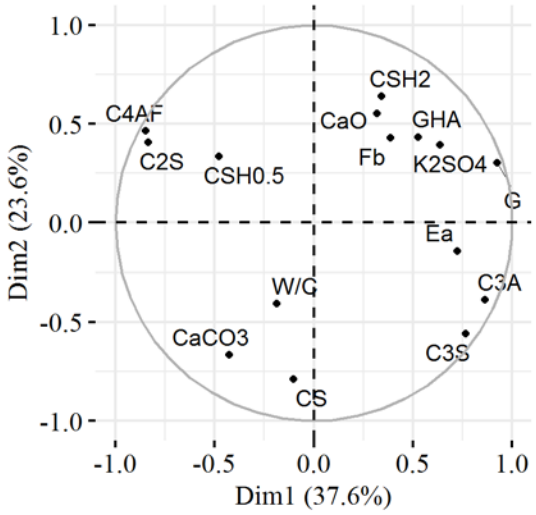

(c) Component plot

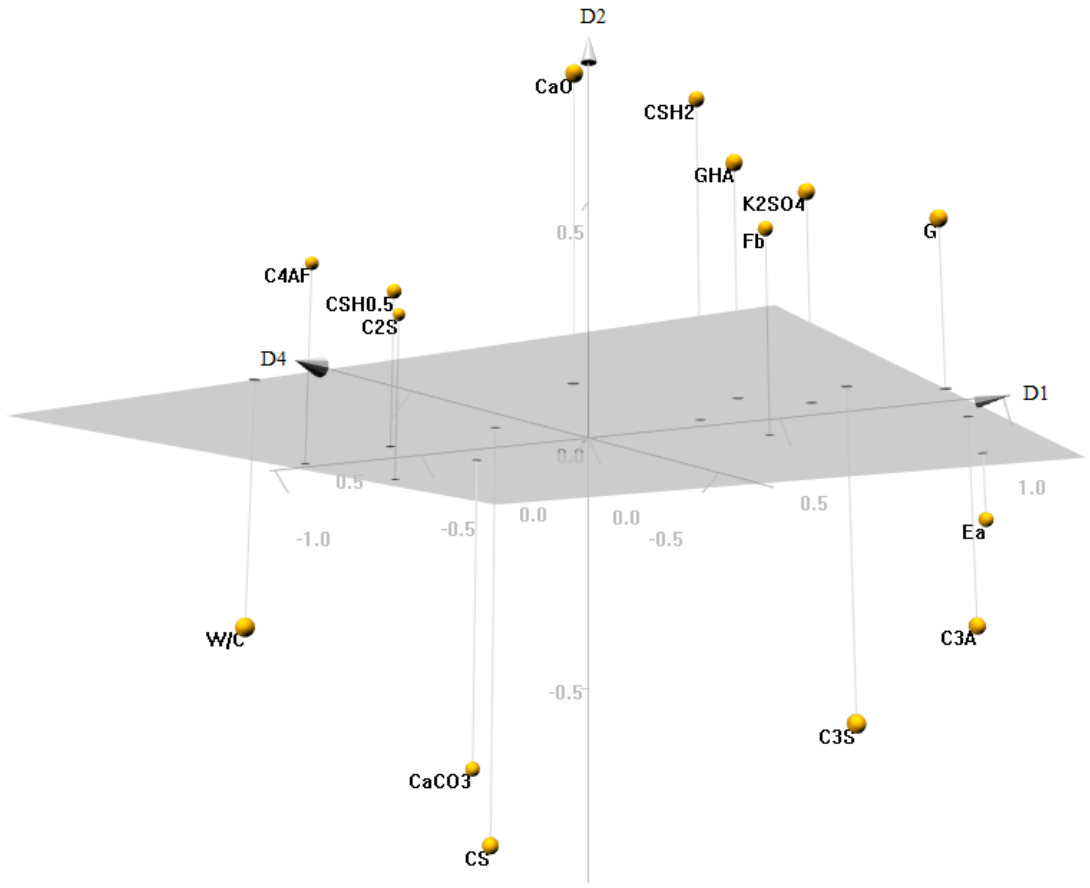

(d) 3D component plot

Figure 4.18 POD results for Poole data used for modelling Eq. 4.05

Fig. 4.18 (a) indicates only about 61% variance explained from first-two components. E_a is well represented in first and fourth components as per Fig. 4.18 (b). Eq. (4.05) includes C_3A, GHA, K_2SO_4, Blaine fineness and W/C as variables to predict E_a. Component plot drawn for first-two dimensions (Fig 4.18 (c)) shows a strong association of E_a with C_2S, C_4AF and C_3S in addition to variables in Eq. 4.05. Their inclusion to address the mismatch in E_a model may be necessary, which can be taken up based on supplementary information. Consideration of third and fourth components may be required for more accurate analysis.

POD can be of great utility in variable selection by dimensionality reduction of complex data which otherwise is difficult to analyse and model. Analysis becomes quick, and modelling can be more assertive. Thus POD can be used as a model refinement tool in concrete computational mechanics.

CHAPTER 5
CONCLUSIONS

Utility of POD in understanding dependence, inter-dependence and independence of variables, interplay of variables in influencing performance, quantification of performance levels and reduction of dimensionality of data has been systematically studied. The need for computational techniques in reorganization and rationalization of concrete data for development of math models, refining of available models has been explained. A method of performance appraisal from POD analysis result interpretation, and quantification of performance level by determination of performance index has been suggested. Possible application of POD in refinement of modelling concrete in performance based design has been illustrated.

5.1 GENERAL CONCLUSIONS

General conclusions that can be drawn from the investigation are,

a) POD is of great utility in handling high-dimensional data and helps in identifying very vital variables that greatly influence system's behaviour. Identification of crucial variables shall help in reduction of computational efforts in math modelling. From the situations addressed, it is clear that first few components are sufficient to capture much of the variation. Also at the expense of computational time and effort POD helps in inclusion of entire exhaustive data in assessing system's behaviour.
b) In experimental investigations, many a time, some crucial data is not acquired. Suggestions for acquisition of such data can be made by analytical investigation employing POD.
c) Qualitative and quantitative assessment of system's behaviour is possible and POD is a valid decision-making tool in comparing, discriminating and selecting from alternatives as demonstrated by exercise on innovative cement combinations.
d) Existing and recognised models can be assessed with available data and the model that best represents the system can be chosen as has been illustrated by the investigation on early-age cracking of concrete.
e) Systems can be investigated by inclusion of new data and assessed for changes in system's behaviour when such new data is available.

f) In the current investigation, the concept of 'whole-to-part' of dimensionality reduction has been attempted. Part-to-whole approach of dimensionality addition is also a possible sequence, wherein, from fringe data, system's behaviour appraisal can be done by addition of data on variables for exploration, verification and validation of possible improvements in performance.

5.2 SPECIFIC CONCLUSIONS

Specific conclusions that can be drawn from the investigation are,

5.2.1 Workability

a) An increase in water and fine aggregate content increases workability; whereas higher coarse aggregate content makes the mix harsher (Section 4.2.4d, e).
b) Use of silica fume as a replacement to fine aggregate influences flow characteristics more than replacement by GGBS or fly ash in self-compacting concrete (Section 4.4.2).
c) In cement - fly ash based and fly ash - GGBS based geo-polymer concrete slump is strongly and positively correlated to fly ash content whereas in cement-GGBS based mixes slump is correlated to cement content (Section 4.5.3).

5.2.2 Strength

a) Higher cement content in mixes and an increase in the ratio of cement to aggregate increases compressive strength but an increase in water-cement ratio decreases compressive strength. Strength is negatively correlated to fine aggregate to cement content and coarse aggregate to cement content ratios (Section 4.2.4a, b, c).
b) In self-compacting concrete, use of GGBS as a replacement to fine aggregate strongly affects, leading to increase in 90 days' cube compressive strength, flexural strength and modulus of elasticity. Silica fume replacement enhances early age and long term strengths, on the contrary, substitution of fly ash affects strength properties adversely (Section 4.4.3).
c) POD analysis of fly ash - GGBS based geo-polymer concrete reveals that strength parameters are positively correlated to GGBS and negatively correlated to fly ash contents. Positive correlations of fly ash content in concrete with weight and strength loss due to acid, thermal and fire exposure are indicators of poor performance. Generally, in geo-polymer concrete mixes, weight and strength loss

due to acid exposure and loss in compressive strength due to thermal shock and fire are negatively correlated to strength of concrete. Incorporation of fibres can vastly help in retaining compressive strength characteristics when fly ash - cement based mixes exposed to fire and GGBS - cement based mixes are subjected to a harmful acid environment (Section 4.5.3).

d) In the innovative cement combination studies, strength variables cluster around total fine content and lie opposite to fine and coarse aggregate contents (Section 4.6.4), indicating superiority of more fines concrete in strength capabilities.

5.2.3 Durability

a) It is observed that in making innovative cement, usage of fly-ash and GGBS in binary blends in addition to cement does not change the interaction of the variables much. Although, their increased percentage in mixes can initiate durability problems (Section 4.6.4).
b) Coarse aggregate majorly affects sorption characteristics and does not affect strength and durability as much as other variables. Increased fine aggregate content in mixes can result in higher sorption and water penetration (Section 4.6.5).
c) Replacement of coarser materials (aggregates) does not have an effect as much as the replacement of finer materials on strength and durability characteristics, unless coarse material is reactive (Section 4.6.3).
d) Percolation characteristics are negatively correlated with strength variables. Hence mixes with high-strength are likely to have low permeability issues (Section 4.6.3).
e) Clustering of variables influencing durability suggests that they are interrelated and one of the variables affecting adversely indicates possibility of issues due to other variables too (Section 4.6.3).
f) The signatures of variable interaction in component plots substantiate that grading of fines and their optimum proportioning are the primary factors that contribute to strength enhancement and durability extension (Section 4.6.3).
g) Utility of SCMs is more effective as a ternary blend. On the whole fly ash based ternary blends are superior to GGBS (Section 4.6.4).

5.2.4 Performance at elevated temperature exposure

Inferences from POD analysis of data on concrete exposed to elevated temperature are,

a) Crushed rock fines content and water-cement ratio are the primary variables that increase weight loss due to concrete exposure up to 200 °C. In this temperature range, higher cement content and cement to aggregate ratio help in retaining weight (Section 4.3.3).
b) For exposure above 200 °C, cement content, cement to aggregate ratio, admixture dosage and concrete grade are the significant parameters that determine the amount of weight loss that can happen. Higher the strength, greater is the weight loss (Section 4.3.3).
c) Fine and coarse aggregate contents do not significantly affect weight loss at elevated temperatures (Section 4.3.4).
d) In all temperature ranges of the data, water-cement ratio shows a positive correlation with residual compressive strength whereas cement content, cement to aggregate ratio, admixture dosages and gel space ratio show a negative correlation with residual compressive strength, indicating loss in strength is greater in higher strength grades (Section 4.3.4).
e) Fine aggregate content has a strong positive correlation with residual compressive strength, indicating beneficial role of fine aggregate in strength retention (Section 4.3.4).

5.3 HIGHLIGHTS AND NOVELTY OF THE PRESENT INVESTIGATION

a) Demonstration of utility of POD in performance based design has been accomplished by illustrations through investigations on available data for
    - Workability
    - Strength
    - Durability
    - Performance at elevated temperature exposure
b) The illustrations demonstrate the power of POD in quantification of influence of variables on concrete performance. The investigations have been carried out on a wide and varied range of data sets available for conventional concrete, geo-polymer, self-compacting concrete, concrete at elevated temperature and innovative cement blends.

c) Available concrete models have been tested for prediction/projection capabilities subjecting them to POD analysis.
d) POD has immense capabilities of dimensionality reduction, qualitative and quantitative representation of system's behaviour, understanding interplay of variables and refinement of concrete models as has been demonstrated by the various illustrations.

PUBLICATIONS

ARTICLES

Manoj, A., and Babu Narayan, K. S., (2019). "Making sense of high dimensional concrete data–a statistical approach." *IOP Conference Series: Materials Science and Engineering*, Vol. 615(1). doi:10.1088/1757-899X/615/1/012019

Manoj, A., and Babu Narayan, K. S., (2021). "Application of proper orthogonal decomposition in concrete performance appraisal" *Recent Trends in Civil Engineering*, Lecture Notes in Civil Engineering, 105, Springer. doi.org/10.1007/978-981-15-8293-6_2

Manoj, A., and Babu Narayan, K. S., (2021). "The utility of proper orthogonal decomposition for dimensionality reduction in understanding behaviour of concrete." *Computers and Concrete*, 28(2), Techno-Press. doi.:10.12989/cac.2021.28.2.129

Manoj, A., and Babu Narayan, K. S., "POD in Concrete Performance Assessment" *Manipal Journal of Science and Technology* (Accepted)

Manoj, A., and Babu Narayan, K. S., "Proper Orthogonal Decomposition for performance valuation of multi-blend Concrete mixes" (Manuscript under preparation)

CONFERENCES

Manoj, A., and Babu Narayan, K. S., (2018). "Application of PCA in Concrete Technology." *7th Int. Eng. Sym.*, Kumamoto Uni., Japan.

Manoj, A., and Babu Narayan, K. S., (2019). "Proper Orthogonal Decomposition for Generation of Organised Data in Concrete Technology." *UKIERI Concr. Congr. The Glob. Build.*, Dr B R Ambedkar National Institute of Technology, Jalandhar, India.

Manoj, A., and Babu Narayan, K. S., (2019). "Making Sense of High Dimensional Concrete Data – A Statistical Approach." *7th Int. Conf. EACEF*, Stuttgart Uni., Germany.

Manoj, A., and Babu Narayan, K. S., (2019). "Application of proper orthogonal decomposition in concrete performance appraisal" *TMSF'19*, DBCE, Fatorda, GOA (Best paper award)

REFERENCES

Aggarwal, R., Kumar, M., Sharma, R. K., and Sharma, M. K. (2015). "Predicting Compressive Strength of Concrete." *Int. J. Appl. Sci. Eng.*, 13(2), 171–185.

Ahmed, M. A., Mallick, J., and Hasan, M. A. (2016). "A study of factors affecting the flexural tensile strength of concrete." *J. King Saud Univ. - Eng. Sci.*, 28(2), 147–156.

Al-Ghalib, A. A., and Mohammad, F. A. (2016). "Damage and repair classification in reinforced concrete beams using frequency domain data." *Mater. Struct.*, 49(5), 1893–1903.

Aldahdooh, M. A. A., Bunnori, N. M., and Johari, M. A. M. (2013). "Evaluation of ultra-high-performance-fiber reinforced concrete binder content using the response surface method." *Mater. Des.*, 52, 957–965.

Anderson, T. W. (1963). "Asymptotic theory for principal component analysis." *Ann. Math. Stat.*, 34(1), 122–148.

Arizio, E., Piazza, R., Cairns, W. R. L., Appolonia, L., and Botteon, A. (2013). "Statistical analysis on ancient mortars : A case study of the Balivi Tower in Aosta (Italy)." *Constr. Build. Mater.*, 47, 1309–1316.

Bal, L., and Buyle-Bodin, F. (2013). "Artificial neural network for predicting drying shrinkage of concrete." *Constr. Build. Mater.*, 38, 248–254.

Bartlett, M. S. (1950). "Tests of significance in factor analysis." *Br. J. Stat. Psychol.*, 3(2), 77–85.

Beltrami, E. (1873). "Sulle funzioni bilineari." *G. di Mat. ad Uso degli Studenti Delle Univ.*, 11(2), 98–106.

Bonifazi, G., Palmieri, R., and Serranti, S. (2018). "Evaluation of attached mortar on recycled concrete aggregates by hyperspectral imaging." *Constr. Build. Mater.*, 169, 835–842.

Boukhatem, B., Ghrici, M., Kenai, S., and Tagnit-hamou, A. (2011a). "Prediction of Efficiency Factor of Ground-Granulated Blast." *ACI Mater. J.*, (108), 1–10.

Boukhatem, B., Kenai, S., Hamou, A. T., Ziou, D., and Ghrici, M. (2012). “Predicting concrete properties using Neural Networks (NN) with Principal Component Analysis (PCA) technique.” *Comput. Concr.*

Boukhatem, B., Kenai, S., Tagnit-Hamou, A., and Ghrici, M. (2011b). “Application of new information technology on Concrete: An Overview.” *J. Civ. Eng. Manag.*, 17(2), 248–258.

British Standards Institution. (2000). *BS EN 206-1:2000 Concrete. Specification, performance, production and conformity*. London.

Calabrese, L., Campanella, G., and Proverbio, E. (2012). “Noise removal by cluster analysis after long time AE corrosion monitoring of steel reinforcement in concrete.” *Constr. Build. Mater.*, 34, 362–371.

Chávez-Arroyo, R., Lozano-Galiana, S., Sanz-Rodrigo, J., and Probst, O. (2013). “On the application of Principal Component Analysis for accurate statistical-dynamical downscaling of wind fields.” *Energy Procedia*, Elsevier, 67–76.

Chou, J., Chiu, C., Farfoura, M., and Al-taharwa, I. (2011). “Optimizing the Prediction Accuracy of Concrete Compressive Strength Based on a Comparison of Data-Mining Techniques.” *J. Comput. Civ. Eng.*, 25(3), 242–253.

Chou, J., Ngo, N., and Pham, A. (2015). “Shear Strength Prediction in Reinforced Concrete Deep Beams Using Nature-Inspired Metaheuristic Support Vector Regression.” *J. Comput. Civ. Eng.*, 30(1), 1–9.

Degala, S., Rizzo, P., Ramanathan, K., and Harries, K. A. (2009). “Acoustic emission monitoring of CFRP reinforced concrete slabs.” *Constr. Build. Mater.*, 23(5), 2016–2026.

Dhir, R. K., Newlands, M. D., McCarthy, M. J., Zheng, L., and Halliday, J. E. (2010). *Innovative Cement Combinations for Concrete Performance–Final Report CTU/5009. Concr. Technol. Unit, Div. Civ. Eng. Sch. Eng. Phys. Math. Univ. Dundee.*

Falchi, L., Varin, C., Toscano, G., and Zendri, E. (2015). “Statistical analysis of the physical properties and durability of water-repellent mortars made with limestone

cement, natural hydraulic lime and pozzolana-lime." *Constr. Build. Mater.*, 78, 260–270.

Filho, F. M. A., Barragán, B. E., Casas, J. R., and Debs, A. L. H. C. El. (2010). "Hardened properties of self-compacting concrete - A statistical approach." *Constr. Build. Mater.*, 24, 1608–1615.

Folliard, K. J., Juenger, M., Schindler, A., Riding, K., Poole, Jonathan, Kallivokas, L. F., Slatnick, S., Whigham, J., and Meadows, J. L. (2008). *Prediction Model for Concrete Behavior—Final Report*. Austin.

Ghizdăveț, Z., Ștefan, B. M., Nastac, D., Vasile, O., and Bratu, M. (2016). "Sound absorbing materials made by embedding crumb rubber waste in a concrete matrix." *Constr. Build. Mater.*, 124, 755–763.

González-Taboada, I., González-Fonteboa, B., Martínez-Abella, F., and Pérez-Ordóñez, J. L. (2016). "Prediction of the mechanical properties of structural recycled concrete using multivariable regression and genetic programming." *Constr. Build. Mater.*, 106, 480–499.

Gower, J. C. (1966). "Some distance properties of latent root and vector methods used in multivariate analysis." *Biometrika*, 53(3–4), 325–338.

Gryllias, K., Koukoulis, I., Yiakopoulos, C., Antoniadis, I., and Provatidis, C. (2009). "Morphological processing of proper orthogonal modes for crack detection in beam structures." *J. Mech. Mater. Struct.*, 4(6), 1063–1088.

Gulotta, D., Goidanich, S., Tedeschi, C., and Toniolo, L. (2015). "Commercial NHL-containing mortars for the preservation of historical architecture. Part 2: Durability to salt decay." *Constr. Build. Mater.*, 96, 198–208.

Hellebois, A., Launoy, A., Pierre, C., Lanève, M. De, and Espion, B. (2013). "100-year-old Hennebique concrete, from composition to performance." *Constr. Build. Mater.*, 44, 149–160.

Hotelling, H. (1933). "Analysis of a complex of statistical variables into principal components." *J. Educ. Psychol.*, 24(6), 417–441.

Hotelling, H. (1936). “Simplified calculation of principal components.” *Psychometrika*, 1(1), 27–35.

Husson, F., Lê, S., and Pagès, J. (2017). *Exploratory Multivariate Analysis by Example Using R*. CRC press.

Jaruszewicz, M., and Mandziuk, J. (2002). “Application of PCA method to weather prediction task.” *Proc. 9th Int. Conf. Neural Inf. Process. 2002. ICONIP ’02.*, IEEE, 2359–2363 vol.5.

Jeffers, J. N. R. (1967). “Two case studies in the application of principal component analysis.” *J. R. Stat. Soc. Ser. C (Applied Stat.*, 16(3), 225–236.

Jolliffe, I. T. (2002). *Principal Component Analysis*. *Int. Encycl. Educ.*, New York: Springer.

Jordan, C. (1874). “Mémoire sur les formes bilinéaires.” *J. Math. Pures Appl.*, 19, 35–54.

Kellouche, Y., Boukhatem, B., Ghrici, M., and Tagnit-Hamou, A. (2017). “Exploring the major factors affecting fly-ash concrete carbonation using artificial neural network.” *Neural Comput. Appl.*, Springer London, 1–20.

Kheder, G. F., Gabban, A. M. Al, and Abid, S. M. (2003). “Mathematical model for the prediction of cement compressive strength at the ages of 7 and 28 days within 24 hours.” *Mater. Struct.*, 36(10), 693–701.

Krzywinski, M., and Altman, N. (2014). “Visualizing samples with box plots.” *Nat. Methods*, 11(2), 119–120.

Lavanya, R. (2018). “An experimental investigation on properties of high strength self-compacting concrete mixes.” Anna University.

Lee, S.-C. (2003). “Prediction of concrete strength using artificial neural networks.” *Eng. Struct.*, 25(7), 849–857.

Li, B., Ren, X., Li, Y., Ma, W., and Li, H. (2017). “Evaluation and selection of sealants and fillers using principal component analysis for cracks in asphalt concrete pavements.” *J. Wuhan Univ. Technol. Sci. Ed.*, 32(2), 408–412.

Li, J. (2009). “A layman’s introduction to principal component analysis.” *Vis. High Dimens. Data*, <http://jamesxli.blogspot.com/2009/09/>.

Liang, Y. C., Lee, H. P., Lim, S. P., Lin, W. Z., Lee, K. H., and Wu, C. G. (2002). “Proper Orthogonal Decomposition and Its Applications—Part I: Theory.” *J. Sound Vib.*, 252(3), 527–544.

Lu, Y., Li, J., Ye, L., and Wang, D. (2013). “Guided waves for damage detection in rebar-reinforced concrete beams.” *Constr. Build. Mater.*, 47, 370–378.

Madandoust, R., Ghavidel, R., and Nariman-Zadeh, N. (2010). “Evolutionary design of generalized GMDH-type neural network for prediction of concrete compressive strength using UPV.” *Comput. Mater. Sci.*, 49(3), 556–567.

Manoj, A., and Babu Narayan, K. S. (2019). “Proper Orthogonal Decomposition For Generation Of Organized Data In Concrete Technology.” *Ukieri Concr. Congr. Concr. Glob. Build.*

Manoj, A., and Narayan, K. S. B. (2021). “Application of Proper Orthogonal Decomposition in Concrete Performance Appraisal.” *Recent Trends Civ. Eng.*, Springer, 13–21.

Mehta, P. K., and Monteiro, P. J. M. (2014). *Concrete: Microstructure, Properties, and Materials*. McGraw-Hill Education.

Moropoulou, A., Polikreti, K., Bakolas, A., and Michailidis, P. (2003). “Correlation of physicochemical and mechanical properties of historical mortars and classification by multivariate statistics.” *Cem. Concr. Res.*, 33, 891–898.

Neville, A. M., and Brooks, J. J. (2010). *Properties of concrete*. London: Pearson.

Newlands, M. D. (2019). “A Concrete Education: Futureproofing for the Digital World.” *Ukieri Concr. Congr. Concr. Glob. Build.*

Ng, S. C. (2017). “Principal component analysis to reduce dimension on digital image.” *Procedia Comput. Sci.*, 113–119.

Ni, H.-G., and Wang, J.-Z. (2000). “Prediction of compressive strength of concrete by neural networks.” *Cem. Concr. Res.*, 30(8), 1245–1250.

Ogallo, L. J. (1989). “The spatial and temporal patterns of the East African seasonal rainfall derived from principal component analysis.” *Int. J. Climatol.*, 9(2), 145–167.

Pan, Y., Prado, A., Porras, R., Hafez, O. M., and Bolander, J. E. (2017). “Lattice modeling of early-age behavior of structural concrete.” *Materials (Basel).*, 10(3), 1–34.

Pearson, K. (1901). “On lines and planes of closest fit to systems of points in space.” *London, Edinburgh, Dublin Philos. Mag. J. Sci.*, 2(11), 559–572.

Poole, J. L. (2007). “Modeling temperature sensitivity and heat evolution of concrete.” The University of Texas at Austin.

Pradeep, B. K., Shashank, B. N., and Karthik, S. U. (2012). “Application of Principal Component Analysis in Civil Engineering.” NITK, Surathkal.

Rampazzi, L., Pozzi, A., Sansonetti, A., Toniolo, L., and Giussani, B. (2006). “A chemometric approach to the characterisation of historical mortars.” *Cem. Concr. Res.*, 36(6), 1108–1114.

Rao, C. R. (1964). “The use and interpretation of principal component analysis in applied research.” *Sankhyā Indian J. Stat. Ser. A*, 329–358.

Raskin, R., and Terry, H. (1988). “A principal-components analysis of the Narcissistic Personality Inventory and further evidence of its construct validity.” *J. Pers. Soc. Psychol.*, 54(5), 890–902.

Rejilin, A. D. R. (2018). “Strength and durability properties of geopolymer concrete.” Anna University.

Riding, K. A., Poole, J. L., Folliard, K. J., Juenger, M. C. G., and Schindler, A. K. (2012). “Modeling hydration of cementitious systems.” *ACI Mater. J.*, 109(2), 225–234.

Sadowski, Ł., Nikoo, M., and Nikoo, M. (2015). “Principal Component Analysis combined with a Self Organization Feature Map to determine the pull-off adhesion between concrete layers.” *Constr. Build. Mater.*, 78, 386–396.

Santos, J. P., Cremona, C., Orcesi, A. D., and Silveira, P. (2016). “Early Damage Detection Based on Pattern Recognition and Data Fusion.” *J. Struct. Eng.*, 143(2),

04016162.

Schindler, A. K., Dossey, T., and McCullough, B. F. (2002). *Temperature control during construction to improve the long term performance of Portland cement concrete pavements*. Austin, TX.

Schindler, A. K., and Folliard, K. (2005). "Heat of Hydration Models for Cementitious Materials." *ACI Mater. J.*, 102, 24–33.

Shalizi, C. R. (2013). *Advanced Data Analysis from an Elementary Point of View*. Cambridge University Press.

Shlens, J. (2003). *A Tutorial on Principal Component Analysis and Singular Value Decomposition. Technical report*. CA.

Smith, L. I. (2002). *A Tutorial on Principal Components Analysis. Technical Report OUCS-2002-12*. New Zealand.

Ta, V. L., Bonnet, S., Senga Kiesse, T., and Ventura, A. (2016). "A new meta-model to calculate carbonation front depth within concrete structures." *Constr. Build. Mater.*, 129, 172–181.

Taffese, W. Z., and Sistonen, E. (2017). "Machine learning for durability and service-life assessment of reinforced concrete structures: Recent advances and future directions." *Autom. Constr.*, 77, 1–14.

Thirumalaiselvi, A., and Sasmal, S. (2019). "Acoustic emission monitoring and classification of signals in cement composites during early-age hydration." *Constr. Build. Mater.*, 196, 411–427.

Tobias, S., and Carlson, J. E. (1969). "Brief report: Bartlett's test of sphericity and chance findings in factor analysis." *Multivariate Behav. Res.*, 4(3), 375–377.

Trejo, D., Shakouri, M., and Vaddey, N. P. (2017). "The need for standardized testing for service life prediction of reinforced concrete." *Int. Conf. Adv. Constr. Mater. Syst.*, Chennai, 125–138.

Yaragal, S. C., Narayan, K. S. B., Venkataramana, K., Kishor, S., Kulkarni, K. S., Gowda, H. C. C., Reddy, G. R., and Sharma, A. (2010). "Studies on Normal Strength

Concrete Cubes Subjected to Elevated Temperatures.” *J. Struct. Fire Eng.*, 1(4), 249–262.

Yi, S.-T., Moon, Y.-H., and Kim, J.-K. (2005). “Long-term strength prediction of concrete with curing temperature.” *Cem. Concr. Res.*, 35(10), 1961–1969.

SCHOLAR DETAILS

Name	: A. Manoj
Student registration number	: 165 037 CV16F01
Contact	: manoja1990@gmail.com
Research interests	: Computational mechanics, POD, math modelling, reinforced concrete structures, pushover analysis.